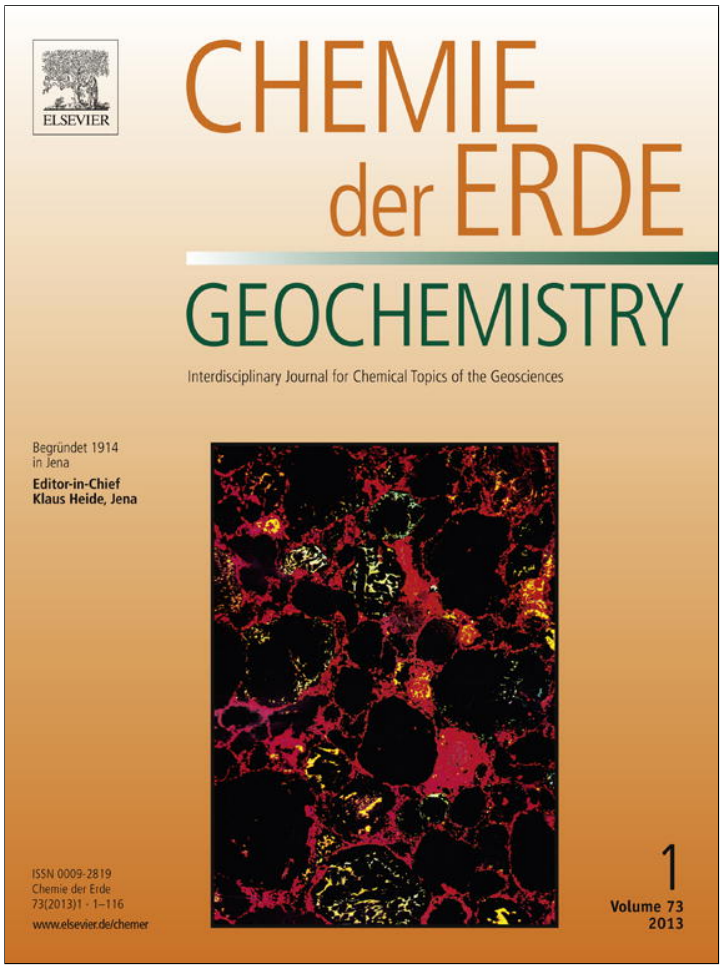

Chemie der Erde 73 (2013) 1–37

Contents lists available at SciVerse ScienceDirect

Chemie der Erde

journal homepage: www.elsevier.de/chemer

Invited review

Luminescence studies of extraterrestrial materials: Insights into their recent radiation and thermal histories and into their metamorphic history

Derek W.G. Sears[a,*], Kiyotaka Ninagawa[b], Ashok K. Singhvi[c]

[a] Space Science and Astrobiology Division, NASA Ames Research Center, MS245-3, Moffett Field, Mountain View, CA 94035, USA
[b] Department of Applied Physics, Okayama University of Science, Okayama, Japan
[c] Physical Research Laboratory, Ahmedabad 380 009, India

ARTICLE INFO

Article history:
Received 4 September 2012
Accepted 4 December 2012

Keywords:
Thermoluminescence
Meteorites
Orbits
Terrestrial age
Metamorphism

ABSTRACT

Early work on meteorite thermoluminescence (TL), influenced by pottery dating and dosimetry applications, demonstrated a relationship between natural thermoluminescence and (1) the orbital perihelion and (2) the terrestrial age (time since fall) of a meteorite. For 14 years natural TL measurements were routinely made on newly recovered Antarctic meteorites to help identify unusual thermal and radiation histories, and to sort them by terrestrial age and perihelion. Two examples of the value of such data are presented, an Antarctic meteorite that underwent a major orbit change prior to fall, and the collection mechanics of meteorites at the Lewis Cliff ice field. A second major area of focus for meteorite TL that has no non-meteorite heritage, is the use of their induced TL to provide an extraordinarily sensitive and quantitative means of exploring metamorphic intensity and palaeothermometry. While especially valuable for unequilibrated ordinary chondrites, these types of measurement have proved useful with virtually every major class of meteorite, asteroidal and planetary. The challenge now is to extend the technique to small particles, micrometeorites, interplanetary dust particles, and cometary particles.

Contents

* Corresponding author. Tel.: +1 510 400 9517; fax: +1 510 604 6779.
E-mail address: Derek.Sears@nasa.gov (D.W.G. Sears).

0009-2819/$ – see front matter © 2013 Elsevier GmbH. All rights reserved.
http://dx.doi.org/10.1016/j.chemer.2012.12.001

1. Introduction: a little history

It is arguable that the first person to observe the luminescence from a mineral – or at least to document it in a modern scientific way – was Boyle (1664). In his book "*Experiments and Considerations Touching Colours*", he described a great many experiments on the optical properties of diamond including one in which he induced diamond to luminesce by prolonged exposure to sunlight. He states "I also brought it to some kind of glimmering light, by taking it to bed with me, and holding it a good while upon a warm part of my naked body". Such was the dedication and keen observation of one of the great 17th century natural philosophers. Nearly 150 years later, Howard (1802), British aristocrat scientist, brother of the 12th Duke of Norfolk, described the first modern chemical analysis of meteorites in a paper given to the Royal Society of London in 1801. Among the many important contributions in this remarkable paper – Howard was clearly a first rate chemist – was the genesis of the work described here. He described how luminescence was produced by the Benares meteorite when "electrical fluid" was passed over its surface (Fig. S1; Howard, 1802): "I ought not to suppress, that in endeavoring to form an artificial black coating on the interior surface of one of the stones from Benares, by sending over it the electrical charge of about 37 square feet of glass it was observed to become luminous, in the dark, for nearly a quarter on an hour: and that the tract of the electrical fluid was rendered black." He actually thought this might be part of the explanation for the brightness of the fireball as the meteorite passed through the atmosphere. The luminescence observed by Howard (1802) was probably caused by the flow of electrons into the crystal lattices, and should therefore be termed cathodoluminescence (CL), luminescence produced by cathode (electron) rays. However since considerable heating of the stone occurred, some part of the light might have been thermoluminescence (TL), luminescence produced by heating. In any event, at the very dawn of the serious scientific studies of meteorites, there is an observation that meteorites have noteworthy luminescence properties.

Throughout the 19th century enormous strides were made in collecting and cataloging meteorites and understanding their properties. Some of the great analytical chemists and geologists were associated with the effort (Burke, 1986). Despite rapidly growing collections, every meteorite fall attracted newspaper headlines as it does even today. Towards the close of the century a meteorite fell on a railway track near Middlesbrough in Yorkshire. A professor from a nearby university, well-known for his interest and expertise in meteors, was almost immediately at the scene. Alexander Herschel (Fig. S2), grandson of the great astronomer William Herschel, wrote a paper for *Nature* describing the fall (Herschel, 1881). A few years later he followed up with a paper on the Middlesbrough meteorite's luminescence properties (Herschel, 1899). He wrote that grains of the meteorite, when sprinkled on a hot plate, produced flashes of light as they hit the hot surface (Fig. S3): "Some fine dust and grains obtained from the interior portion of the mass of the Middlesborough aërolite, were found, to my considerable surprise, to glow quite distinctly, though not very brightly, with yellowish-white light, when sprinkled in the normal way for these experiments on a piece of nearly red-heated iron in the dark." He correctly suggested that the mineral responsible for the thermoluminescence was feldspar (Herschel, 1899). A great many recent

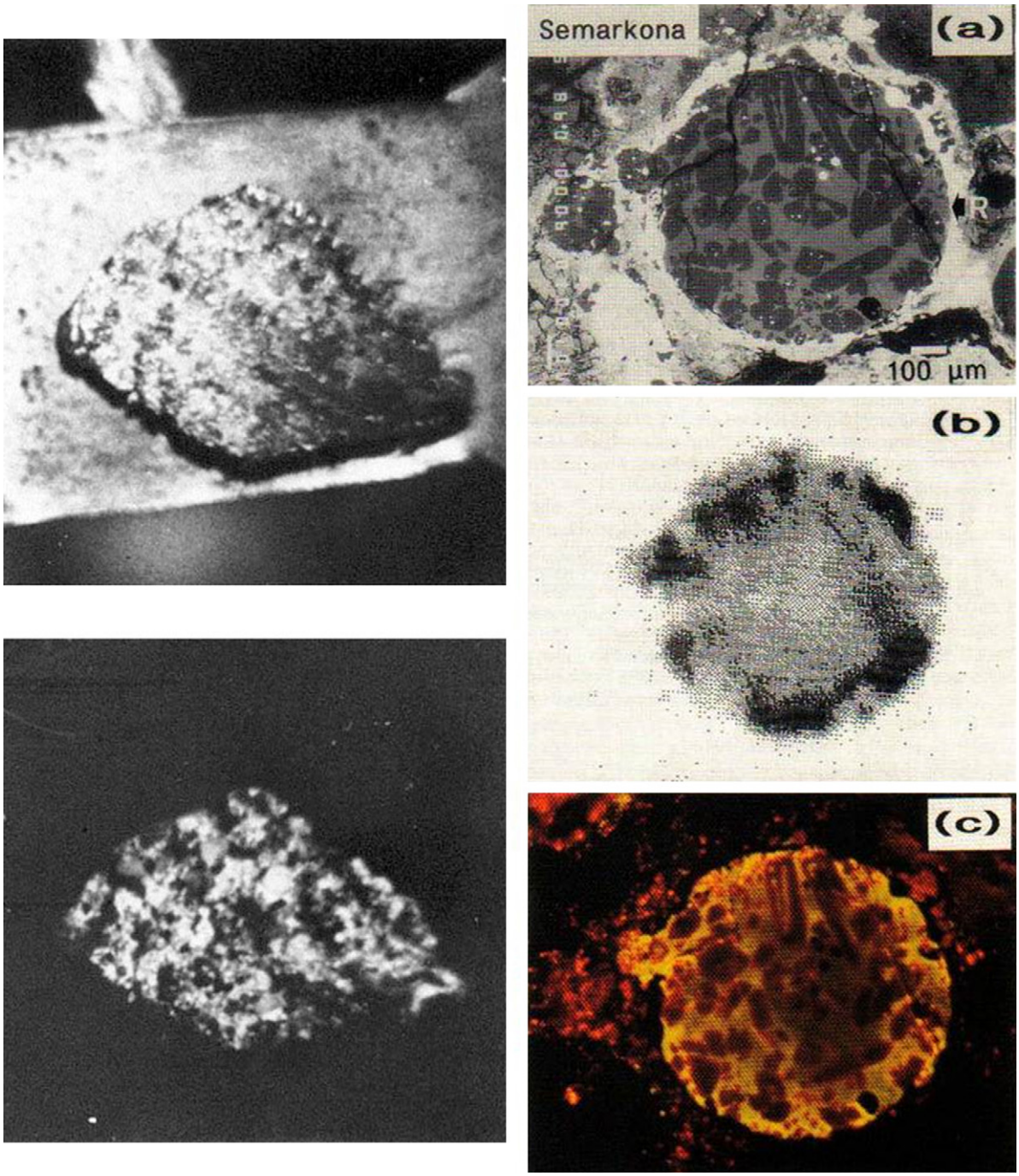

Fig. 1. Left, thermoluminescence of the Holbrook ordinary chondrite. A slice about 1 cm across and a millimeter thick lies on a nichrome heating strip prior to closing the apparatus. Heated to 250 °C in the dark the meteorite slice produces enough TL to be readily photographed in real-time. For the purposes of this photograph, the slice had been irradiated with a high dose of ^{60}Co gamma radiation. Right, three images of a large chondrule from the Semarkona chondrite. (a) Backscattered electron image. (b) Thermoluminescence image obtained by a CCD camera. (c) Cathodoluminescence obtained by a low-powered CL microscope. The luminescent area is not apparent in the BSE image, but the TL and CL are higher in the same outer regions of the chondrule mesostasis. Subsequent analysis by electron and ion microprobes showed the outer regions were higher in volatile elements and lighter in oxygen isotopes (in a non-mass-dependent way) relative to the interior (Sears, 1974; Matsunami et al., 1993).

studies involving mineral separation (Table 1) and low-powered cathodoluminescence mosaics of ordinary chondrite polished thin sections have confirmed this suggestion (Lalou et al., 1970; Sears et al., 1991a; Akridge et al., 2004). Fig. 1 is an image of the thermoluminescence of an ordinary chondrite in which it can be seen that only the feldspar is glowing. Herschel (1899) had also argued that the thermoluminescence of the grains of Middlesbrough was proof that the interior of the meteorite was not heated significantly during its passage through the atmosphere. Thermal gradients in meteorites produced by atmospheric heating have been documented by later authors using thermoluminescence (Vaz, 1971; Sears, 1975b; Singhvi et al., 1982).

The history of luminescence studies has been documented in considerable detail by Harvey (2005), and in the early 20th century significant progress was made in understanding the solid state properties and luminescence mechanisms of solids (Garlick and Gibson, 1948; Randall and Wilkins, 1945a,b; McKeever, 1985). By the mid-century, textbooks were available describing how it is

Table 1
Mineral separations and the thermoluminescence carriers in the St. Severin ordinary chondrite (Lalou et al., 1970).

Fraction	Thermoluminescence (whole powder = 1)	
	Induced	Natural
Whole powder	1.0	1.0
Merrillite/Whitlockite	2.1	1.3
Olivine	1.4	0.47
Olivine/Pyroxene	0.40	0.17
Pyroxene	0.4	0.17
Metal/Sulfide	0.05	0.03
Plagioclase	13	11

possible to quantify the thermoluminescence process (e.g. Garlick, 1949) and the ideas in them remain the basis of modern descriptions.

There are two widespread uses of thermoluminescence that exploit the radiation dosimetry properties of insulating solids like natural minerals. These are pottery or sediment dating, in which the build-up of dose is a measure of the time since some resetting event, such as exposure to sunlight and burial (in the case of quaternary sediments) or firing (in the case of pottery dating). Luminescence dating now occupies a preeminent place in quaternary sediment dating and pottery dating and studies on human evolution and migration. The principles of the methods are the same. The radiation dose equivalent to the TL signal is determined in the laboratory by appropriate calibration experiments and this dose (termed equivalent dose) is divided by the experimentally measured dose rate at the burial site to arrive at an age (Aitken, 1985).[1] Laser stimulated emission is used to measure the TL signal in the case of quaternary dating while heating the sample is used in the case of pottery dating. Second, it is equally commonplace for thermoluminescence to be used for radiation dosimetry, where a highly sensitive crystal is placed in a badge worn by personnel working with radiation and the signal built up is a measure of dose absorbed by the worker.

As with many current avenues of meteorite research, luminescence studies picked up in the 1960 due to the tremendous impetus from the Apollo program. Much of this work was prompted by the possibility that luminescence might be behind the Transient Lunar Phenomena observed in certain craters (Nash and Greer, 1970; Garlick et al., 1972), but mineralogical and physical studies were also reported (e.g. Garlick and Robinson, 1971; Dalrymple and Doell, 1970; Geake et al., 1972; Hoyt et al., 1972). The present contribution describes luminescence studies of extraterrestrial materials from about the time of the Apollo missions to the present. We will describe studies based on the natural ("as received") thermoluminescence followed by thermoluminescence induced based on laboratory irradiation. Next we discuss the major cathodoluminescence properties of extraterrestrial materials. Finally, we also present some recent work on small particles, micrometeorites and 10 μm samples of the matrix of a particularly primitive meteorite. Measurements on such small materials represent a new research frontier for luminescence studies of cosmic samples. However, first we will briefly outline the basic theory as this is necessary to understand the interpretations and concepts – which are sometimes quite subtle – that have appeared in the literature.

[1] The units of absorbed radiation dose normally used in the meteorite literature are krad, however this is not an SI unit and some authors prefer to use the Gray (Gy). We use krad here, since the conversion is trivial (10 Gy = 1 krad).

2. Some theoretical and experimental background

2.1. The TL mechanism: the nature of the glow curve

Since TL is the light produced by heating, the raw data of a TL measurement are plots of light intensity emitted versus the temperature to which it has been heated. This plot is referred to as the "glow curve". The mechanism responsible for this curve is described, along with the mechanism for the closely related phenomenon of cathodoluminescence, in Fig. 2.

An insulating crystalline mineral is thought of as a band of energy states in which electrons are associated with individual atoms, the Valence Band (VB), and a band of higher energy states in which electrons are mobile, associated with the crystalline network but not associated with individual atoms, the Conduction Band (CB). Conductors have their CB populated with electrons; insulators do not. Semi-conductors (like most silicates) can have their CB populated under special circumstances. Ionizing radiation separates an electron from an atom and provides sufficient energy to promote it to the CB where it enables current flow. This is the basis of semiconductor detectors like Ge(Li) and Si(Li) which are used in X-ray and γ-ray spectroscopy.

Within the crystal lattice there are localized defect sites at which an electron might reside with lower energy than the CB, typically ~1–2 eV below the CB. These are the electron "traps". Although the average thermal energy of an electron even at 500 °C is low ~0.066 eV, an ensemble of electrons has a Maxwellian distribution and this implies that the some of the trapped electrons have energies at the higher edge of distribution with energies exceeding ~1–1.5 eV. These electrons are energetic enough to escape the trap and on their escape the lattice vibrations reestablish the equilibrium quickly for the next electron to be released. Given the complexity of the crystal lattices and variety of intrinsic and impurity defects, there are usually many kinds of trap in a given solid, especially geological materials not made in the highly controlled conditions of the laboratory. All else being equal, deeper traps require higher temperatures to empty them. The traps can have various energy depths beneath the conduction bands which imply variable time scales on which they are able to retain charges in them from seconds to Ma at ambient temperature. The physical nature of the traps is usually an impurity center, such as a transition metal replacing Ca^{2+} in the feldspar lattice, or an intrinsic defect, such as a displaced lattice ion. Once released from the traps the electrons can become re-trapped by the same traps or, more likely, by shallower traps, or find their way to a recombination center via a variety of pathways where it can radiatively recombine to give light, whose characteristics are determined by the electronic characteristics of the site where the recombination occurs. Typically, luminescence centers are transition metals, where transitions from one d orbital to another produce photons in the visible range. Rare earth ions can also give rise to luminescence centers, where f–f transitions are responsible for the luminescence. The spectroscopy of transition metals and the splitting of the d- and f-orbitals by the crystal field environment are described in many textbooks and summarized in the form of Orgel Diagrams (e.g. Cotton and Wilkinson, 1968; Burns, 2005).

2.2. Measurements of natural versus induced thermoluminescence of meteorites

Two very different types of measurement can be made using the thermoluminescence of natural materials. These are the measurements of natural and induced TL, and these yield different types of information about the materials under study (Sears and Hasan, 1986).

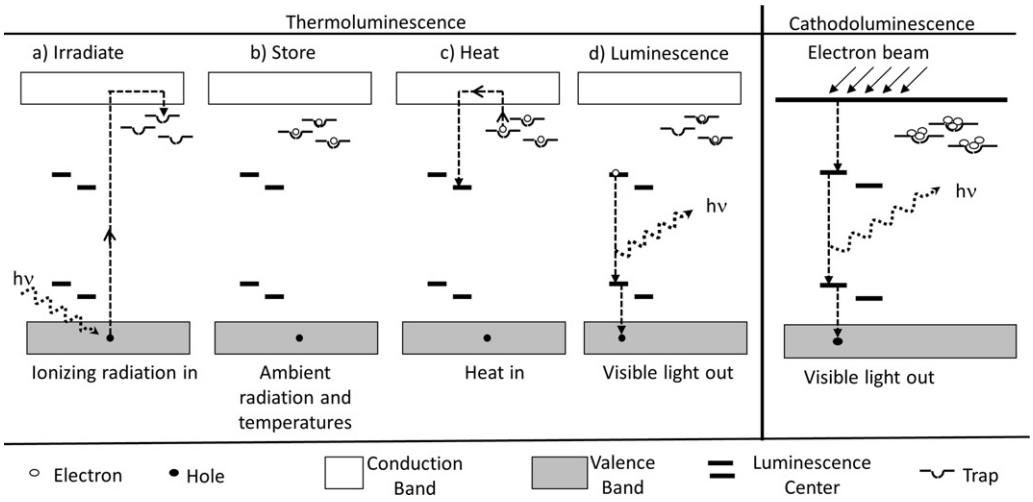

Fig. 2. Energy level diagrams for the thermoluminescence and cathodoluminescence mechanisms. Ionizing radiation separates an electron from an atom and provides sufficient energy to promote it to the Conduction Band (CB). Within the crystal lattice there are traps below the CB with a Gaussian distribution about a mean of ~1 eV. Once released from the traps the electrons can find their way to the ground state (the Valence Band, VB) via a luminescence center to produce TL. In the case of CL, the CB is saturated with electrons that fall directly into the luminescence centers.

Measuring the natural TL, the TL of an "as-received" sample, informs on the extent of stored charges in the traps and thereby the absorbed dose and ambient temperature. The intensity (photon counts/s) of the TL signal depends on the availability of traps and luminescence centers, their saturation limit, and these are mineral dependent. The TL intensity can be converted to radiation dose, by irradiating the material with a known beta or gamma dose (normally beta for easier shielding options) and using this intensity for calibration. The most common applications of TL, radiation dosimetry, pottery dating, and dating of sediments, apply this strategy, although there are a great many variations in detail that arise largely due to changes in luminescence response to dose each time the sample is given a thermal or optical treatment (Aitken, 1985, 1999; McKeever and Yukihara, 2011; Boetter-Jensen, 1997). Alternatively, the natural TL signal can be normalized by dividing the TL observed at low glow curve temperatures, which is more sensitive to thermal and radiation history, by the TL observed at high glow curve temperatures which is less sensitive to thermal and radiation histories. Thus it is sometime helpful to determine the peak height ratio, LT/HT, where LT and HT refer to the intensity of the two major TL peaks in the natural TL glow curve. If the peaks are not well resolved, then very similar information is obtained by dividing the TL signal at 250 °C by the TL signal at 400 °C in the glow curve. Theoretically it is preferable to take LT and HT at fixed temperatures (say, 250 °C and 400 °C) because the physics of the process depend on temperature. However, because of the sharpness of the LT peak small errors in temperature result in large errors in TL intensity. In practice, measuring TL intensity at the top of the peak is preferable. In addition, peak positions depend on intensity, since the peak shifts to higher temperatures as it decreases in intensity (e.g. Garlick, 1949). Thus again it is preferable to measure intensity at the top of the peak.

The laboratory induced TL, referred to as the "induced TL", provides information on the number and type of traps and therefore provides insights into the mineralogy and crystallography of the phases responsible for the TL signal. This in turn provides important information on the degree of metamorphism and post-metamorphic cooling histories. A large number of meteorite classes and lunar materials have been investigated this way. Because of the difficulty of absolute calibration of TL apparatus, normalization of the induced TL level is normally done by dividing the signal by the signal produced by a standard meteorite usually the Dhajala, an H3 chondrite, which lies in the middle of the observed range on a logarithmic scale. The Dhajala-normalized induced TL signal is referred to as the normalized "TL sensitivity". Occasionally the Kernouve H5 chondrite has also been used for normalization, where Kernouve has a TL sensitivity of 22 on a Dhajala-normalized scale (e.g., Sears et al., 1980).

2.3. The shape of the glow curve and its information content

The TL process can be quantified as follows (after, e.g., Garlick, 1949). Thermal excitation out of the traps is described by an Arrhenius equation

$$p = s\exp\left(\frac{-E}{kT}\right) \tag{1}$$

where p is the probability of an electron escaping the traps, s is a constant with dimensions of frequency (the "frequency-factor"), E is the depth of the trap below the conduction band (in units of eV), k is Boltzmann's Constant, and T is absolute temperature (K). If n is the number of electrons in the trap being emptied, then the intensity of light emitted at time t is given by

$$I = \frac{-\mathrm{d}n}{\mathrm{d}t} = ns\exp\left(\frac{-E}{kT}\right) \tag{2}$$

To determine the TL produced as a function of temperature as the sample is heated, we may rearrange (2):

$$I = \frac{-\mathrm{d}n}{n} = s\exp\left(\frac{-E}{kT}\right)\mathrm{d}t \tag{3}$$

and set $\mathrm{d}T = \beta\mathrm{d}t$ where β is the heating rate in degrees/second which is assumed to be a constant. Then we can integrate (3) to give:

$$\log\left(\frac{n}{n_o}\right) = -\int \frac{s}{\beta\exp(-E/kT)}\mathrm{d}t \tag{4}$$

where the limits of integration are from T_0 to T. This can be written:

$$n = n_o\exp\left\{-\int \frac{s}{\beta\exp(-E/kT)}\mathrm{d}t\right\} \tag{5}$$

so that the light emitted as a function of temperature is given by

$$I = n_o s\exp\left(\frac{-E}{kT}\right)\exp\left\{-\int \frac{s}{\beta\exp(-E/kT)}\mathrm{d}t\right\} \tag{6}$$

with the limits of integration are from 0 to *T*. The theoretical shape of glow curves of various values of *s* and *E* are shown in Fig. S4.

As most solids contain numerous trapping sites, in general their glow curves are the sum of individual peaks, each of which is described by Eq. (6). An analysis of meteorite glow curves was performed by McKeever (1980) in which numerous curves described by Eq. (6) were fitted to the glow curve using a least squares fit. A typical set of results is shown in Fig. S5. Most of these peaks are expected to be due to different trapping sites within the feldspar responsible for the major TL emission. A more recent study of the glow curve peaks present in the high-temperature region of the curve was reported by Akridge et al. (2001). These authors found they could explain the glow curve with six peaks in the temperature region above ~300 °C and they reported *E* and *s* values for each of them. Such data for more stable, higher temperature glow peak corresponding to deeper traps, expand the range of applications to larger time spans, but such possibilities are yet to be explored.

While the TL glow curve can be described in terms of *E* and *s* values, a rigorous analysis would be required for complete identification of all of the individual peaks. However, the variety of TL characteristics observed for meteorites are so large that a rigorous glow curve analysis for each is not possible. A simpler approach is to use bulk parameters that amount to summarizing these detailed variations in individual peaks. Fig. S6 shows a glow curve for the Allan Hills A77011 ordinary chondrite in which the three parameters commonly used, the height of the peak at maximum intensity, the temperature of the peak at maximum intensity, and the full-width-half-maximum of the peak, are shown. The second and third parameters are referred to as the "peak shape parameters", or simply "peak temperature" and "peak width".

2.4. The cathodoluminescence mechanism

Cathodoluminescence arises when traps and the CB receive such a stream of energetic electrons that cascade down the luminescence centers without the need for heating. While the process cannot be quantified in the manner of TL and the glow curve, the method can be used with petrographic polished sections so CL petrography is possible. In fact, if the CL stage is attached to an electron microprobe, detailed comparison can be made of the CL and composition of minerals and the technique is especially valuable in locating compositional profiles (Steele, 1986, 1989b, 1998).

2.5. The minerals responsible for TL and CL

Early work described the essential luminescence properties of feldspars and the role of various impurities on CL color and spectra (Derham and Geake, 1964; Derham et al., 1964; Geake and Walker, 1966a,b, 1967; Benoit et al., 2001). In ordinary chondrites, the CL emission, like the TL, is in the blue green region of the spectrum, and has commonly been associated with Mn^{2+} impurity ions in the plagioclase. In more Ca-rich feldspars, the CL, and presumably TL emissions, are in the yellow region, suggesting a different crystal field for the Mn^{2+}. Traces of Fe^{2+} substituting for Ca^{2+} in the lattice reduces the CL and TL of the mineral to insignificant levels. Thus Fe^{2+} is usually referred to as a "quencher" of luminescence. The mechanism involves providing a more efficient electron pathway to the ground state that does not produce emission in the visible range.

While abundant in ordinary chondrites, olivine and pyroxene do not produce measurable CL or TL because of quenching by Fe^{2+}. However, the forsterites (Mg_2SiO_4, Fo) and enstatites ($MgSiO_3$, En) that are found in unequilibrated ordinary chondrites, where fayalite (Fe_2SiO_4, Fa) and ferroslilite ($FeSiO_3$, Fs) are below about 1 mol%, do produce measurable CL and TL. Forsterite is also an important phosphor (producer of luminescence) in CI and CM chondrites and enstatite is a luminescing phase in enstatite chondrites (Reid and Cohen, 1967; Grögler and Leiner, 1968; Keil, 1968; Leitch and Smith, 1982; McKinley et al., 1984; Marshall, 1988; Steele, 1989b; Dehart and Lofgren, 1994, 1995; Weisberg et al., 1994). Forsterite and enstatite can have either red or blue CL depending on minor element chemistry. Studies that elucidate trace chemistry and CL spectra are shown in Fig. S7. Synthetic forsterites doped with Mn have red CL, while those doped with Ti have blue CL. Weisberg et al. (1994) used CL to identify and study textural relationships of trace element (Mn, Cr)-bearing enstatite, Fe-rich enstatite and near-pure enstatite in E3 chondrites, which showed red CL, no CL and blue CL, respectively. There is an interesting transition from red to blue CL throughout the EH chondrites, and red to magenta throughout the EL chondrites, as the meteorites undergoe increasing metamorphism, solid state recrystallization and homogenization due to subsolidus heating. Zhang et al. (1996a) suggest that this difference in CL properties of EH and EL chondrites is thermal history which affects crystal structure. It is important to keep in mind that crystal structure as well as composition can affect luminescence and other optical properties of minerals.

Other phases for which there are CL (and limited TL) observations reported in the literature are most of the refractory phases associated with calcium–aluminum-rich inclusions (CAIs) commonly found in CV chondrites and in minor amounts in other classes (Grossman, 1980).

2.6. Instrumentation and procedures for TL and CL

The essential elements of the equipment to record CL and TL data are shown in Fig. S8. Both are very simple in principle. For TL, a control unit provides precise linear heating of the sample, with feedback from a thermocouple attached to the underside of the heating strip, and a photomultiplier tube specially designed for TL application (high sensitivity, high gain, quartz window) detects the light and passes it through a preamplifier and a digitizer to a computer (Mills et al., 1977; Boetter-Jensen, 1997). Critical aspects in the design of the apparatus are color glass or interference filters to remove the black-body radiation and increase the effective temperature range of the measurement, and a geometry that maximizes the signal from the sample while minimizing background from the heating strip.

Measurements are made in an inert nitrogen atmosphere (with oxygen and water content at <10 ppm level), at about 1 bar. Oxygen causes chemiluminescence and a vacuum inhibits heat transfer from the strip to the sample. Samples are handled in red light, since fluorescent laboratory lights with high energy blue and UV emission can drain the TL of some samples. Ideally, a monolayer of silicates from the meteorite (cleaned with dilute HCl and its magnetic fraction separated) are placed on a copper cup or stainless steel discs in the apparatus. These typically contain 2–4 mg of sample in the form of grains of ~200 μm diameter that freely flow like sand and do not clump (like flour) when poured. After recording the natural luminescence of ("as is"), the samples are irradiated in a gamma cell or on the heater plate itself and a known β or γ dose is imparted and the induced TL is recorded after taking the sample through a preheat cycle to remove thermally unstable signal. This may be repeated several times for replicate measurement or with incremental doses. The radiation sources commonly used are ^{60}Co γ-radiation or ^{90}Sr β-radiation, the latter is safer to handle but since β particles have a smaller penetration depth, the net dose delivered becomes dependent on the thickness of the samples and calls for care while irradiating with sample powder on cups. For sample powders on a stainless steel SS disc fixed with silicone oil, there is an inherent assurance that the sample does not get disbursed and its thickness remains unchangeable. The laboratory irradiation especially populates the very shallow traps. In fact, some of these

shallow traps are so shallow that they decay during the time interval between irradiation and TL measurement, so the time between irradiation and measurement is standardized or samples are "preheated" to ~50 °C to empty the shallow traps. Standard phosphors (e.g., the Dhajala meteorite) are recorded at beginning and end of each day and between samples of different meteorites. Samples are typically run in triplicate and a black-body curve obtained for each sample; this is obtained by reheating the sample after its TL has been recorded. Multiple heating of a sample does reduce the sensitivity of induced TL by about 20% on the first run but then no further sensitivity change takes place (Sears and McKeever, 1980).

The CL apparatus is conceptually even simpler, whether attached to a bench top optical microscope (Marshall, 1988) or an electron microscope such as an SEM or electron microprobe (Reed, 2005). In the bench top, low-powered, CL microscopes, a polished thick section is placed on a slide in a vacuum stage attached to a microscope. The stage is evacuated and a cold cathode electron gun attached to the stage provides the electron beam. The beam is defocussed and forms an ellipse a centimeter long and half a centimeter wide. In this case, coating to avoid charge build-up can be avoided, and multiple images can be obtained as the sample is moved systematically under the beam. The gas pressure is critical to success, since a high vacuum prevents an ionized pathway for the electron beam and a weak vacuum prevents electrons from leaving the cathode. Typically, the optimum vacuum is ~10 mTorr with a beam current of ~7 μA and accelerating voltage of ~14 keV.

Cathodoluminescence detectors are now routinely attached to the electron microprobe and electron microscopes. This is an excellent technique for observing zoning and compositional variations in minerals that may not be easily visible by optical microscope or standard backscatter electron imaging. This also allows CL studies at finer scales. In these instruments the beam is focused, rastered, or defocussed to form a circle 50–100 μm wide and a light coating is necessary to prevent charge build-up. The main difference between the two types of CL instruments, other than magnification, is that higher accelerating voltages and smaller currents are used in the analytical instruments, so comparisons should be made with caution. Bench top CL and CL apparatus attached to analytical instruments provide very different information. Bench top CL apparatus usually involves low-powered microscopy and irradiates the entire thin section, say 1 cm across, with electrons of ~15 eV. On the other hand, electron microscopes are usually used in spot mode, or rastered over a field of view a few hundred μm, often in conjunction with a chemical analysis. Thus the low-powered microscope provides an opportunity for large scale petrography while the high powered instruments enable complementary micrometer scale profiling and compositional studies.

3. Studies of natural thermoluminescence of meteorites

Natural thermoluminescence data that are available in the literature have been collected together for this article and appear in Table S1 with the relevant metadata in Table 2.

3.1. The process

3.1.1. A quantitative description of the process

The equilibrium level of natural TL can be calculated using simple kinetic concepts. The rate at which electrons are promoted to traps can be described by a second order rate equation such as:

$$\frac{dn}{dt} = \alpha R(N - n) \tag{7}$$

where n is the number of trapped electrons, N is the number of traps, and R is the dose rate, t is time, and α is a rate constant. Similarly,

Table 2
Metadata for supplemental table on natural TL data for meteorites.

Filename	Natural TL data
Number of meteorites:	1381
Field 1:	
Abbreviation	Name
A	Asuka
ALH	Allan Hills
BOW	Bowden Neve
DOM	Dominion Range
EET	Elephant Moraine
GRA	Graves Nunataks
GRO	Grosvenor Mountains
HaH	Hammada al Hamra
LEW	Lewis Cliff
MAC	MacAlpine Hills
MET	Meteorite Hills
WSG	Mount Wisting
OTT	Outpost Nunatak
PCA	Pescora Escarpment
QUE	Queen Alexandra Range
RKP	Reckling Peak
TIL	Thiel Mountain
WIS	Wisconsin Range
Y	Yamato
Field 2:	Class and type
Field 3:	Natural TL (krads)
Field 4:	Standard deviation for natural TL

the rate at which electrons leave the traps can be described by a first order equation:

$$\frac{dn}{dt} = -\varepsilon(T)n \tag{8}$$

where $\varepsilon(T)$ is the rate constant for this process for a given temperature and since the rate is determined by the size of an energy barrier, the trap depth, we can again write Eq. (1):

$$\varepsilon(T) = s\exp\left(\frac{-E}{kT}\right) \tag{9}$$

and thus:

$$\frac{dn}{dt} = -n\,s\exp\left(\frac{E}{kt}\right) \tag{10}$$

Since at equilibrium the rate of promotion to traps and the rate of decay from traps must be equal, we can set (7) equal to (10) and rearrange to get:

$$\phi = \frac{\phi_s}{\{1 + [s/\alpha R\exp(-E/kt)]\}} \tag{11}$$

where ϕ (Gy, absorbed dose, which is proportional to n) is the level of natural TL, ϕ_s (Gy) is the value of TL at saturation (which is proportional to N), dimensionless parameter s is the Arrhenius factor, α is the reciprocal of the mean dose (the dose to fill 1/e of the traps, Gy^{-1}), R is the dose rate (Gy/s), E is the trap depth (eV), k is Boltzmann's constant (eV/K) and T (K) is temperature. A considerable amount can be learned from examining Eq. (11) and most of the natural TL studies of extraterrestrial materials can be quantitatively understood applying the equation or its derivatives.

Eq. (11) suggests that two types of factors control natural TL levels in meteorites, viz., (1) those that describe the solid state properties of the luminescing phase (s, α, and E), and (2) those that describe the meteorite environment both pre and post capture on the Earth (R, and T). The thermoluminescence properties of the solid can be determined by the laboratory methods described in Garlick's (1949) book applied to meteorites and in a great number of research papers (e.g. Correcher et al., 2007). The value of natural TL measurements of extraterrestrial materials lies in the insights

they provide into dose rate and temperature and the lessons that can be learned from these insights.

3.1.2. Properties of the solid, s, α, and E

Probably the most straightforward way of determining the number of glow peaks present in a glow curve and for determining E and s, is to write a simplified form of Eq. (6) for low temperatures. Then

$$I = n_o s \exp\left(\frac{-E}{kT}\right) \quad (12)$$

where I is the intensity of the luminescence and the other terms are as defined previously. Thus a plot of $\log I$ versus $1/T$ for the onset of a peak produces a line whose slope is $-E/k$ and intercept is s. This is known as the "initial rise" method. If the TL is read out by a number of successive heating events such that in each cycle, the sample is taken incrementally to higher temperatures (stopping temperature increased incrementally), then a plot of E versus stopping temperature inform on the spectrum of traps. A recent application to meteorites is that of Correcher et al. (2007) who found that the natural TL glow curve of the Villalbeto de la Pena L6 chondrite has four peaks with trap depths (and glow curve temperatures) of 1.2 eV (270 °C), 1.4 eV (290–300 °C), 1.6 eV (350–370 °C) and 1.7 eV (390–430 °C). These values are input parameters for numerical modeling the glow curves, as in Fig. S6, and these are used to further refine values for E and s. Results from McKeever's (1980) study are listed in Table S2. The rate constant α can be determined by administering radiation doses in the laboratory and producing a plot of TL against dose absorbed (e.g., Sears and Mills, 1974).

3.1.3. Properties of the environment, R, and T

The radiation doses received by a meteorite consist of those due to internal radioactivities and those due to cosmic ray bombardment. Melcher (1981b) suggested that the cosmic ray dose rate was 10 mrad/year. Biswas et al. (2011) estimated that the cosmic ray dose rate effective for luminescence for meteorites of preatmospheric size range 10–50 cm is 41–85 krad/year. Assuming chondritic abundances of ^{238}U, ^{232}Th, ^{40}K and ^{87}Rb are 13 ppb, 40 ppb, 840 ppm and 2 ppm respectively (Mason, 1971), the dose rate due to internal radioactivity was calculated to be 0.001 mrad/year by Biswas et al. (2011). Thus cosmic ray dose rates are almost 10^4 times the dose rates due to internal radioactivity. Thus the meteorite formation ages are $\sim 10^3$ times cosmic ray exposure ages (the time the body fragmented and attained dimensions on the order of meters are required for cosmic radiation to register in them), and total doses from both sources for most meteorites should be comparable within an order of magnitude. This is further discussed in Section 3.5.

Theoretical calculations (e.g. Benoit and Sears, 1993b; Biswas et al., 2011) and experiments in which large meteorites or large meteorite mock-ups are irradiated with energetic radiation (Lalou et al., 1970), suggest that the variation in natural TL through meteorites of a large range of sizes is less than ~30% (Fig. 3). This is borne out by measurements along cores and bars cut from large meteorites (Sears, 1975a; Vaz, 1971; Lalou et al., 1970; Singhvi et al., 1982) and by measurements on a large (60 cm × 50 cm) slab of the Estacado chondrite (Sears, 1975a). Contrary to the conclusions of Barton et al. (1982), ^{26}Al shows similar variations across the slab as natural TL, about 60 dpm/kg in the center, where the natural TL was ~1300 (arbitrary units), and about 50 dpm/kg around the periphery, where the natural TL was ~1100 (arbitrary units) (Fig. 3). The depth profile of natural TL and ^{26}Al were also similar, both reflecting the preatmospheric shape of the meteorite. It can reasonably be concluded that dose rate variations throughout the meteorite causes relatively minor differences in equilibrium level because, as with low-energy cosmogenic isotopes such as

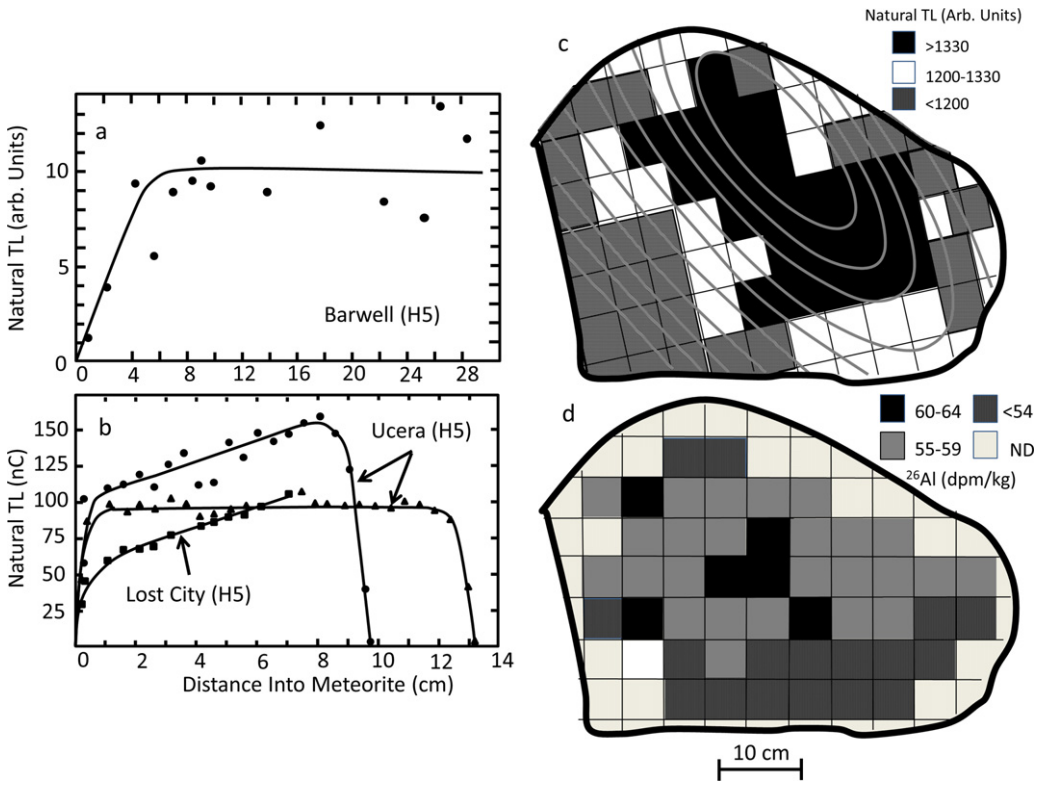

Fig. 3. Theoretical and observed profiles in natural TL through meteorites. Top left, theoretical profiles calculated by Benoit et al. (1993c). Top right, natural TL profiles along bars from the Ucera chondrite (Vaz and Sears, 1977). Bottom figures, a slab of the Estacado chondrite on which both natural TL and ^{26}Al measurements have been made. Both measurements indicate an increase along a central diagonal with values falling off to either side. This reflects the preatmospheric contours of the object.
Data from Sears (1975a,b) and Barton et al. (1982).

^{26}Al, attenuation of the primary radiations is balanced by the build-up of secondary radiations.

It is worth pointing out that the heating of the meteorite as it passes through the atmosphere can be detected as a sudden drop in TL over the outer few millimeters of the TL profiles (see Fig. 3). The temperature gradient in a meteorite during atmospheric passage is determined by the ablation rate, which is given by:

$$v_w = \left(\frac{k}{y}\right) \ln\left(\frac{T}{T_i}\right) \quad (13)$$

where k is thermal diffusivity, T_i is temperature at the surface, and T is temperature at depth y (Sears and Mills, 1973). Then the thermal gradient can be calculated from:

$$\frac{dT}{dy} = v_w T_i k^{-1} \exp(y v_w k^{-1}) \quad (14)$$

and depends on the orientation of the meteorite's local surface during flight. Beyond a few millimeters, the profile is no longer governed by ablation but follows the normal path determined by conductivity.

Sears (1975b) performed laboratory heating experiments to obtain a calibration curve for this process and thereby obtained experimental temperature profiles for comparison with the theory. On the basis of this work, a standard requirement for meteorite samples obtained for natural TL work is that the samples be taken at least 6 mm from any potential fusion crust. Herschel (1899) pointed out that the display of bright TL by the Middlesbrough meteorite demonstrated that the interior had not been significantly heated during atmospheric passage. This has also been discussed by Bhandari et al. (1980), Singhvi et al. (1982), Bhandari (1985) and Wagner (1985).

In fact, Eq. (13) predicts that for an oriented meteorite the penetration of heat into a meteorite depends on the orientation of the face, frontal faces suffer greatest ablation, rear faces suffer least, and lateral faces suffer intermediate ablation. Thus heat penetration increases in going from frontal to lateral to rear faces (Sears and Mills, 1973; Sears, 1975a; Singhvi et al., 1982).

The other environmental factor for determining natural TL intensity is the ambient temperature during the orbit and after fall. The temperature of a meteorite in orbit can be calculated by the inverse square law and Stefan's law, and is given by:

$$T = 279\left(\frac{\theta}{d^2}\right)^{1/4} \quad (15)$$

where θ = the ratio of the absorbed radiation to that of the emitted radiation and d is the distance to the Sun. Melcher (1981b) used this effectively to show that some meteorites had smaller perihelion distances, as discussed in Section 3.3.

3.1.4. Natural thermoluminescence: peak height ratio and equivalent dose

For most applications of natural TL to typical meteorite studies, it is the signal at low glow curve temperatures (~250 °C) that is interesting. As discussed in Section 2.3, there are two ways to handle the data to remove unwanted effects. We can calculate LT/HT or we can divide the natural TL by the TL induced by a dose administered in the laboratory. The first is more precise, but the second has the advantage of yielding absolute units with the proviso that there is no sensitivity change due to heating associated with the recording natural TL. In natural TL studies of meteorites both parameters for several hundred meteorites were measured and a regression line plotted to provide a conversion relationship (Hasan et al., 1989). Thus LT/HT is measured, with high-precision, and converted to the reported natural TL (NTL), with its absolute units, using the equation:

$$\log(\mathrm{NTL}) = \frac{[\log(\mathrm{LT/HT}) + 0.844]}{0.775} \quad (16)$$

The term NTL is used to distinguish the measurements obtained this way from the equivalent dose.

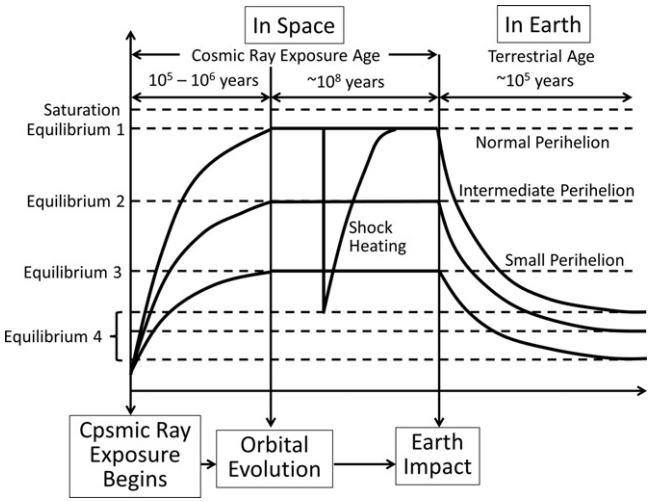

Fig. 4. Schematic diagram showing the history of natural thermoluminescence levels in a meteorite as it passed through a typical history of formation by break-up of a larger object, exposure to cosmic rays and adjustment to an equilibrium value depending on orbit – this may be interrupted by stochastic evens such as impact shock – and adjustment to a lower value after fall on Earth (Benoit et al., 1993c).

3.1.5. Natural thermoluminescence and the expected history of meteorites

Fig. 4 is a schematic diagram showing the manner in which the natural TL varies throughout the history of a typical meteorite (Benoit et al., 1991). When deeply buried inside the parent body, the TL level is expected to be low because the only source of radiation is internal radioactivity. While dose rates are low, the duration of irradiation is long. Offset against this, over long time spans, internal heating becomes significant and the TL is drained. The net TL in the parent body can therefore be considered as low. Once the parent body breaks up, the fragments are small enough to be exposed to cosmic radiation, solar energetic particles near the surface, and galactic cosmic radiation throughout (Eugster et al., 2006). In about 10^5–10^6 years equilibrium is reached, the final TL level depending on perihelion. For the bulk of the duration of exposure to cosmic radiation (~10^8 years), natural TL levels in meteorites stay close to equilibrium, being interrupted occasionally by stochastic events such as heating during impact. The meteorite then undergoes orbital evolution through a variety of possible mechanisms, impact, resonant interaction with Jupiter, and thermal radiation processes (Nesvorný et al., 2002), until it encounters Earth's gravity well and falls to its surface. Once on Earth, the natural TL decays to its new equilibrium value that will be lower because of higher temperatures (~300 K) and low cosmic ray and environmental dose rates on Earth. During this adjustment to the new equilibrium values, it is in principle possible to use natural TL as a measure of terrestrial age since the lower the TL level, the higher is the terrestrial age.

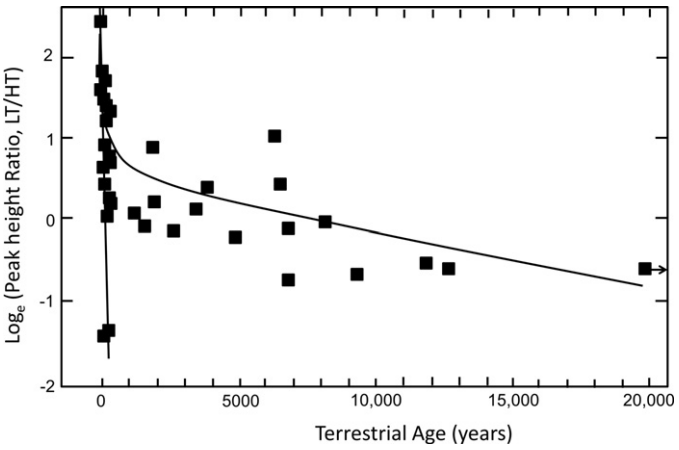

Fig. 5. Natural thermoluminescence against terrestrial age determined from ^{14}C measurements using accelerator mass spectrometry (Sears and Durrani, 1980). Most meteorites plot on or near the curve indicated, but a few have natural TL too low for a large terrestrial age and are assumed to be meteorites that have been heated by close solar passage.

3.2. Measurements of natural TL and the terrestrial age of meteorites

3.2.1. Terrestrial age dating using natural decay

The terrestrial age can be determined by measuring the present level of natural TL in a sample and calculating the time required to decay from an assumed extraterrestrial natural TL value to the present level. The required kinetic parameters for such a computation can be measured in the laboratory. The assumed natural TL value at the time of fall is determined by averaging the values for a number of recent observed falls. The major unknown is the storage temperature at which the decay occurred. This has to be estimated from the known history of the sample. We then have:

$$\frac{dI}{dt} = -s\,I_0 \exp\left(\frac{-E}{kt}\right) \tag{17}$$

The actual treatment is complicated by the existence of several peaks with different E and s parameters.

Several authors pointed out that the natural TL of ordinary chondrites decreases with increasing terrestrial age. Sears and Mills (1974) and Melcher (1981a) studied large numbers of ordinary chondrite observed falls and found this expected decrease. A comparison of terrestrial ages obtained from natural TL and radiocarbon dating for meteorites from the US Prairie States obtained by Boeckl (1972), who used beta counting, showed poor agreement between the two techniques. However, this changed dramatically when the old radiocarbon ages were replaced with ages determined by accelerator mass spectrometry (Fig. 5; Jull et al., 1980; Sears and Durrani, 1980; see also Benoit et al., 1993a). The better radiocarbon data showed that for most meteorites the level of natural TL was a reflection of terrestrial age. Benoit et al. (1993b) summarized the data for meteorites from a variety of find sites, hot deserts (Otto, 1992; Bevan and Binns, 1989), prairies (Sipiera et al., 1987), and Antarctica (Cassidy et al., 1977, 1992; Cassidy, 2003), and showed that decay followed the expected theoretical curves if mean summer temperatures were assumed for the various sites (Fig. 6). The mean effective temperatures inferred were 30 °C, 20 °C and 0 °C for hot deserts, prairies, and Antarctica, respectively corresponding to approximate age spans for which the technique is applicable of 10^3 years, 10^4 years, and 10^6 years, respectively. Interestingly, a few percent of the meteorites at every site had natural TL values too low to be explained by terrestrial age. We return to this in the next section.

In the case of Antarctic meteorites there is the complication that there is an additional phase of their history in which they are buried in the ice where they are protected from cosmic rays and solar insolation, so that the terrestrial age determined in this case is probably the duration of exposure on the surface (Sen Gupta et al., 1997a,b). This complication aside, typical terrestrial ages are 10^4 years for hot deserts, 10^5 years for Prairies and other open grasslands, and 10^6 years for Antarctic meteorites.

3.2.2. Terrestrial age dating using the fusion crust method

The fusion crust of a meteorite is the surface produced by melting during the heating of atmospheric passage. As mentioned above, heat penetration in meteorites during passage through the atmosphere was studied by Sears and Mills (1973) and its effect on natural TL was examined by Sears (1975a,b). The frontal face has greater ablation and steeper thermal gradients than rear faces, and thus heat penetration is less at the front than at the rear. However, many meteorites tumble during flight and this effect is averaged out. Temperatures of ~250 °C are experienced by the meteorite within a few millimeters of the surface. Thus immediately beneath the fusion crust there is a zone that has been heated sufficiently to drain the natural TL but to not melt it. Thus instead of using the decay of the natural TL as the meteorites adjust from the high radiation, low-temperature environment of space to their low radiation, high-temperature conditions on Earth, it is also possible to measure the terrestrial build-up in natural TL of the drained zoned just below the crust (Miono et al., 1990; Miono and Nakanishi, 1994; Sen Gupta et al., 1997a,b; Akridge et al., 2000).

A total of 50 meteorites have been examined in this way, and all four papers report similar results. There is reasonable measure of agreement between the terrestrial ages determined from the TL-fusion crust method and terrestrial age determined from radioisotopes ^{14}C and ^{36}Cl for ages up to about 200 ka when the TL saturates. An occasional instance of the ^{36}Cl ages being a factor of two or so larger than the TL-fusion crust age was attributed to either periods of burial under the ice, which would lower the TL age, or to unidentified problems with the ^{36}Cl, such as unusual shielding. Minor adjustments to some of the assumed TL parameters might also resolve these issues. Recent developments in imaging luminescence systems might improve the TL estimates of terrestrial ages since it could enable better separation of the TL signal from just under the fusion crust and the TL signal from interior grains that always contaminate samples removed from the meteorite physically.

3.3. Measurements of natural TL and meteorite orbits

3.3.1. Meteorites with normal natural TL (5–100 krad)

While natural TL levels in the range 5–100 krad are primarily a reflection of terrestrial age, as with cosmogenic isotopes, meteorites enter the atmosphere with a range of values, typically 20–100 krad. Variation in the TL levels of recently fallen meteorites is primarily due to differences in orbit (Melcher, 1981b; McKeever and Sears, 1980; Benoit et al., 1991; Benoit and Sears, 1997). In fact, the distribution of natural TL levels for recent falls is very similar to the distribution of perihelia observed for near-Earth asteroids with the majority having perihelia of 0.8–1.0 AU (Sears et al., 2011).

3.3.2. Meteorites with low-natural TL (<5 krad)

About 5% of the meteorites, regardless of their class, have natural TL levels <5 krad (Hasan et al., 1987; Benoit et al., 1991, 1993b; Sears et al., 1991c). This value is too low to be explained by an especially long terrestrial age. Under most realistic conditions, natural TL values decay asymptotically to values much

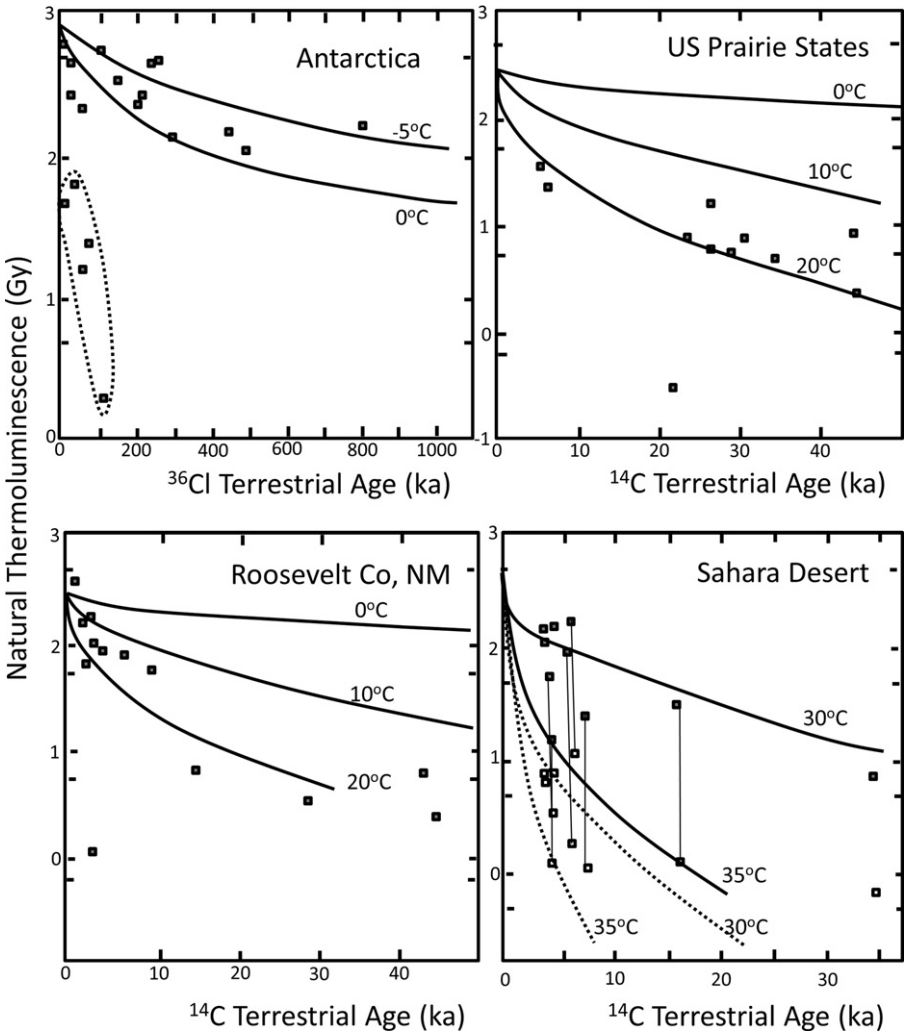

Fig. 6. Natural TL against terrestrial age determined by isotopic methods compared with theoretical predictions. (a) Meteorites from Antarctica which plot near the 0 °C and −5 °C theoretical lines except for five with lower values which are assumed to have small perihelia before encountering Earth. (b) Meteorites from the Prairie States in the US plot near the 20 °C theory line, but in this case one meteorite has unusually low-natural TL. (c) Meteorites from Roosevelt County in New Mexico also plot near the 20 °C line. (d) Meteorites from the Sahara Desert. In this case the natural TL at 300 °C in the glow curve (top of the tie lines) is also plotted, because at these temperatures the 250 °C TL decays rapidly (bottom of the tie lines).
Figure from Benoit et al. (1993c).

above 5 krad (see Fig. 6, for example). However, 5% is also the proportion of near-Earth asteroids with perihelia <0.85 AU (Sears et al., 2011), so it seems likely that these low-natural TL meteorites are meteorites whose orbits have small perihelia. This is also true of the ordinary chondrites with known orbits. However, in this case the values extend to smaller perihelia, say 0.5–0.6 AU, which would account for TL levels being low (<5 krad). Hasan et al. (1987) found that the Antarctic meteorites with natural TL <5 krad also have high values of cosmogenic ^{26}Al (>70 dpm/kg) and they suggested that while solar heating had drained the TL, irradiation with solar particles at small perihelion distances had caused the higher ^{26}Al levels (Michel et al., 1996; Nishiizumi et al., 1990).

3.3.3. *Meteorites with high natural TL (>100 krad)*

When a field party from Germany visited the Allan Hills field site in Antarctica in 1988/1989 it was after the area had previously been thoroughly searched by American teams. Initially they found little. After a 3 days storm, in which the team was trapped in their tents, they found a large number of meteorites that had weathered out of the ice (Wlotzka, 1990, 1991). The meteorites were distributed along an escarpment with larger meteorite masses at one end of the line, as if they still retained the pattern observed in strewn fields. Perhaps the pattern was retained with the help of a crevasse, the strewn field being blown into the crevasse and relative positions of the meteorites frozen.

Benoit and Sears (1993b) found that many of the meteorites recovered by the German field party had natural TL levels about a factor of two higher than the previous highest levels observed among recent falls. After considering various possibilities, they concluded that these were pieces of a single meteorite that had fragmented in the atmosphere, and that the parent meteorite had recently changed orbit. These meteorites were displaying the levels of natural TL expected for a meteorite with a perihelion of ~1.2 AU, where the relatively cooler temperatures would sustain the higher natural TL levels. Apparently, the Earth had captured this meteorite before its natural TL could adjust to the Earth-crossing orbit, say within 10^5 years. The dynamics of asteroids in the inner solar system is a matter of considerable interest, and this discovery adds a new perspective to the process (Bottke et al., 2006) and suggests that in some cases asteroid orbits can be perturbed on short timescales.

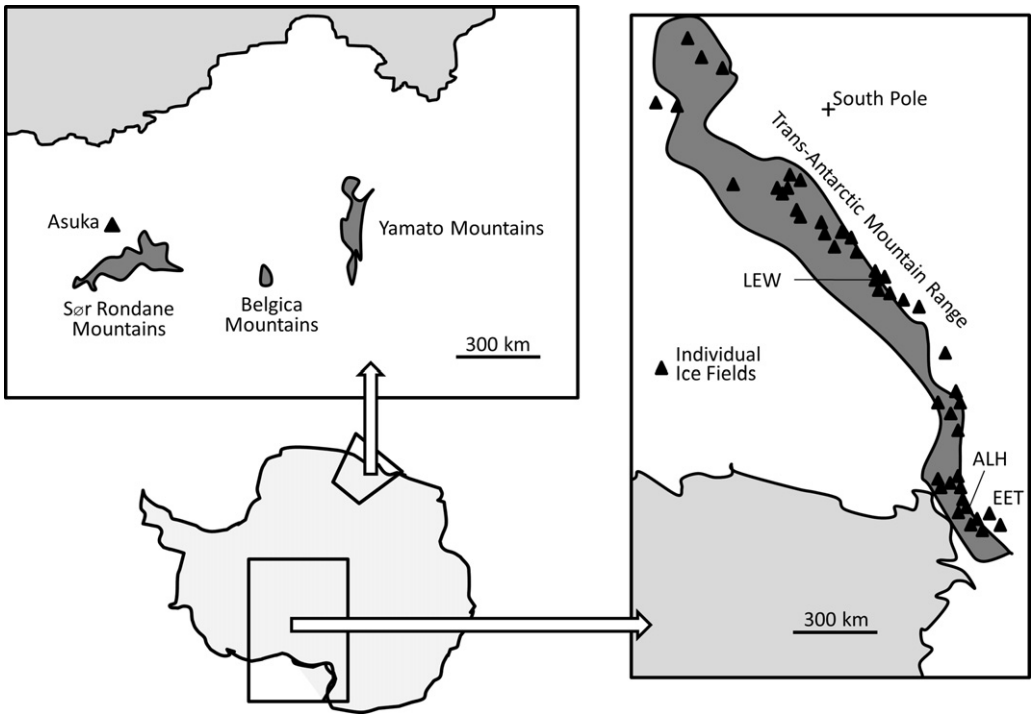

Fig. 7. Map of Antarctica showing the locations of meteorite ice fields discussed in this paper. From Yanai and Kojima (1991) and Righter et al. (2011).

3.4. The survey of natural TL of Antarctic meteorites

3.4.1. The background to the survey

Meteorites have been recovered from Antarctica in a systematic way since 1978, on the order of a few hundred to a few thousand being returned each year (Fig. 7; Cassidy et al., 1977; Cassidy, 2003). The collection is noteworthy for the primitive, lunar, and martian meteorites it has returned. Natural TL measurements have been used to survey Antarctic meteorites because of the insights they provide into orbit, terrestrial age and the mechanisms by which ice concentrates the meteorites at the find sites. Meteorites can accumulate at ice fields because they fall on the ice sheets, become buried below the surface due to later snow fall or sinking, and are then carried towards the continental margins by the pressure of ice overload at the South Polar Dome. Normally the ice escapes to the sea as icebergs. However, towards the west side of the continent is a range of mountains, the Transantarctic Mountain Range, that blocks the movement of the ice sheet and forces it upwards where it is ablated by strong winds and evaporated to produce the blue ice fields, consisting of ice that once had been at depth and, through overburden, lost its air inclusions which causes the ice to be white. Meteorites trapped in the ice sheets then accumulate on the blue ice fields. It is also possible for meteorites to fall directly onto some of these ice fields. Once exposed on the surface, meteorites can move across the ice and concentrate in crevasses and moraine edges. Similar accumulations of meteorites have also been found around the Japanese Antarctic research bases in the Queen Fabiola Mountains in Eastern Antarctica (Fig. 7). These are the Yamato and Asuka meteorites.

In the light of this scientific background and the challenge of getting the maximum scientific value from these large accumulations (Sutton and Walker, 1986), a pilot study of the natural TL of 23 samples of known ^{26}Al was organized by the Antarctic Meteorite Working group of NASA, NSF, and the Smithsonian Institution. Aluminum-26 is a cosmogenic isotope that decays at about the same rate as natural TL under Antarctic conditions (Hasan et al., 1987; Wacker, 1990). The pilot study showed that for 80% of the samples, natural TL correlated with ^{26}Al, since both decayed at a similar rate with increasing terrestrial age (Fig. 8a; Hasan et al., 1987). The remaining 20% of the samples had low-natural TL values and high ^{26}Al due to close passage to the Sun (see Section 3.3.2). As a result of this pilot study the systematic determination of natural TL of Antarctic meteorites was incorporated into their preliminary examination. The data appeared in NASA's Antarctic Meteorite Newsletter (Table 3; now on-line http://www-curator.jsc.nasa.gov/antmet/amn/amn.cfm). A similar program for the systematic study of the natural TL of Antarctic meteorites has been in operation in Japan, focusing on meteorites returned from Eastern Antarctica (e.g., Ninagawa et al., 1998, 2000). The natural TL distribution for meteorites from Western Antarctica and Eastern Antarctica is similar (Fig. 9), implying similar terrestrial age and preterrestrial histories for both populations.

The U.S. natural TL survey of Antarctic meteorites operated for 14 years and resulted in many scientific papers (Benoit et al., 1992, 1993b, 1994; Benoit and Sears, 1993b, 1999). Because of the different sampling limitations of natural TL and ^{26}Al, not all samples could be analyzed by both techniques, but data for 120 common samples were obtained and are compared in Fig. 8b (Sears et al., 2011). There appear to be two major terrestrial age trends reflecting normal and small perihelia meteorites, and a group of meteorites (mostly paired) with intermediate orbit and little spread in terrestrial age. The contours in Fig. 8b delineate the role of terrestrial age and orbit in determining natural TL levels. Terrestrial ages obtained from Fig. 8b are compared with terrestrial ages obtained by isotopic methods in Fig. 10. There is a reasonable agreement, especially since both techniques carry large uncertainties, the few outliers being readily explained in terms of anomalous radiation histories.

When the natural TL data for meteorites with natural TL <5 krad are compared with terrestrial ages calculated from ^{36}Cl, another cosmogenic isotope with a decay rate on Antarctic meteorite terrestrial age scales (half-life 301,000 year), there is a trend in which

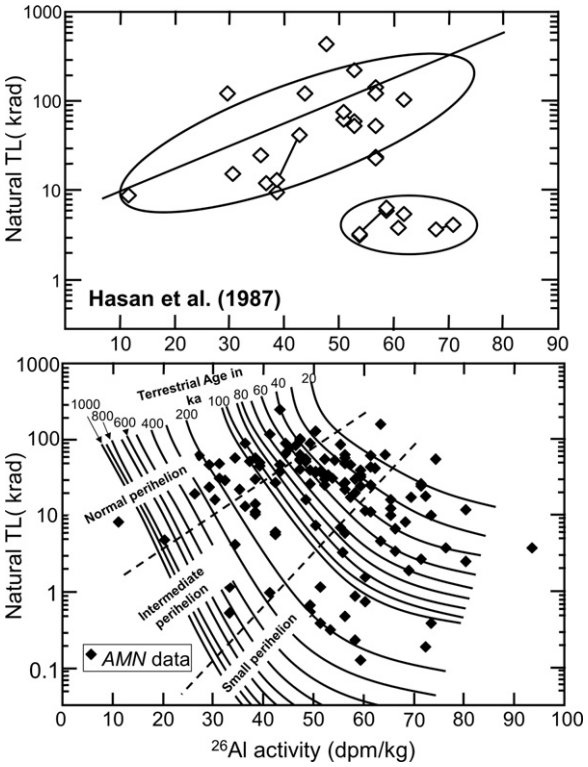

Fig. 8. Natural TL plotted against ^{26}Al for Antarctic meteorites. (a) The plot originally produced by Hasan et al. (1987) based on a comparison of 23 meteorites. (b) The 120 Antarctic meteorites for which both ^{26}Al and natural TL data have been published in the Antarctic Meteorite Newsletter (AMN) interpreted in terms of perihelion and terrestrial age, based on the analyses discussed in this paper. On the basis of these data and our favored interpretations, it is possible to sort the meteorites by perihelion and terrestrial age (Sears et al., 2011).

Table 3
Antarctic meteorite newsletters containing data from the natural TL survey of Antarctic meteorites.

Authors	Year	Vol (Issue), Page
Hasan, F.A., Score, R.	1989	12 (1), 21
Myers, B., Sears, H., Hasan, F., Score, R., Sears, D.	1990	13 (2), 25–27
Benoit, P.H., Myers, B., Sears, H., Sears, D.	1990	13 (3), 20–22
Benoit, P., Sears, H., Sears, D.	1991	14 (1), 15
Benoit, P.H., Roth, J., Sears, H., Sears, D.	1992	15 (1), 19
Benoit, P.H., Roth, J., Sears, H., Sears, D.	1992	15 (2), 34–35
Benoit, P.H., Roth, J., Sears, H., Sears, D.	1993	16 (1), 21
Benoit, P.H., Roth, J., Sears, H., Sears, D.	1993	16 (2), 21
Benoit, P.H., Roth, J., Sears, H., Sears, D.	1994	17 (1), 23
Benoit, P.H., Roth, J., Sears, H., Sears, D.	1994	17 (3), 20–21
Benoit, P.H., Roth, J., Sears, H., Sears, D.	1995	18 (1), 17
Benoit, P.H., Sears, D.	1996	19 (1), 20–21
Benoit, P.H., Sears, D.	1996	19 (2), 14–15
Benoit, P.H., Sears, D.	1997	20 (1), 15
Benoit, P.H., Sears, D.	1997	20 (2), 12
Benoit, P.H., Sears, D.	1998	21 (1), 15
Slinker, J., Benoit, P.H., Sears, D.	1998	21 (2), 19
Slinker, J., Benoit, P.H., Sears, D.	1999	22 (1), 19
Cosmochemistry Group	1999	22 (2), 13
Benoit, P.H., Sears, D.W.G.	2000	23 (1), 21
Benoit, P.H., Sears, D.W.G.	2000	23 (2), 21–22
Benoit, P.H., Sears, D.W.G.	2001	24 (1), 14
Cummings, M., Benoit, P.H., Sears, D.W.G.	2001	24 (2), 21–22

natural TL decays with increasing terrestrial age but with a high rate of natural TL decay (Benoit et al., 1993c). Apparently, the recent radiation filled the less stable low-temperature peaks which decay rapidly. This idea is testable, since low TL–high ^{26}Al meteorites should have lower temperature TL peaks.

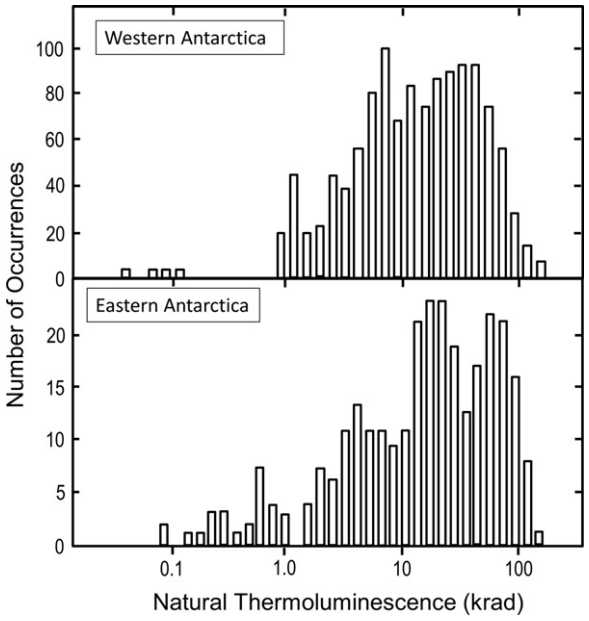

Fig. 9. Natural TL levels for meteorites from Western and Eastern Antarctica. The similarity in the distributions suggests similar preterrestrial and terrestrial histories (Benoit et al., 1992, 1993c, 1994; Benoit and Sears, 1993b, 1999; Ninagawa et al., 2000, 2002, 2005; Matsui et al., 2010; Takeda and Ninagawa, 2005).

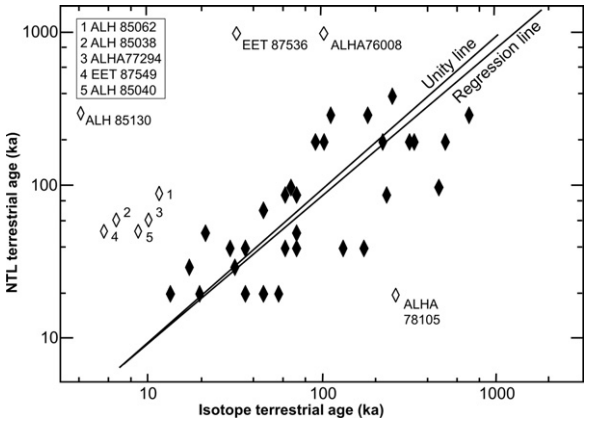

Fig. 10. Plot of terrestrial ages determined from natural thermoluminescence of Antractic meteorites against terrestrial age determined from cosmogenic isotope measurements. For the terrestrial age determined from natural TL, the middle of the range is plotted, while for isotopic ages the reported value is plotted and this has a typical uncertainty of 20–70%. Data for isotopic terrestrial ages are from Jull et al. (1998), Nishiizumi et al. (1979, 1989), and Michlovich et al. (1995). Nine outliers are indicated by open symbols and are thought to have unusual radiation histories. The remaining 34 meteorites (out of 43 on the plot) lie within a factor of 2 of a regression line through the data, which is indistinguishable from the unity line (Sears et al., 2011).

3.4.2. *The perpetual problem of "pairing"*

When a meteorite is decelerated through the atmosphere it not only heats and ablates, it normally breaks into fragments because of numerous cracks in the original meteorite. If it fragments high in the atmosphere, the individual fragments become rounded through ablation and uniformly covered in fusion crust. If it fragments near the end of atmospheric passage, the pieces that reach the ground may be only partially covered in fusion crust and on occasion can actually fit together. Once on the ground, repeated thermal cycling due to daily and seasonal changes and physical stresses such as windblown movement can also break the meteorite into small fragments. So meteorites are usually found in elliptical strewn fields with the larger masses located at the furthest end of the field

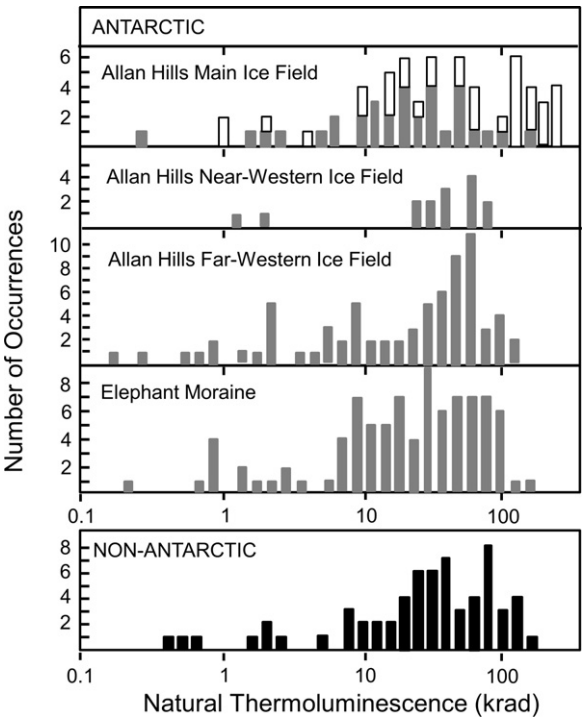

Fig. 11. Natural TL data for ordinary chondrites of weights >20 g (to avoid samples heated during atmospheric passage). The Allan Hills data are shown as an individual histograms for each of the ice fields. Meteorites collected by the German 1988/1989 expedition are indicated by open boxes in the Main ice field data. Data for Elephant Moraine and non-Antarctic ordinary chondrites are shown for comparison. Figure from Benoit et al. (1993c).

in the direction of flight. Wind and ice movement can disperse these strewn fields or they can create new distributions by collecting the rocks in crevasses or along moraine edges. Thus there is a universal problem, where large numbers of meteorites are found in large concentrations, of identifying members of a single fall. Although the meteorite fragments can be 10–50 in number, the process of linking them is termed "pairing".

Members of a given meteorite class are usually very similar in mineralogy and petrology, so there is no single technique that can reliably pair meteorites. Induced and natural TL are useful in this respect because of the large range overall but narrow range within a given meteorite, but TL data are always used with find location, class, petrography, and sometimes degree of weathering. Using a combination of techniques 167 meteorites from Allan Hills were thought to represent 129 or fewer individual meteorite falls (Benoit et al., 1993c), 107 meteorites from Elephant Moraine were thought to represent fewer than 73 individual meteorite falls (Benoit et al., 1994), and 302 meteorites from Lewis Cliff were thought to represent 230 or fewer falls (Benoit et al., 1992). There is similarity in the level of pairing at these three sites, 22%, 31% and 24%, respectively.

3.4.3. Systematics of natural TL of meteorites collected at the Allan Hills

The Allan Hills collection site in Western Antarctica consists of numerous discrete ice fields, each with its own characteristics (Fig. 11). Benoit et al. (1993c) suggested that while natural TL values for the main ice field are fairly low, say 5–30 krad, reflecting terrestrial ages ~400 ka, the Far Western Field has values of 30–80 krad, reflecting terrestrial age of <150 ka. These interpretations are suggestive of what can be done with data of this sort, but a statistical treatment is required. Benoit et al. (1993c) also suggested that there were trends in natural TL within individual ice fields that could indicate the directions of ice movement at these sites during the period of meteorite concentration.

3.4.4. The Elephant Moraine meteorites and their natural TL properties

The Antarctic meteorites from Elephant Moraine are noted for their high natural TL levels and suggest this population typically has terrestrial ages of <12,500 year (Fig. 11). The ice fields formed through shallow ablation of ice (Benoit et al., 1994). Unlike the Allan Hills sites to the south, lateral transport is probably less important relative to the in-fall of meteorites in concentrating meteorites on these ice fields.

3.4.5. Ice collection mechanics at the Lewis Cliff

In the case of the Lewis Cliff Ice Tongue, ice is being pushed in a narrow field northwards against a moraine (Cassidy, 1990). Half way along the tongue is a morphological and geophysical discontinuity, marked by firn and a step in the ice. Large numbers of meteorites accumulate on the tongue, concentrated mostly towards the western side (Fig. 12). If these were static collection surfaces, meteorites of all terrestrial ages and thus natural TL values, would be randomly mixed along the length of the tongue. However, the distribution of natural TL levels for the meteorites is not random (Benoit et al., 1992). Meteorites with "young" terrestrial ages, with natural TL >80 krad, occur in the upper and low tongue, but avoid a region just south of the discontinuity. On the other hand, "old" meteorites (natural TL <30 krad) plot uniformly across the tongue regardless of the discontinuity. Intermediate meteorites (30–80 krad) show intermediate behavior. Benoit et al. (1992) interpreted this to indicate that the ice sheet had faulted at the discontinuity and that the southern tongue was turning up and ablating and abrading as other meteorites are being exposed where old ice is brought to the surface (Fig. 13). The small perihelion meteorites (<5 krad) are randomly scattered about the ice field, their natural TL levels being determined by orbit rather than terrestrial age.

3.5. Anomalous fading, natural TL, and cosmic ray exposure ages

Many types of terrestrial feldspar, most notably those from volcanic regions, undergo "anomalous fading", which is uniform fading across all glow curve temperatures that can be observed on the scale of days or weeks (Wintle, 1973, 1977). The process has been thought of in terms of the traps "leaking" and is caused by the finite overlap of wave functions for the electrons in the traps and recombination centers (Garlick and Robinson, 1971). Hasan et al. (1986) found that most ordinary chondrites did not display anomalous fading, while Hasan et al. (1986) found that basaltic meteorites did. As a result of anomalous fading, basaltic meteorites have natural TL values about an order of magnitude lower than those of chondritic meteorites (Sears et al., 1991c). Hasan et al. (1986) argued that the amount of anomalous fading observed for a given meteorite was determined by the relative amounts of ordered and disordered feldspar. They argued that ordered feldspars show anomalous fading while disordered feldspar did not and that it was the shorter distance between oxygen and cations in the feldspar lattice of ordered feldspars that facilitated orbital overlap. Bhandari et al. (1985) found that shergottites had much lower natural TL than ordinary chondrites which they attributed to either shock heating or close solar passage, but the explanation is most probably that the TL of shergottites, like that of HED meteorites, is also undergoing anomalous fading. While anomalous fading might be considered a problem in the application of natural TL to meteorite problems, Biswas et al. (2011) recently argued that this phenomenon could be used to advantage. Small amounts of anomalous fading observed after long periods of time might allow the high-temperature

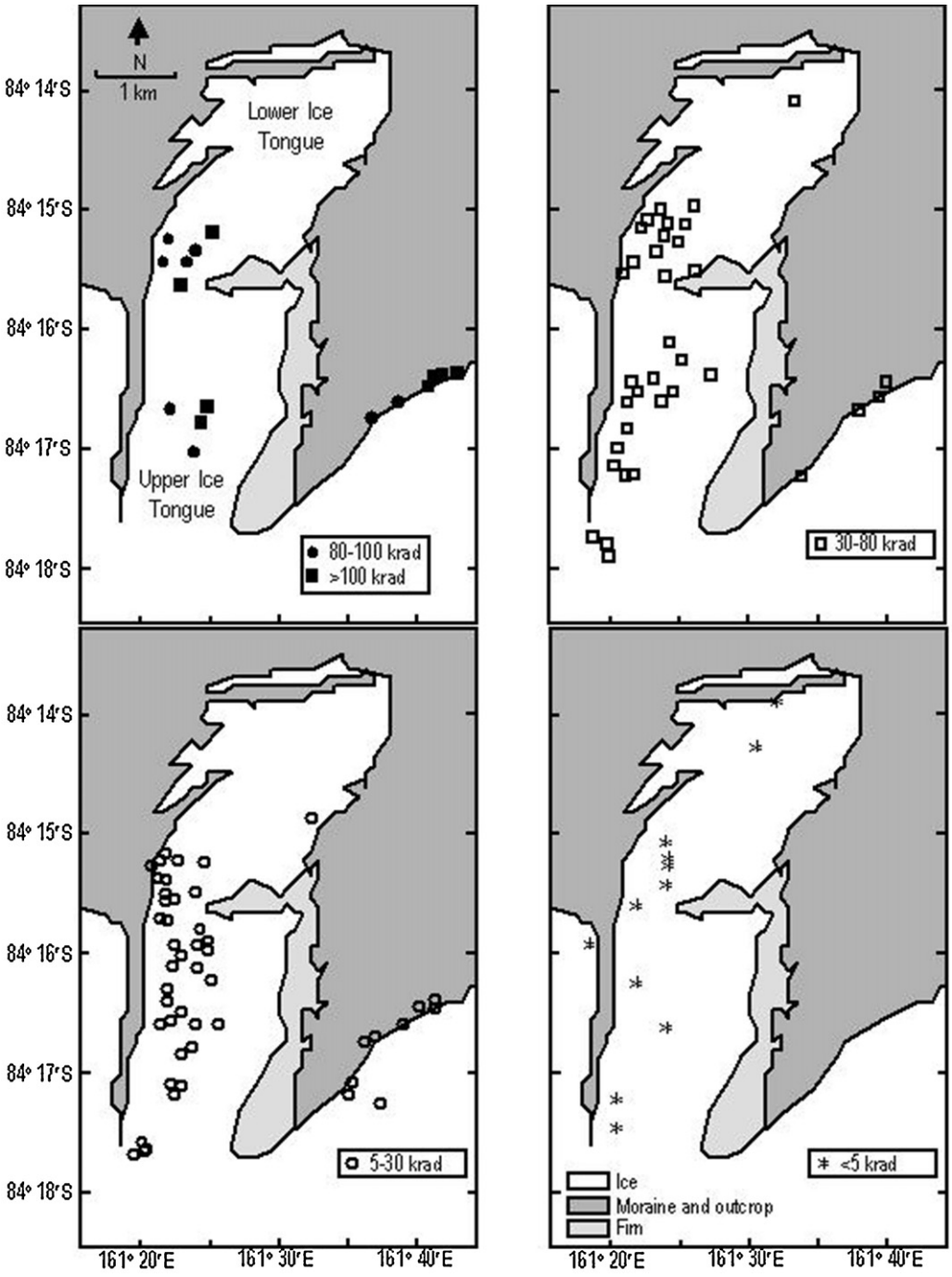

Fig. 12. Distribution of meteorite finds at the Lewis Cliff Ice Tongue in Antarctica, separated by natural TL level. Ice is being pushed towards a moraine at the north and has faulted half way along its length. The fault's outcrop at the surface is marked by firn, unconsolidated snow. Meteorites with low-natural TL (large terrestrial ages) are spread uniformly across the field, while high natural TL meteorites (small terrestrial ages) avoid the area south of the fault. Meteorites with intermediate natural TL display intermediate behavior. This is interpreted as indicating that the ice is turning up at the fault line exposing old meteorites, as the ice is ablated and evaporated. Apparently, the rate at which old meteorites are brought in from depth is greater than rate of fall (Benoit et al., 1992).

natural TL to be used for determining cosmic ray exposure ages.

One of the enigmatic results in meteorite luminescence was that despite the exposure ages of Ma and higher, and the fact that higher temperature glow peaks corresponded to stability of charges in traps in excess of 100 Ma, the stored luminescence never exceeded 100 krad suggesting exposure ages of 10 ka, assuming a cosmic ray dose of ~0.01 krad/year. Using the GEANT4 simulation toolkit, Biswas et al. (2011) found that the cosmic ray dose rate in the interior of the meteoroid body of a preatmospheric radius 9–40 cm was ~0.0043 krad/year, not sufficiently different from ~0.01 krad/year to explain the low equivalent dose observed. Biswas et al. (2011) also examined the natural TL at red wavelengths, and while these resulted in higher equivalent doses, again the values are much lower than expected on the basis of dose rate and cosmic ray exposure age. They therefore concluded that the low equivalent doses were due to anomalous fading and found that for four meteorites the anomalous fading rates decreased with CRE ages. Perhaps there was a loss of centers due to radiation damage. In any event, the data suggest that the anomalous fading rate and the equivalent

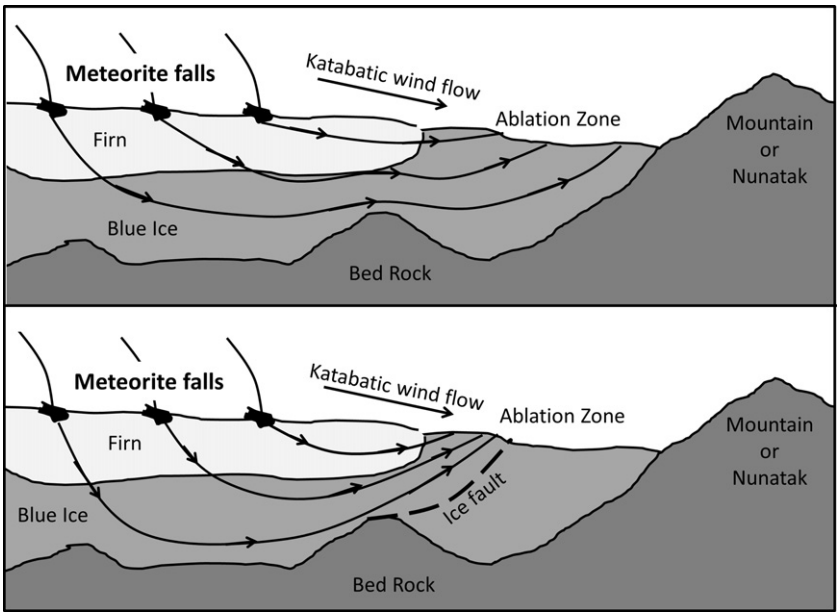

Fig. 13. Schematic diagrams showing the accumulation of meteorites on blue ice fields in Antarctica and with a possible explanation for the distribution of terrestrial ages inferred by the natural TL data for meteorites at the Lewis Cliff Ice Tongue.

dose could be used to determine the cosmic ray exposure age. It would be useful to confirm this relationship between CRE and high-temperature natural TL by performing the measurements on a much larger sample set.

3.6. Extraterrestrial materials other than ordinary chondrites

Despite the recovery of large numbers of meteorites in Antarctica, the recovery of the first lunar meteorite was a true surprise and resulted a high level of agreement in a series of papers in *Geophysical Research Letters* (cited as "GRL, 1983" in the references). We now know of over 50 meteorites on Earth that were ejected from the Moon and most of these were recovered from Antarctica, with some from hot deserts. Natural TL measurements have been used to estimate the duration of the meteorites' exposure to radiation in space, and to link meteorites ejected by a common ejection event. Most of the transit ages determined are very short, typically <2500 years (Sutton and Crozaz, 1983; Benoit et al., 1996). The Bhandari et al. (1985) work on shergottites was mentioned above (Section 3.5).

While not involving measurements on meteorites, but on sandstone and limestone from the target rocks, the age of the impact that created the Barringer Crater in Arizona has been determined by natural TL methods. Barringer Crater is the first recognized and most famous of the meteorite impact craters on Earth. Calculating dose rates from concentrations of U, Th, K, and from cosmic radiation, confirming the estimates using TL dosimeters buried at the site, and using natural TL to measure the absorbed dose, Sutton (1985) calculated a value of 49,000 ± 3000 years for the age of the crater. This is about twice the previous best estimate and is now widely accepted. The Lonar Crater in India, which is unusual for being an impact structure in basalt, was also dated by natural TL techniques by Sen Gupta et al. (1997a,b) who found that the mean age of three pieces of impact glass was 52,000 ± 6000 years.

4. Studies of induced thermoluminescence

Studies of induced TL produce information of meteorite mineralogy and crystallography. This in turn provides information on the degree of metamorphism, post-metamorphic cooling histories, shock and regolith histories. In fact, any phase in the history of a meteorite that affects its luminescent components (usually feldspar) leaves an imprint on induced TL properties. Available induced thermoluminescence data appear in Table S3 with the relevant metadata in Table 4.

Table 4
Metadata for supplemental table for induced TL data for meteorites.

Filename	Induced TL data
Number of meteorites:	918
Field 1:	Meteorite name
Abbreviations for meteorite names:	See Table 2
Field 2:	TL sensitivity (Dhajala = 1)
Field 3:	Standard deviation for TL sensitivity
Field 4:	TL peak temperature (°C)
Field 5:	Standard deviation for TL peak temperature
Field 6:	TL peak width (°C)
Field 7:	Standard deviation for TL peak width

4.1. More on the nature of thermoluminescence traps and the effects of shock on induced TL

When modern studies of the thermoluminescence of meteorites were beginning, in the 1960s, several authors in Russia and Switzerland assumed that the most likely cause of electron traps was not impurity centers but defect sites that were produced by radiation damage. It was thought that such defects would increase in number with radiation exposure and thus provide a new solid state mechanism for dating (Houtermans and Leiner, 1969; Leiner and Geiss, 1968). The idea was prompted in part by work of Komovsky (1961) who found that several meteorites had induced TL levels that increased with K–Ar age, as if beta decay from ^{40}K was creating traps, an observation that was confirmed a few years later in a much larger study by Leiner and Geiss (1968).

Sears (1980) tested these ideas by exposing meteorite samples to α, β, γ, and proton radiations to levels in excess of those expected during the lifetime of the meteorite. He found that these radiation doses produced no change in induced TL. Thus Sears (1980)

proposed that the relationships observed by earlier workers were caused by shock heating. Meteorites with low K–Ar ages are noted for their large numbers of shock effects (Heymann, 1967). The shock experienced by these meteorites not only caused the loss of Ar but also converted the luminescent phase, feldspar, into glass. Geological glasses have little or no ability to luminesce because the lack of even short range order precludes the establishment of the discrete energy levels associated with crystals (Fig. 2). It was realized that induced TL reflects the solid state history of meteorites – the history that is reflected in the ability of the meteorites to luminesce whereas the natural TL that reflects recent temperature and radiation history – providing insights into the geology of the meteorites. Thus it might be said that while natural TL is largely the realm of the physicist, induced TL is mostly the realm of the geologist.

While shock can decrease the level of induced TL by about a factor of 100, metamorphism can cause the induced TL of chondrites to increase by factor of $\sim 10^5$. To be able to quantify the level of metamorphism in chondrites in a quantitative fashion over such a large range has profound importance for meteorite studies. The discovery that the induced TL could detect and quantify differences in the petrologic properties of meteorites initiated several decades of meteorite research using induced TL.

4.2. Studies of induced TL of ordinary chondrites

4.2.1. Metamorphism of ordinary chondrites

While most ordinary chondrites have suffered high levels of parent body metamorphism (solid state alteration by high temperatures), there are a few, like Semarkona, Bishunpur and Krymka, where this is negligible or minimal (Dodd et al., 1967; Van Schmus and Wood, 1967). The unmetamorphosed meteorites are especially important as they provide a record of solar system material prior to its alteration on asteroid parent bodies. However, for most meteorites, once accreted into the interiors of asteroids, heat produced by radioactive decay of ^{26}Al (Lee et al., 1976) caused metamorphic alteration and an almost complete destruction of many of the primary properties of the meteorites.

A suite of mineral and phase properties, compositional changes, and textural changes are used to determine the petrologic type 1–6 of a chondritic meteorite (Dodd et al., 1967; Afiattalab and Wasson, 1980; Huss et al., 1981; Schultz and Franke, 2004). There is a gradation from unmetamorphosed to heavily metamorphosed chondrites which has been described in terms of petrographic types 3–6, the type 3 sometimes being referred to as unequilibrated and the types 4–6 as equilibrated chondrites. The word "equilibration" reflects a move towards a state of chemical equilibration within and between minerals as heat allows diffusion of atoms within the meteorite (Dodd et al., 1967; Dodd, 1969; Van Schmus and Wood, 1967). Types 1 and 2 are now thought to owe their properties to aqueous alteration, which increases from type 3 to type 2 to type 1, most of the alteration occurring throughout the CM2 chondrites (Browning et al., 1996; Rubin et al., 2007). Similarly, CR chondrites range from type CR1 to CR3 with a wide range within the CR2s (Weisberg et al., 1993).

Arguably the most notable effect of metamorphism in ordinary chondrites (and probably CO and CV chondrites) is to convert the glass characteristic of primitive ordinary chondrites, into large crystals of feldspar. Glass in these meteorites generally has no induced TL, feldspar has considerable induced TL. Thus the measurement of induced TL in these meteorites can provide a quantitative and extraordinarily sensitive means of assessing the degree of metamorphic alteration (Sears et al., 1980). Cathodoluminescence images provide a means of understanding the mineralogical changes controlling the induced TL properties (Akridge et al., 2004). Several research groups used this new means of assessing metamorphism within the type 3 ordinary chondrites in their efforts to understand early solar system processes (e.g. Grady et al., 1982; McNaughton et al., 1982; Huss, 1991). The technique is also being systematically applied to the Japanese Antarctic meteorite collection (Ninagawa et al., 2000).

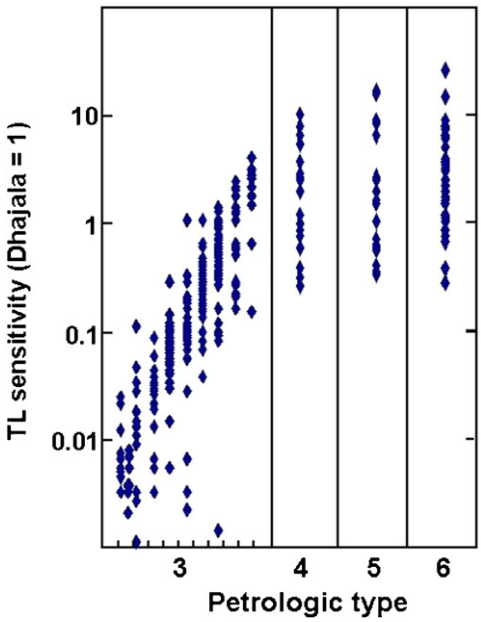

Fig. 14. The intensity of the low-temperature TL peak induced in a sample by a laboratory test dose (and normalized to that of the Dhajala meteorite) is referred to as "TL sensitivity". The dynamic range of TL sensitivity displayed by the type 3 ordinary chondrites is large, especially when compared with the other types, and clearly relates to the metamorphic alterations being described by the petrologic types. The horizontal axis is determined by a suite of mineralogical and compositional data. Thus subdivision into types 3.0–3.9 was proposed by Sears et al. (1980).

Fig. 14 shows data for the TL sensitivity of ordinary chondrites, with shocked meteorites, meteorites known to be brecciated, and meteorites with poor agreement between duplicates, removed. As discussed above these data reflect the history of feldspar. Throughout petrologic type 3, metamorphism causes crystallization of the feldspar in the primary glass. Above type 3 levels of metamorphism the feldspar increases in grain size throughout the type 4–6. Coarsening does not affect TL sensitivity significantly but some influence on TL might be expected as metamorphism removes trace elements that might quench the TL or adds trace elements that enhance the TL.

A wide variety of properties of type 3 ordinary chondrites also depend on metamorphism and these co-vary with TL sensitivity or petrographic type derived from TL sensitivity (Fig. 15). By exploring these trends processes associated with metamorphism and thereby the identification of physical and chemical properties inherited from the primary material prior to parent body metamorphism can be made. Olivine and kamacite compositions homogenize with metamorphism and when the fine-grained matrix crystallizes the amount of iron relative to magnesium in the matrix decreases as iron is reduced and coalesces into metal grains. With increasing metamorphism, carbon becomes isotopically heavy and hydrogen becomes lighter. Finally, interstellar diamonds are destroyed by lower levels of parent body metamorphism and oxygen isotopes are heavier in the lower petrologic types. Most of these changes reflect an approach of the mineral lattice to chemical and physical equilibrium, but some changes reflect the loss of volatiles, for example the move to heavier oxygen seems to reflect the loss of CO or CO_2 during metamorphism (Sears and Weeks, 1983; Clayton et al., 1991). Using TL sensitivity and the correlations observed for these mineral and phase properties, petrologic type 3 has been subdivided into types 3.0–3.9 in the manner described in Table 5.

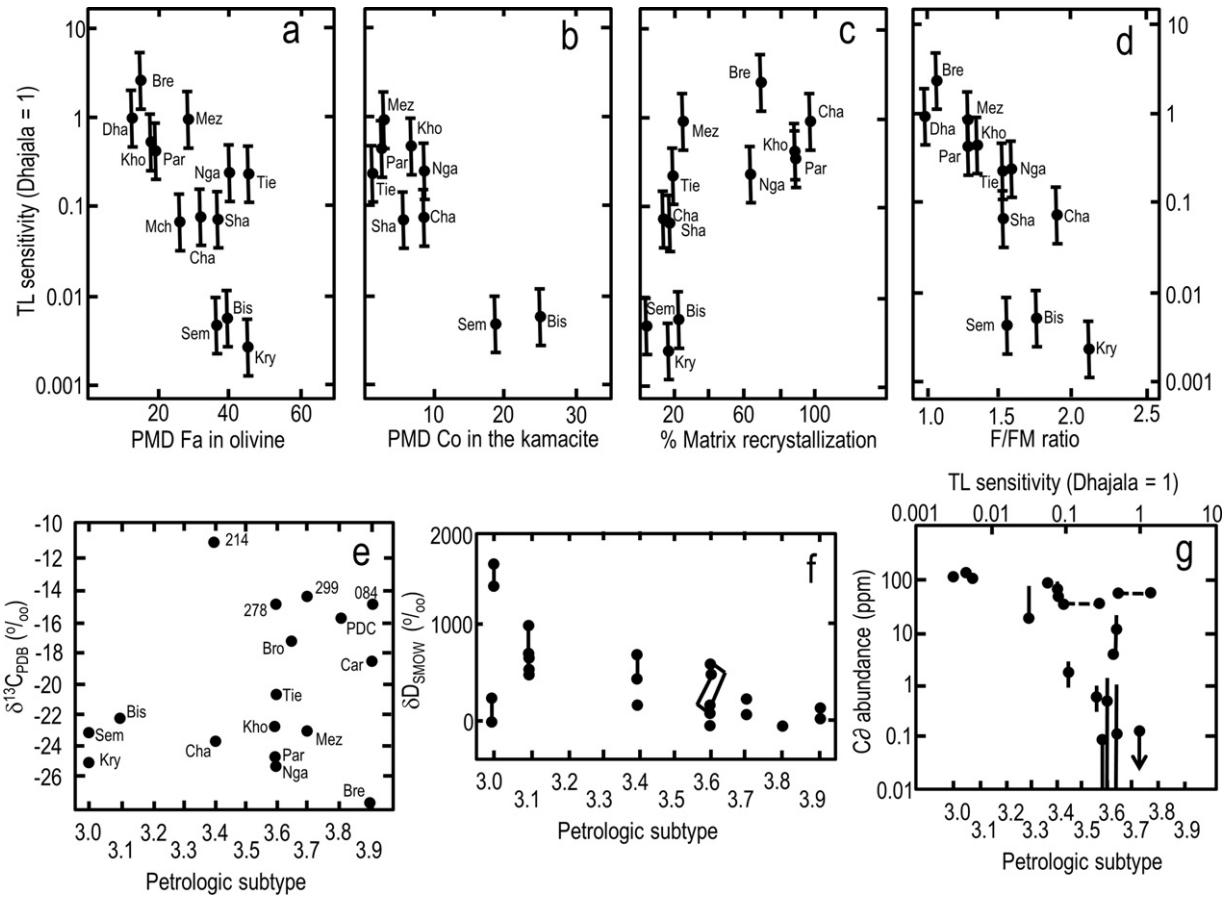

Fig. 15. Thermoluminescence sensitivity and/or the equivalent (petrologic type 3.0–3.9) compared with a variety of properties that are sensitive to parent body metamorphism. (a) The heterogeneity of olivine, expressed as the percent mean deviation of fayalite. (b) The heterogeneity of kamacite (low-Ni Fe,Ni alloy), expressed as the percent mean deviation of Co. (c) Amount of fine-grained matrix that is crystalline. (d) The composition of the matrix expressed as the Fe/(Fe + Mg) ratio. Plots (a) to (d) are from Sears et al. (1980). (e) Hydrogen isotopic composition expressed as δ*D* (McNaughton et al., 1982). (f) Carbon isotopic composition (Grady et al., 1982). (g) Abundance of interstellar diamond (Huss, 1991). (h) Oxygen isotopes (Sears and Weeks, 1983; Clayton et al., 1991).

Since metamorphism was a gradual and uninterrupted process, the subdivisions are arbitrary and selected to give equal steps on a logarithmic scale. Of course it should be borne in mind that these petrologic types give a sense of the degree of alteration of an individual meteorite in a suite of meteorites. It is not necessarily clear that types can carry-over from one class to another, nor is the case that all classes had the same time–temperature history, or that all systems have the same kinetics, notwithstanding simplistic comparisons that have been made in recent years.

Grossman and Brearley (2005) proposed further subdivision at the lowest end of this range, into types 3.00, 3.05, 3.10 and 3.15, based on Cr contents of olivine. Kimura et al. (2008) added that metal compositions also enable finer subdivision of the lower types, in agreement with earlier work (e.g. Afiattalab and Wasson, 1980; Rambaldi et al., 1980). Cathodoluminescence data suggest further subdivision at the low end of the petrographic range is meaningful but this has yet to be fully explored. A combined study of the cathodoluminescence and high-precision induced TL properties of type 3.0–3.2 chondrites would be worthwhile.

It is significant that the distribution of petrographic types is not the same for each ordinary chondrite class. Higher types are preferred for H class, lower types are preferred for the LL class, and the L chondrites are intermediate (Fig. 16). This behavior has not been fully explained but might imply that some correlation between burial depth (and level of low grade metamorphism) and composition such as described in Huang et al. (1996). This is the "onion skin" model often used to describe the meteorite parent body structure and is consistent with the recent interpretations of reflectivity spectra for asteroids (Gietzen et al., 2012). In order to explain the data in Fig. 16 we propose that throughout the type 3 thermal zone of the asteroids, LL chondrites were nearer the surface, then L chondrites, and deepest were H chondrites. This is also consistent with suggestions that the metal-silicate separation that gave rise to the three classes were caused by size-density sorting in the megaregolith of a small body (Huang et al., 1996).

4.2.2. Palaeothermometry

In a PhD thesis and a conference abstract, Pasternak (1978) and Levy (1978) showed that the shape of the feldspar glow curve was governed by its crystallography. In particular, for feldspars crystallizing at low temperatures the Al–Si backbone was ordered, while for feldspar crystallizing at higher temperatures the backbone was disordered such that the Al–Si were randomly arranged along the chain. The order–disorder transformation occurs at about 500–600 °C for feldspars of ordinary chondrite composition and can be monitored by X-ray diffraction measurements (McKie and McConnell, 1963). Pasternak (1978) showed that for ordered feldspars the induced TL peak was narrower and at lower glow curve temperatures, than for disordered feldspar.

Guimon et al. (1984) found that the same changes in TL properties could be brought when heating a petrographic type 3.4 ordinary chondrite (Fig. S9). The narrow peak at low glow curve temperature characteristic of type 3.4 chondrites was converted into the broad high-temperature peak characteristic of equilibrated ordinary chondrites by heating at 900 °C for 200 h. In fact, if the TL peak temperature is plotted against the heating temperature for the

Table 5
Definition of the subtypes of ordinary chondrites (Sears et al., 1980).

Type	TL sensitivity (Dhajala = 1)	PMD olivine[a]	PMD metal[a]	Matrix recrystal-lization (%)	Matrix FeO/FeO + MgO	C (wt%)	$^{36}Ar10^{-8}$ cc g
3.0	<0.0046	>42	>21	<10	>1.9	≥0.6	≥65
3.1	0.0046–0.010	40–42	17–21	10–20	1.7–1.9	0.5–0.6	55–65
3.2	0.010–0.022	38–40	13–17	10–20	1.6–1.7	0.43–0.50	45–55
3.3	0.022–0.046	36–38	10–13	10–20	1.5–1.6	0.38–0.43	35–45
3.4	0.046–0.10	33–36	8.0–10	~20	1.4–1.5	0.33–0.38	27–35
3.5	0.10–0.22	29–33	6.0–8.0	~50	1.3–1.4	0.30–0.33	18–27
3.6	0.22–0.46	25–29	4.0–6.0	>60	1.2–1.3	0.27–0.30	13–18
3.7	0.46–1.0	20–25	2.5–4.0	>60	1.1–1.2	0.24–0.27	8–13
3.8	1.0–2.2	15–20	1.5–2.5	>60	1.0–1.1	0.21–0.24	4–8
3.9	2.2–4.6	5–15	<1.5	>60	<1.0	≤0.21	<4

[a] PMD, percent mean deviation, can be converted to coefficient of variation (CV) by division by 0.80, where CV is σ/mean (Scott et al., 1982; Sears and Weeks, 1983).

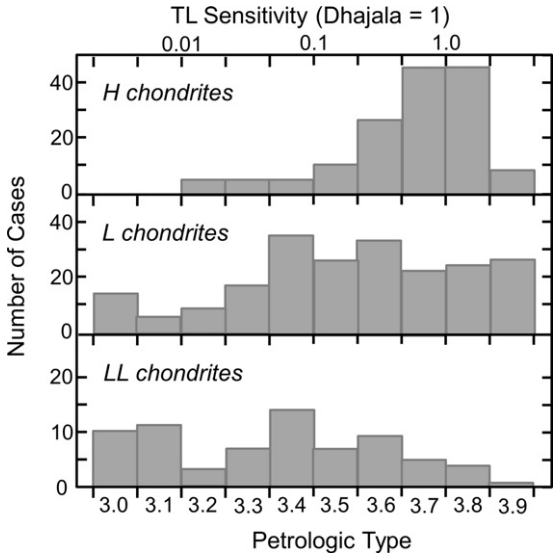

Fig. 16. Histograms for H, L, and LL chondrites showing their distribution over the petrologic types. Preferred petrologic type within each class decreases along the H, L and LL chondrite sequence.

ALHA77011 LL3.4 chondrite, they agree very well with Pasternak's (1978) data for Amelia albite (Fig. S10). Repeating Pasternak's (1978) experiments with other terrestrial feldspars, Guimon et al. (1985) found similar results, namely that the move to TL peak temperatures ~250 °C was associated with an increase in the $\Delta 2\theta$ parameter corresponding to the disordered phase (Fig. 17). As Pasternak (1978) noted, the increase in peak temperature actually precedes disordering, and has lower activation energy, suggesting that it is defect formation during the early stages of disordering that is actually being detected by the TL changes.

On a plot of TL peak temperature against TL peak width, the Guimon et al. (1985) data for ALHA77011 plot in a fairly well defined field around 100 °C (peak temperature), 100 °C (peak width), until heated above 600 °C, where it moves to a higher and equally well defined field with peak temperatures ~175 °C and widths ~150 °C (Fig. 17). Similarly, plotting the data for a large number of type 3 ordinary chondrites produces two clusters similar to the heating data (Fig. 18). Presumably these data indicate the presence of ordered feldspar in the low-temperature group and disordered feldspar in the other. The types 3.0–3.1, which have little if any feldspar, tend to scatter on the diagram. Thus we have a paleothermometer, suggesting that the middle of the type 3 metamorphic spectrum corresponds to metamorphic temperatures of ~500 °C. This is the temperature suggested by the laboratory heating experiments and might shift to lower values if geological times were available, but probably not much since this value is consistent with rather approximate petrographic estimates. Independent confirmation that induced TL peak shape was reflecting thermal history came from an unexpected direction discussed below.

Dodd (1981) suggested that type 3 ordinary chondrites as a whole had experienced metamorphic temperatures of 400–600 °C, but there are few literature estimates for metamorphic temperatures for type 3 chondrites since most geothermometers

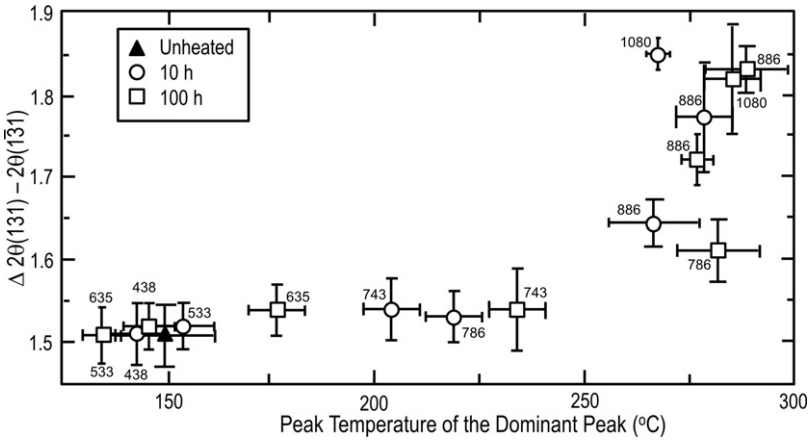

Fig. 17. Increases in peak temperature upon heating compared with the $\Delta 2\theta$ parameter which is a measure of the degree of structural disordering in terrestrial oligoclase (Smith, 1974). The numbers alongside the data points refer to heating temperatures in degrees Celsius with heating times indicated by the symbols. The $\Delta 2\theta$ parameter increases from ~1.5 to 2.0 as the structural order of the feldspar changes from being ordered to disorder. It is suggested that the change in the TL peak temperature is associated with disordering; however the activation energy for the TL changes is lower than the activation energy for disordering, suggesting that the relationship is indirect. Pasternak (1978) suggested that the TL is detecting defect formation that precedes disordering.
From Sears et al. (1997).

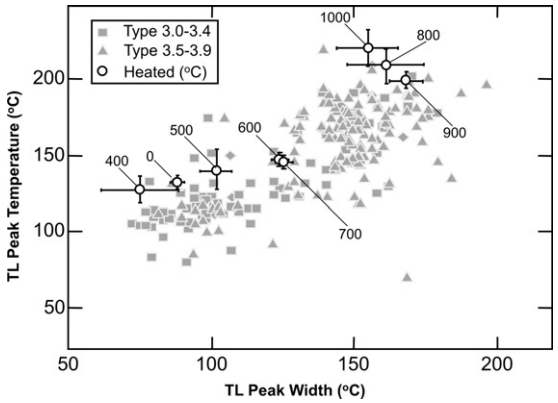

Fig. 18. Thermoluminescence peak temperature against peak width for samples of Allan Hills A77011 heated at the temperatures indicated (°C, open circles, 0 = unheated) compared with these TL parameters for type 3 ordinary chondrites. There is a bimodal distribution in the data with type <3.5 in the lower cluster and type >3.5 in the upper cluster, and Allan Hills A77011 can be transferred from one cluster to the other by heating above 500 °C (Guimon et al., 1985, updated for the present work).

require chemical equilibrium between phases. Despite this, the Cr spinel-olivine thermometer has been used to ascribe 525–700 °C to types 3.7–3.8 (Wlotzka, 1985, 1987; McCoy et al., 1991), and indicators not based on phase equilibria have been used to ascribe metamorphic temperatures to type 3 chondrites. Alexander et al. (1989) set an upper limit of ~260 °C for Semarkona based on phyllosilicate composition. Rambaldi and Wasson (1981) suggested 300–350 °C for Bishunpur (LL3.1) on the basis of Ni content of the matrix, and Brearley (1990) suggested 350–400 °C for type 3.4–3.6 chondrites based on the degree of graphitization of carbon. Huss and Lewis (1994) proposed temperatures ranging from ~200 °C for type 3.0 to ~600 °C for type 3.6 based on pre-solar diamond abundance. All-in-all, these independent estimates are consistent with TL palaeothermometry.

Several studies have been reported on the induced TL properties of individual chondrules to see if they yield new insights into metamorphism and chondrule history. Fig. 19 shows data for chondrules from five ordinary chondrites of increasing petrographic type. For the low types, Semarkona and Bishunpur, the data show no tendency to plot in either the high or low field. Their luminescence comes from a variety of minerals including forsterite, calcic glass in the chondrules, and the occasional chondrule with Na-rich feldspar in their mesostases. When feldspar starts to crystallize, it essentially plots in the low field (Chainpur) and then with higher metamorphism it plots in the high field (Allegan). Dhajala, which is intermediate to Chainpur and Allegan, has chondrules that plot mostly in the high field but with a significant number in the low field. Since all these chondrules experienced the same thermal history, this suggests that chondrules respond differently to metamorphism and that there is a kinetic barrier for conversion of certain chondrules from low to high-form.

4.2.3. *The secular variation in the nature of meteorites falling to earth and post-metamorphic cooling rates*

In the histogram of cosmic ray exposure ages, the H chondrites are conspicuous in having a very sharp peak at 8 Ma, suggesting that a relatively recent major break-up event produced most of the members of this class of meteorite. Looking systematically at peak shapes for equilibrated meteorites, Benoit and Sears (1992, 1993a, 1996) found that H chondrites with 8 Ma cosmic ray exposure ages that were recovered from the Antarctic had slightly higher peak temperatures than H chondrites with 8 Ma cosmic ray ages recovered from the rest of the world (Fig. 20). The main difference in these two populations is terrestrial age. Antarctic meteorites have terrestrial ages typically of ~40 ka, whereas the H chondrites from elsewhere are largely meteorites observed to fall in the last <250 years.

As pointed out in Section 2.2, a typical meteorite glow curve consists of multiple peaks that reflect various trapping sites in the crystal. Since we now know that structural order has a major effect

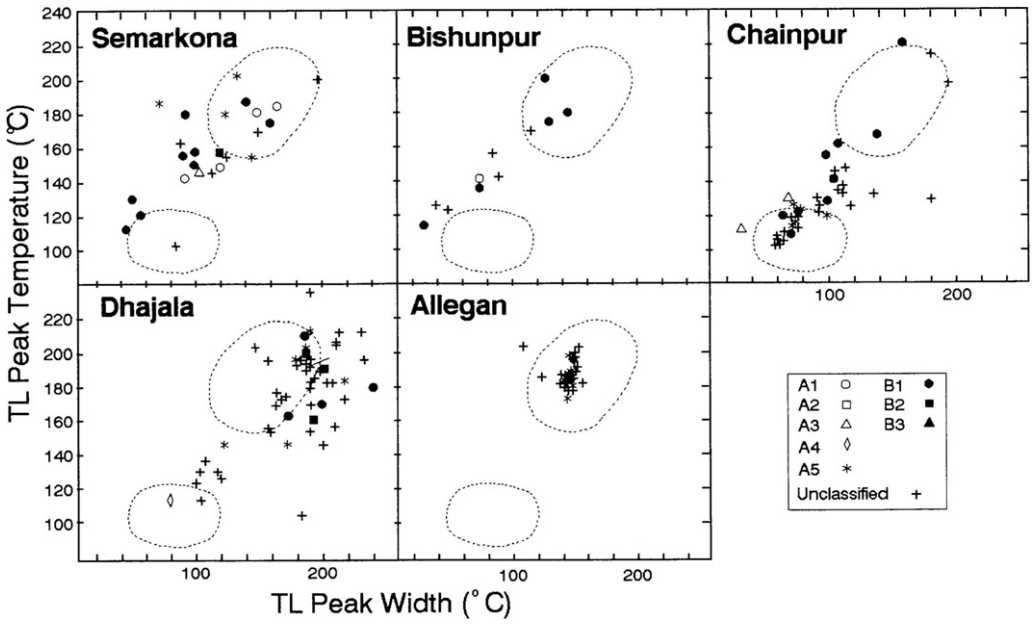

Fig. 19. Plots of TL peak temperature against peak width for chondrules from ordinary chondrites. The two fields refer to type 3 ordinary chondrite samples heated in the laboratory and are thought to be due to low- and high-temperature feldspar in the lower-left field and upper right fields, respectively. Semarkona and Bishunpur chondrules show a correlation between these parameters but do not plot preferentially in either of the two fields. On the other hand, Chainpur chondrules plot preferentially in the low field or between the fields and Dhajala chondrules plot in the upper field (displaced slightly to the right) or between the fields. Allegan chondrules plot in a tight cluster (two chondrules aside) in the upper field. These trends are also consistent with metamorphism being the major factor in determining the TL properties of chondrules from type 3 ordinary chondrites (Sears et al., 1995).

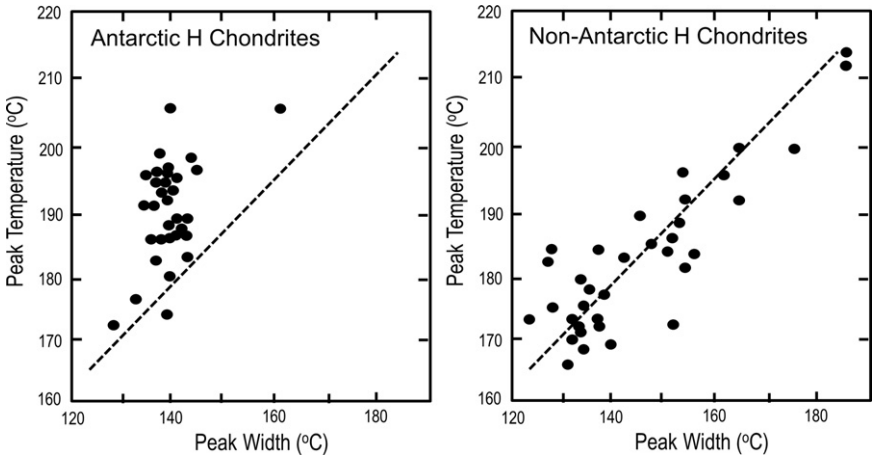

Fig. 20. (a) Induced TL peak temperature against peak width for a suite of 31 Antarctic H chondrites. Data are from Haq et al. (1988). (b) Equivalent data for 37 non-Antarctic (i.e., modern falls) H chondrites. Dashed line is a regression line through the non-Antarctic data. Note presence of a cluster of Antarctic meteorites with peak temperatures >190 °C which do not appear to be the result of either weathering or shock (Benoit and Sears, 1993a).

in the shape of the glow curve, various mixtures of ordered and disordered feldspar will result in increasing the complexity of the glow curve. In fact, the rate of cooling after peak metamorphism influences the glow curve shape since it will determine the relative proportions of ordered and disordered feldspar. Thus as a meteorite cools from peak temperatures above the order–disorder transition, it will form crystals in the disordered form. As it cools below the transition temperature, the new feldspar crystallizing from the glass will be in the low-form. However, transformation from the high- to the low-form of feldspar is slow, so high-form feldspar remains. Therefore it is expected that faster cooling results favor higher glow curve temperatures, while slower cooling results favor lower glow curve temperatures. Meteorites that were never metamorphosed above the transformation temperature will only contain ordered feldspar with its narrow peak at low glow curve temperatures. These predictions can be tested by using an independent technique to measure cooling rate. For example, the Ni profiles in the taenite which also reflect cooling around 400 °C.

Benoit and Sears (1993a) found that the H chondrites with higher peak temperatures cooled more rapidly than those with low peak temperatures (Fig. 21). This is not only independent

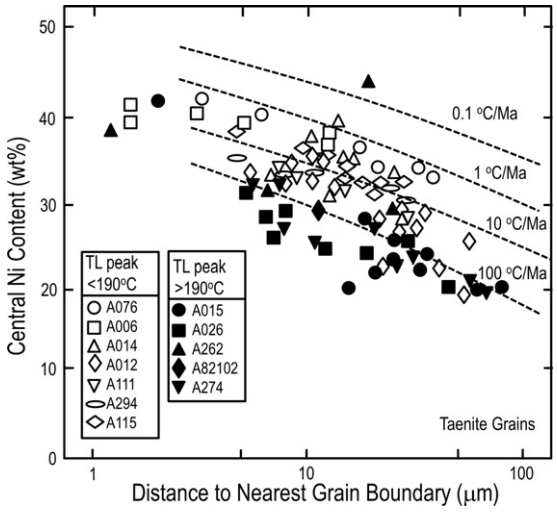

Fig. 21. Central Ni content for taenite (high Ni, Fe,Ni alloy) grains in Antarctic H5 chondrites. Cooling rate lines are from Willis and Goldstein (1981). Sample names are abbreviated from the full listing in Haq et al. (1988). The two groups clearly have different cooling rates and the >190 °C group clearly cooled rapidly (Benoit and Sears, 1992).

confirmation for our understanding of induced TL peak shapes, but it shows that H chondrites associated with the 8 Ma CRE event and arriving on Earth 40,000 years ago came from a different metamorphic region on their asteroid parent object than those currently falling on Earth. Such a secular variation might result from different parts of the disrupted asteroid being placed on different Earth-bound orbits. If one compares temperature-width distributions for H chondrites from a variety of sites, see Fig. S11, there is a sequence that seems to agree with the terrestrial age distributions for these sites as determined by natural TL measurements.

There has been much discussion of whether meteorites found in the Antarctic are somehow different from those falling elsewhere in the world. In general, this idea has met with skepticism because of the arguments are based on elemental abundances which may have been disturbed in these highly weathered meteorites (Dennison and Lipschutz, 1987; Koeberl and Cassidy, 1991; Wolf and Lipschutz, 1992). Weathering is not an issue with TL peak shape data, or the metallographic cooling rate estimates. Glow curve shapes have proved to be independent of weathering – the TL signal from weathering products is minor compared to the meteorite signal – and, in any event, weathering products are easily removed from TL samples by a simple acid wash. In the case of the metallography, unweathered metal grains can easily be distinguished from weathered grains.

4.2.4. Shock effects in ordinary chondrites

Subsequent to the study of Sears (1980) that showed shock intensities of ~30 GPa could decrease induced TL levels by a factor of about 100, Haq et al. (1988) made a study of a large number of naturally shocked ordinary chondrites and found a similar range of induced TL levels. Shock is so prevalent in ordinary chondrites that the petrographic and mineralogical effects have been studied at some length and shock classification schemes have been developed (Stöffler et al., 1988, 1991). With shock, crystal structures are changed, iron and sulfide phases form eutectic melt veins, and crystalline feldspar melts and flows through the veins. It is undoubtedly this damage to feldspar that causes the decrease in the induced TL levels. The shock levels inferred from the TL decrease are consistent with shock levels inferred for mineralogical changes. By comparing induced TL data with ^{40}Ar, which is released by shock at 800 °C, it is possible to sort the meteorites into three groups (Fig. 22). Those heated to <800 °C (~63%) form a trend in which TL sensitivity weakly correlates with ^{40}Ar, suggesting that thermally induced degassing is associated with heating that lowers TL sensitivity, perhaps by darkening or loss of crystallinity. Heating

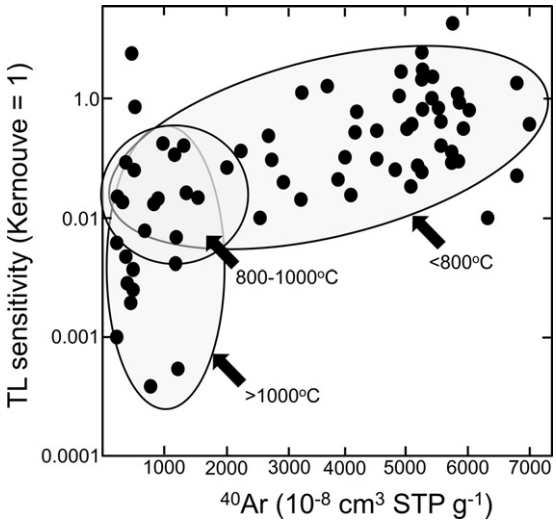

Fig. 22. Plot of TL sensitivity again ^{40}Ar for shock heated ordinary chondrites. Indicated are post-shock residual temperatures based on TL sensitivity, ^{40}Ar and the heating data in Fig. 5 of Haq et al. (1988), assuming uniform post-shock cooling rates and that the shock event occurred recently (<1 Ga). The meteorites plotted can be divided into three post-shock temperature reginmes (Haq et al., 1988).

to >1000 °C (~23% of the samples) has caused major ^{40}Ar loss and major loss of TL signal caused by shock-melting of the feldspar. In the overlap region are meteorites (~14%) heated enough to cause gas-loss but not enough to melt feldspar. We assume they experienced temperatures of 800–1000 °C.

Hartmetz et al. (1986) measured the induced TL properties of terrestrial feldspar previously shock-loaded and studied by Ostertag (1983). Again they found the behavior was similar to the data of Haq et al. (1988) who examined the TL properties of samples of the Kernouve H5 chondrite, similarly shock-loaded. The similarity between the meteorite and the feldspar was not restricted to TL sensitivity (Fig. S12), but also extended to changes in peak temperature as the feldspar (in this case oligoclase) was heated above the order–disorder transformation by the heat associated with the shock events.

A special case of shock effects in meteorites that can be followed by TL studies are the martian meteorites which are discussed below.

4.2.5. Regolith breccias

The regolith breccias are meteorites whose constituents have clearly spent most of their history at or close to the surface of their airless parent bodies (Keil, 1982). They are very distinctive in appearance consisting of sizeable clasts of normal chondrite material embedded in a very dark matrix rich in solar wind gases and carbon. They also contain charged particle tracks caused by energetic particles emitted by the Sun. Most xenolithic clasts in regolith breccias usually are CM or CM-like material (Wilkening, 1976). In fact, they are often referred to as gas-rich regolith breccias, because they were first identified through their high inert gas contents.

Haq et al. (1989) found that the dark matrix of these meteorites had TL sensitivities lower than the adjacent clasts and that the ratio of the TL sensitivity of the dark matrix to the TL sensitivity of the clasts was a measure of the maturity of the matrix. The TL ratio correlated with several of the parameters that characterize regolith breccias, inert gas content, carbon content, and track density. At one time there was controversy over the origin of the dark matrix, whether it was a new kind of primary material (Binns, 1967; Wilkening, 1976; Bart and Lipschutz, 1979; Lipschutz et al., 1983) or whether it was comminuted and contaminated clast material (Fredriksson and Keil, 1963; Suess et al., 1964; Müller and Zähringer, 1966; Mazor and Anders, 1967; Ashworth and Barber, 1976). However, cathodoluminescence and other studies show that the matrix is comminuted clast material (Akridge et al., 2004). The process and mechanism for lowering TL sensitivity during regolith working is seen in lunar soil cores and is the destruction of crystalline feldspar by melting during long term micrometeorite impact (Section 5.5).

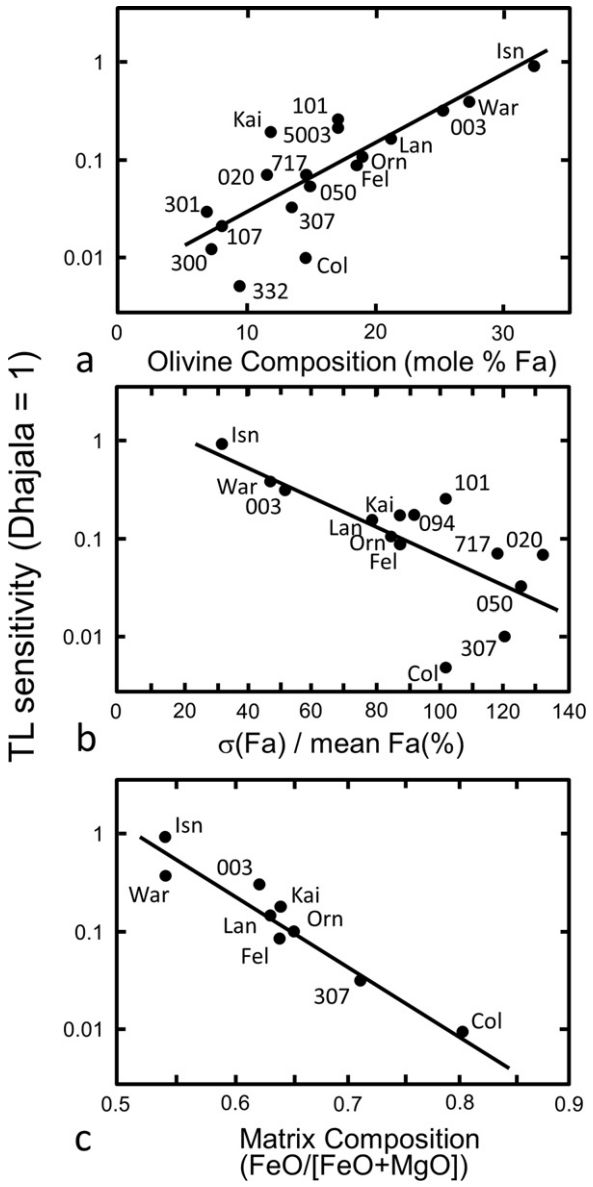

Fig. 23. Thermoluminescence sensitivity of the 120 °C peak for CO chondrites against (a) olivine composition (mol%), (b) the heterogeneity of the olivine composition (the coefficient of variation, σ/mean), and (c) FeO/(FeO + MgO) of the fine-grained matrix. As TL sensitivity increases, the olivine becomes richer in iron and less heterogeneous while the matrix decreases in iron. The iron content of the matrix of Colony may have been increased by weathering (Sears et al., 1991b).

4.3. Carbonaceous chondrites and their inclusions

4.3.1. Carbonaceous chondrites

Induced TL studies on meteorites other than ordinary chondrites have followed similar lines to those on ordinary chondrites. While >90% of the meteorites observed to fall are ordinary chondrites, equally important are the small classes like CO and CV carbonaceous chondrites (Weisberg et al., 2006), with TL properties somewhat similar to those of the ordinary chondrites.

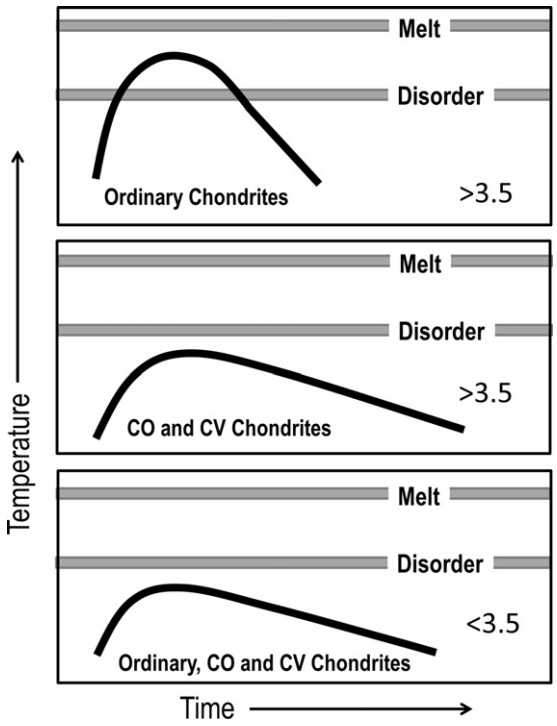

Fig. 24. Schematic diagram of the time–temperature histories of ordinary, CO, and CV chondrites based on TL and other studies. The CV and CO chondrites of petrologic type <3.5 did not experience sufficient peak metamorphic temperatures to produce disordered feldspar, while ordinary, CV, and CO chondrites of petrographic types >3.5 were metamorphosed to a higher degree but still below the order–disorder transformation temperature for feldspar. Ordinary chondrites of petrographic types >3.5 were heated to temperatures or for times that varied with petrographic type (Guimon et al., 1995).

The CO and CV meteorites have been classified into petrographic types, much like ordinary chondrites (Scott and Jones, 1990; Sears et al., 1991b; Guimon et al., 1995; Chizmadia et al., 2002). Olivine composition, olivine heterogeneity, and fine-grained matrix composition showed the expected trends with TL sensitivity justifying subdivision into types 3.0–3.9 (Fig. 23). With increasing metamorphism, and increasing TL sensitivity, olivine becomes more fayalitic and less heterogeneous and the matrix becomes poorer in iron as it coarsens to form discrete metal grains (McSween, 1977a,b; Rubin et al., 1985). Additionally, Ni in kamacite increases and Co decreases, Cr in kamacite decreases, and bulk C and ^{20}Ne decrease so that all these parameters can be used in defining the petrographic type (Table 6). Similar data can be used to subdivide the CV chondrites (Table 7). It should be stressed that the subdivisions proposed for CO and CV (like those for UOC) are based on empirical correlations observed between the TL data and a wide variety of mineralogical, textural, and compositional data, and not on our understanding of the underlying mechanism (Bonal et al., 2006, 2008).

There are, however, major differences in the TL peak shape data, and therefore the metamorphic history, between these C chondrites and the ordinary chondrites. This is summarized in Fig. 24. The peak shape parameters indicate that while TL sensitivities suggest levels of alteration equivalent to high type 3 ordinary chondrites, metamorphism occurred below 500 °C because the peak shape remained in the ordered field. In fact, to achieve the TL sensitivities suggestive of types >3.5, CO and CV chondrites must have spent longer periods below ~500 °C than the ordinary chondrites. Contrary to the comment of Huss et al. (2006; p. 579), this conclusion is not based on assumed temperatures but purely on glow curve shape.

Huss et al. (2006) suggest that CO3.0 chondrites had experienced ~200 °C and that Kainsaz CO3.2 experienced ~300 °C, based on a variety of mineralogical and compositional data, but in the absence of estimates for types >3.5 there is no mineralogical evidence to confirm or refute the TL palaeothermometry.

4.3.2. Calcium–aluminum-rich inclusion (CAIs) in the Allende CV chondrite

The refractory inclusions in meteorites, particularly Allende, have attracted considerable attention because they appear to be the first formed solids in the solar system and contain a number

Table 6
Definition of the subtypes of CO chondrites (Sears et al., 1991a).

Type	TL sens (Dhajala = 1)	Mean Fa (mol%)	σFa/Fa (%)	Matrix FeO/(FeO + MgO)	Kam Ni (wt%)	Kam Co (wt%)	Kam Cr (wt %)	C (wt%)	^{20}Ne 10^{-8} cc/g
3.0	<0.017	<11.0	>126	>0.77	<4.4	<0.2	>0.5	>0.65	>19
3.1	0.017–0.030	11.0–13.5	112–126	0.73–0.77	4.4–4.6	0.2–0.4	0.47–0.50	>0.65	>19
3.2	0.030–0.054	13.5–16.0	102–112	0.70–0.73	4.6–4.8	0.4–0.6	0.34–0.47	0.55–0.65	16–19
3.3	0.054–0.10	16.0–18.5	90–102	0.67–0.70	4.8–5.0	0.6–0.8	0.26–0.34	0.45–0.55	13–26
3.4	0.10–0.17	18.5–21.0	78–90	0.63–0.67	5.0–5.2	0.8–1.0	0.18–0.26	0.35–0.45	10–13
3.5	0.17–0.30	21.0–24.0	64–78	0.60–0.63	5.2–5.4	1.0–18	0.10–0.18	0.25–0.35	10–7l
3.6	0.30–0.54	24.0–27.5	46–64	0.57–0.60	5.4–5.7	<0.10	<0.15	0.15–0.25	7–4
3.7	0.54–1.00	27.5–31.0	28–46	0.53–0.57	5.7–6.0	<0.10	<0.15	<0.15	<4
3.8	1.0–1.7	31.0–35.0	8–28	<0.53	6.0–6.4	<0.10	<0.15	<0.15	<4
3.9	>1.7	>35.0	<8	<0.53	6.4–6.7	<0.10	<0.15	<0.15	<4

Table 7
Definition of the subtypes of CV chondrites (Sears et al., 1995).

Type	TL sensitivity (Dhajala = 1)	Mean Fa (mol%)	σFa (%)	Ni in sulfide[a] (wt%)	C (wt%)	H_2O (wt%)
3.0	<0.017	<8.0	>110	<17	>1.05	>3.5
3.1	0.017–0.030	8.0–10.0	90–110	17–20	0.75–1.05	2.5–3.5
3.2	0.030–0.054	10.0–11.0	70–90	20–22	0.60–0.75	2.5–3.5
3.3	0.054–0.10	11.0–12.0	50–70	20–23	0.45–0.60	2.0–2.5
3.4	0.10–0.17	12.0–13.0	40–50	23–24	0.40–0.45	1.5–2.0
3.5	0.17–0.30	13.0–13.5	30–40	24–25	0.30–0.40	1.3–1.5
3.6	0.30–0.54	12.5–14.0	20–30	25–26	0.20–0.30	0.8–1.3
3.7	0.54–1.00	13.5–14.0	5–20	26–28	0.15–0.20	0.5–0.8
3.8	1.0–1.7	14.0–14.5	<5	>28	<0.15	<0.5
3.9	>1.7	>14.5	<5	>28	<0.15	<0.5

[a] Applicable to oxidized subgroup of the CV chondrites only.

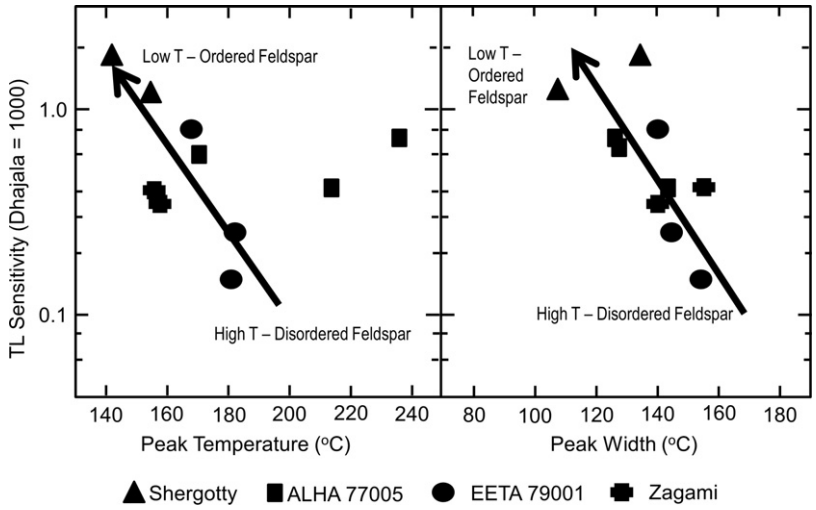

Fig. 25. Thermoluminescence sensitivity of Shergottites (normalized to Dhajala = 1000) plotted against the temperature at which TL emission is at a maximum (left diagram) and the width of the peak at half its maximum intensity, FWHM (right diagram). The trend lines indicate the expected path for a cooling series (Hasan et al., 1986).

of unusual isotopic properties (Grossman, 1980). They consist of a number of Ca- and Al-rich minerals, most of which are expected to have high TL and CL levels. This is found to be the case. Sears et al. (1995) reported TL data for six Allende inclusions and mineral separates from Allende inclusions which are shown in Fig. S13. These authors suggested that the induced TL data demonstrate the effects of metamorphism, suggested by Meeker et al. (1983), during which low-feldspar was converted to high-feldspar that was in turn converted to melilite $[(Ca,Na)_2(Al,Mg,Fe^{2+})(Si,Al)_2O_7]$.

4.4. Planetary meteorites

In addition to the chondrites, there are many classes of meteorites that are not asteroidal and may be considered "planetary". Martian meteorites (once known as the SNC meteorites) (Papike et al., 2009), basaltic meteorites (also known as HED meteorites, after the Howardite, Eucrite and Diogenite meteorites), which are thought to be ejecta from the large asteroid, 4 Vesta (Keil, 2002), and lunar meteorites (Korotev, 2005). Mention should also be made of lunar samples returned by the Apollo program (Heiken et al., 1991).

4.4.1. Martian meteorites

In the case of the martian meteorites, the component that is feldspathic in composition and has the outline of crystalline feldspar, is in fact an unusual glass called maskelynite (Milton and de Carli, 1963). In these cases, shock has apparently caused the conversion of feldspar to glass by a solid state transformation without melts being involved. Maskelynite is an extremely unstable glass that readily crystallizes. As a result, Shergottites placed in an oven for, say, 1 h at 900 °C, show a 100-fold increase in induced TL levels (Hasan et al., 1986). This suggests that since formation of the maskelynite, these meteorites have suffered little if any thermal events. The structure of the glow curve provides information on the conditions of shock. After the shock formation of maskelynite, trace amounts of feldspar formed during cooling. The relative amounts of ordered and disordered feldspar produced depended on the time spent in each field, in other words, the cooling rate. Thus plots of TL sensitivity against peak temperature and peak width show trends that can be interpreted in terms of cooling rate (Fig. 25). We postulate that slow cooling of the feldspathic glass favors the formation of trace amounts of crystals and therefore increases the TL sensitivity. Slow cooling also favors the formation of low-temperature (ordered) feldspar, with its lower peak temperatures and broader peaks. Thus there are trend lines in both plots in Fig. 25, going from bottom right to top left, reflecting decreasing cooling rate.

4.4.2. HED meteorites

The eucrites, while essentially basalts, have also experienced parent body metamorphism that can be quantified using induced TL measurements (Batchelor and Sears, 1991a). The mineral responsible for the TL emission is still feldspar, but the range in TL sensitivity is smaller than for the ordinary chondrites. The TL sensitivity data are shown in Fig. 26 where it can be seen that unequilibrated eucrites have lower TL sensitivity than equilibrated and cumulate eucrites. In fact, if one assigns petrologic types on the basis of the TL sensitivity as shown in the figure, the types are in excellent agreement with those proposed by Takeda et al. (1983) based on pyroxene chemistry. The only exception is Ibitira, an unusual vesicular eucrite, which clearly has a unique history involving surface flow. One would assume this has left the feldspar as glass, and hence the

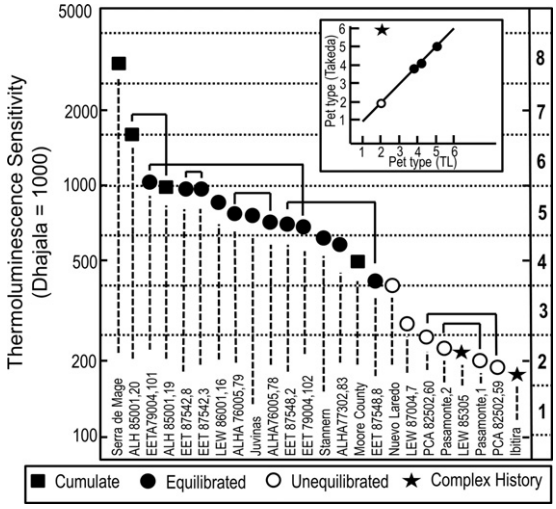

Fig. 26. Induced TL sensitivities for whole-rock samples of equilibrated, unequilibrated and cumulate eucrites and lavas (i.e., Ibitira) have lower TL sensitivity than the equilibrated eucrites and cumulates. The inset compares petrographic type assigned by Takeda et al. (1983) based on pyroxene properties. Except for the anomalous Ibitira, the type assignments on the basis of TL and pyroxene data show excellent agreement (Sears et al., 1997).

Table 8
Definition of the subtypes for eucrites (Takeda et al., 1983; Batchelor and Sears, 1991a,b).

Type	TL sensitivity (Dhajala = 1000)	Pyroxene characteristics	Meteorites
1	<160	Extensive Mg–Fe zoning trend in pyroxene, Fe-rich augite	Y-75011, clasts in Y074450 and Y-75015
2	160–250	Fe-rich pyroxene not seen, Mg–Fe–Ca trend preserved	Pasamonte, Ibititra, LEW850305, PCA82502, clasts in Y-74159
3	250–400	Mg–Fe zoning mostly disappeared, Fe–Ca trend from core to rim preserved	LEW87004, Y-790226
4	400–630	Trend from host to exsolved augite dominant, original Fe–Ca trend can be recognized	Stannern, Nuevo Laredo, Millbillillie, Moore Co., EET87548, ALHA77302
5	630–1000	All zoning has disappeared, exsolution trend dominant	Juvinas, Haraiya, Sioux Co., LEW85303, EETA79004, EET87542, LEW86001. ALHA76005
6	1000–1600	Partial to complete inversion of pigeonite to orthopyroxene	ALH85001
7	1600–2500	Partial to complete inversion of pigeonite to orthopyroxene	–
8	>2500	Partial to complete inversion of pigeonite to orthopyroxene	Serra de Mage

low TL sensitivity, while its pyroxenes were highly equilibrated. The descriptions of the petrologic types for eucrites appear in Table 8.

The cause for the variations of induced TL in eucrites is not the formation of crystals from glass but the diffusion of Fe^{2+}, a luminescence quencher, out of the feldspar (Batchelor and Sears, 1991b). This was evident from the CL mosaics and the literature on the composition of feldspars in these meteorites. Again induced TL peak shapes can be used for their insights into thermal history and indicate that the unequilibrated eucrites contain feldspar in the low-temperature form while equilibrated eucrites contain the high-form, so again we have a palaeothermometer for this class of meteorites (Sears et al., 1997). As with chondrites and terrestrial feldspars, heating experiments confirm this interpretation (Fig. S14). The howardites have TL properties reflecting their brecciated nature, being a mixture of eucrite and diogenite components.

4.5. Lunar samples

On a plot of TL sensitivity against peak temperature it is possible to recognize four fields, highland material and mare material, high-temperature feldspar and low-temperature feldspar (Fig. 27). Thus lunar sample types (Apollo samples and lunar meteorites) can be identified on the basis of their induced TL properties. Location on this plot reflects the nature and amount of feldspar, and thus the mixing and thermal history of the various samples (Fig. 27; Batchelor et al., 1997). Fig. S15 is an attempt to simply describe the history of lunar surface rocks in terms of their feldspar properties and thus induced TL properties.

The Apollo 16 and 17 regolith cores show variations in induced TL properties with maturity (amount of surface gardening), reflecting the destruction of feldspar by micrometeorite bombardment that converts surface material into agglutinates, which are irregular

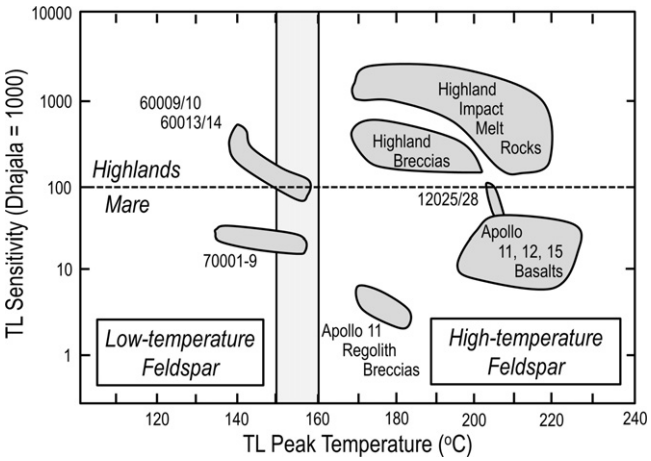

Fig. 27. Schematic diagram showing the fields for lunar rocks and soils on a plot of TL sensitivity against peak temperature, compared with proposed boundaries for mare/highlands and low- to high-temperature state, which is related to order/disorder. The lunar highland materials have TL sensitivities about an order of magnitude higher than the mare materials, but two soil cores have much lower peak temperatures than rocks from the same region. Regolith breccias are displaced to lower TL sensitivities and peak temperatures relative to other rocks of similar lithologies. The only pristine highland sample in our study and one clast-poor impact melt rock have a second peak at lower temperatures (Batchelor et al., 1997).

glassy fragments on dust. The process also converts low-feldspar to high-feldspar as it decreases TL sensitivity by destroying feldspar producing the negative trend lines in Fig. 27. The CL trends caused by this process are discussed below.

5. Cathodoluminescence studies of extraterrestrial materials

While induced TL is a highly sensitive means of looking at bulk properties of a geological sample, cathodoluminescence provides a means of looking at the petrography of the luminescent phases. It thus provides information that enhances the information obtained from TL measurements and provides a bridge to an array of techniques available to the geologist. For the ordinary chondrites, particularly the type 3 ordinary chondrites, the differences observed in CL properties as a function of metamorphism could not be more sweeping. Over 150 mosaics of the CL of extraterrestrial materials have been prepared by Akridge et al. (2004) who published 60 in an on-line supplement to their article (Table 9).

5.1. Ordinary chondrites – metamorphic trends

Fig. 28 summarizes the CL images of 12 type 3 ordinary chondrites of virtually all of the petrologic types. High-resolution versions are available via Akridge et al. (2004). Most of the details of these photomosaics have not been explored in any depth, but the broad sweep trends are as follows. The lowest petrologic type meteorites have CL images that are dominated by ubiquitous fine-grained material with bright red CL, in fact the color is identical to the large chondrule grains of forsterite observed in many chondrules. This fine-grained ubiquitous phase quickly disappears with the onset of metamorphism, becoming coarser and patchy by type 3.2. However, the majority of chondrule grains do not luminesce. Some of the forsterite rich chondrules have mesostases that produce a spectacular yellow CL. A few chondrules have blue mesostases. With increasing metamorphism red luminescing phases disappear and blue phases become more abundant until by petrologic type 3.9, the meteorites show a fairly uniform blue CL caused by feldspar. The trends in CL between these extremes are gradational to a point that it is possible to ascribe a

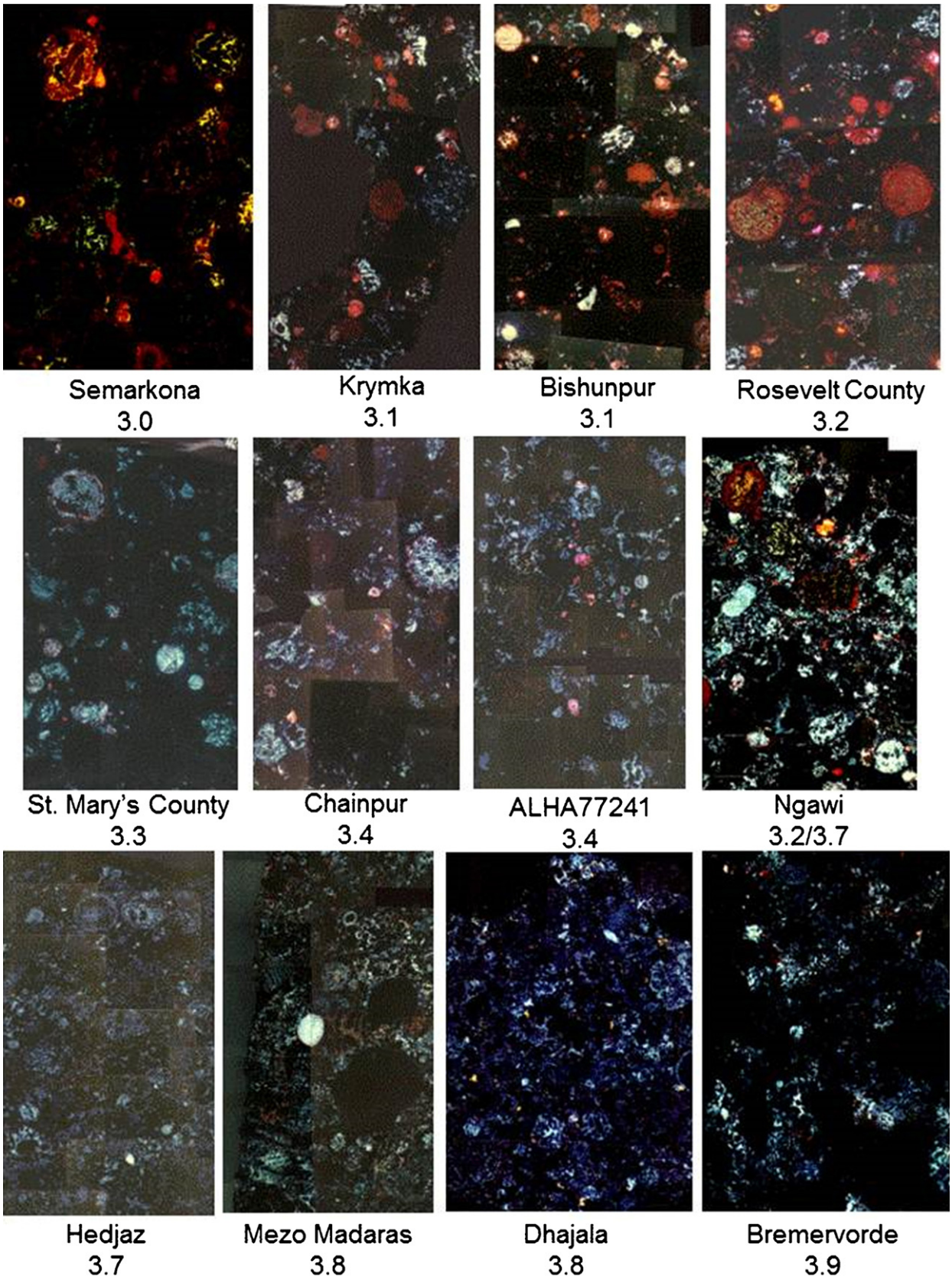

Fig. 28. Photomosaics of the cathodoluminescence of 12 unequilibrated ordinary chondrites (all at same scale, about a centimeter across) showing how the CL properties change systematically with petrographic type. High-resolution versions of these images are available in the on-line supplement of Akridge et al. (2004). These changes are quantified in the next figure.

Table 9
Cathodoluminescence mosaics of extraterrestrial samples in Akridge et al. (2004): samples, class, and figure number.

Carbonaceous chondrites		
Murchison	CM2	A1
Colony	CO3.0	A2
Allan Hills A77307	CO3.1	A3
Kainsaz	CO3.2	A4
Lance'	CO3.4	A5
Allan Hills A77003	CO3.4	A6
Isna	CO3.7	A7
Ordinary chondrites		
Semarkona	LL3.0	A8
Semarkona	LL3.0	A9
Semarkona	LL3.0	A10
Semarkona	LL3.0	A11
Semarkona	LL3.0	A12
Semarkona	LL3.0	A13
Krymka	LL3.1	A14
Bishunpur	LL3.1	A15
Roosevelt County 075	H3.1	A16
St. Mary's County	LL3.3	A17
Allan Hills A77214	LL3.4	A18
Chainpur	LL3.4	A19
Yamato 790448	LL3.6	A20
Hedjaz	L3.7	A21
Ngawi	LL3.2/3.7	A22
Mezö-Madaras	LL3.4/3.7	A23
Dhajala	H3.8	A24
Acfer 028	H4	A25
Allan Hills 81029	H4	A26
Fayetteville	Regolith breccia	A27
Plainview	Regolith breccia	A28
Eucrites and Howardite		
Pasamonte	Eucrite type 2	A47
Pasamonte	Eucrite type 2	A48
Juvinus	Eucrite type 5	A49
Kapoeta	Howardite	A50
Enstatite chondrites		
Allan Hills 84206	EH3	A29
Allan Hills 84170	EH3	A30
Pecora Escarpment 91085	EH4	A31
Pecora Escarpment 91238	EH4	A32
Saint-Sauveur	EH5	A33
Lewis Cliff 88180	EH5	A34
Allan Hills 85119	EL3	A35
MacAlpine Hills 88184	EL3	A36
MacAlpine Hills 88136	EL3	A37
Thiel Mountains 91714	EL5	A38
Reckling Peak A80259	EL5	A39
Allan Hills 81021	EL6	A40
Atlanta	EL6	A41
Khairpur	EL6	A42
Lewis Cliff 88135	EL6	A43
Lewis Cliff 87119	EL6	A44
Lewis Cliff 87223	EL3an	A45
Happy Canyon	ELan	A46
Lunar highland regolith breccias		
14318		A51
14318		A52
14135		A53
14318		A54
Pristine highland sample		
60015		A55
Lunar soils		
60009		A56
60009		A57
60009		A58
60009		A59
60010		A60

petrographic type on the basis of CL photomosaics alone. In fact, there is some suggestion that the CL has higher resolution for the lowest levels of metamorphism than TL.

Akridge et al. (2004) attempted to quantify these trends by defining a blue-red color index for each mosaic (Fig. 29). This is the ratio of the number of blue pixels in the image divided by the number of red pixels, as determined by Adobe Photoshop software. The area in question was essentially the entire thin section and is thus a precise description of that section. Uncertainties are comparable with the symbol size. Scatter within a meteorite can be judged from the replicates for Semarkona, which should be a worse case because it is an especially heterogeneous meteorite. Throughout the type 3 ordinary chondrites the index increases steadily from ~0.5 to ~3.0 as subtype increases. We will discuss Fig. 29 as we discuss each class in turn.

5.2. Ordinary chondrites – chondrules

Even a cursory look at the CL photomosaics is sufficient to show the importance of chondrules in determining the CL of type 3 ordinary chondrites and their range of properties. Since chondrules have been extremely well studied it is generally a simple matter to interpret the CL patterns in terms of phase and mineral chemistry. DeHart et al. (1992) sorted chondrules into classes on the basis of their CL and pointed out both primary variations and variations due to metamorphism. The DeHart et al. (1992) classes are shown in Fig. 30.

In terms of CL there are two main trends, one that starts with luminescent chondrules and one that starts with nonluminescent chondrules. As metamorphism proceeds the chondrules undergo systematic changes until the two trends evolve into the uniform blue CL characteristic of equilibrated chondrules. In addition to the two main trends, about 5% of the chondrules in the least metamorphosed chondrites have blue mesostasis and nonluminescent grains similar to the chondrules in equilibrated chondrites. Initially they have heterogeneous compositions that homogenize during metamorphism but this does not affect the CL of these chondrules. DeHart et al. (1992) subdivided the gradational trends into chondrule classes on the basis of their CL using the definitions in Table 10.

The compositional classification scheme for chondrules can be seen as a natural next step in the long history of chondrule classification (Sears, 2004). An initially solely petrographic scheme has evolved, over several decades, into a system that combines petrology with mineral chemistry, and now has reached pure mineral chemistry. The number of past schemes is noteworthy, with petrographic nomenclature having a half-life of about a decade, reflecting the subjective nature of petrography (Table 11). Making graphs that capture mineral chemistry and defining fields for classification is quantitative and objective, and this aspect of the

Table 10
Compositional classification of chondrules according to the CL of the major chondrule components and mesostasis composition.

Group	Mesostasis		Chondrule grains
	CL	Composition	
A1	Yellow		Red
A2	Yellow		None/Dull Red
A3	Blue		Red
A4	Blue	High An	None/Dull Red
A5	Blue	Low An	None
B1	None/Dull Blue	High Qz	None/Dull Red
B2	Dull Blue	Mid Qz	None/Dull Red
B3	Purple	Low Qz	None

Adapted from DeHart et al. (1992).[a]

[a] An, anorthite (as determined from the compositional norm); Qz (normative quartz).

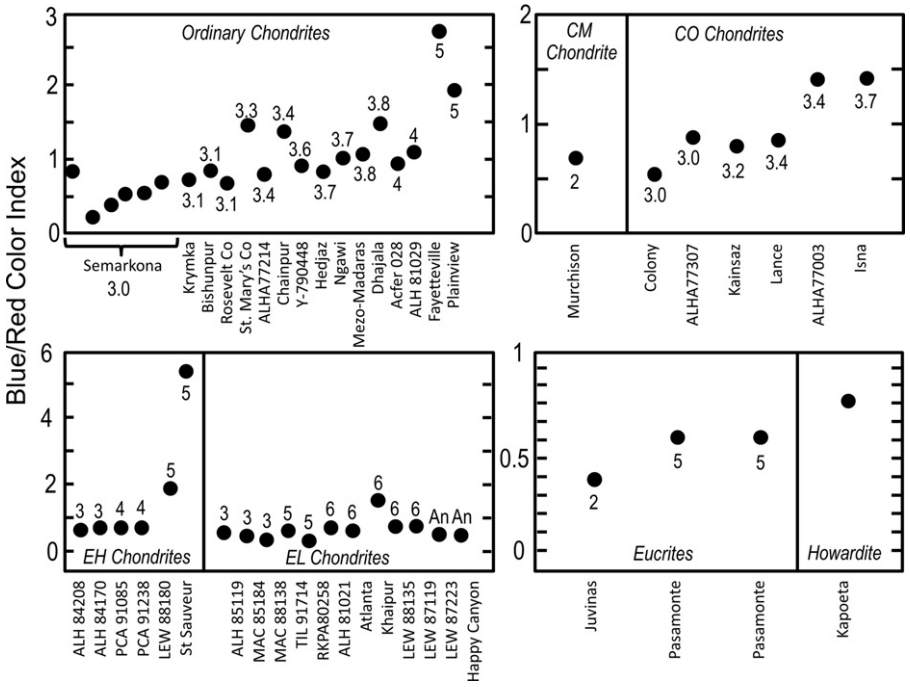

Fig. 29. Blue to red color index (ratio of the number of blue pixels to the number of red pixels in the digital image) for meteorites. (a) For ordinary chondrites, the index increases as a function of petrologic type as forsterite (with red CL) gains Fe and loses its luminescence while feldspar (with blue CL) is formed by crystallization of glass in response to metamorphism. (b) C chondrites also increase their blue-red color index as a function of metamorphism as forsterite is lost and feldspar forms. (c) The blue-red color index of EH chondrites increases with petrologic type, but this is not true of EL chondrites. This difference in CL trends between the EH and EL chondrites does not appear to reflect differences in mineral chemistry but seems to be related to difference in thermal history and pyroxene structure. Abbreviations: LEW, Lewis Cliff; MAC, MacAlpine Hills; RCP, Reckling Peak; TIL, Thiel Mountains. (d) Blue to red color index for two eucrites and a howardite. The feldspar of eucrites decreases in Fe, a quencher of CL, with increasing petrologic type. The feldspar in unmetamorphosed eucrites has a red-brown appearance, where the feldspar in metamorphosed eucrites has a bright yellow CL (Akridge et al., 2004).

compositional classification scheme has not been criticized. The problem has been one of implementation. It has proved difficult to define the class boundaries. In response to criticisms of the class boundaries for olivine from Scott et al. (1992), Sears et al. (1995) redefined and simplified the boundaries to those shown in Fig. S16. Criticism of the mesostasis field boundaries by Grossman and Brearley (2005) are more problematic. Without CL data these authors argued that the mesostasis boundaries needed revision because the mesostasis of DeHart et al. (1992) suffered sodium loss. They argued support from Scott et al. (1992) – who used a different analysis technique – but refuted analyses in four independent groups who had CL data and were well aware of the difficulties of analyzing for sodium and knew how to handle them. Further work is needed here, perhaps to define the mesostasis boundaries in terms of less controversial elements.

Fig. 31 shows how the abundance of the various chondrule compositional (CL) classes varies with petrographic type as the minerals and phases respond to equilibration during metamorphism. The

Table 11
The compositional classes of chondrule, previous equivalents, and deduced properties.

	Previous approximate equivalents		Deduced properties			
Group	Description	Reference	Temperature	Reduction	Mass loss	Cooling rate
A1	Droplet chondrules	Kieffer (1975)	High	Yes	Yes	Slow, phenocrysts and mesostasis at equilibrium
	Nonporphyritic chondrules Metal-rich microchondrules Type IA chondrules	Gooding and Keil (1981) Dodd (1978a,b) Scott and Taylor (1983)				
A2	Poikilitic pyroxene	Scott and Taylor (1983)	High	Yes, but less than A1	Yes, but less than A1	Slow, phenocrysts and mesostasis at equilibrium
	Type IB Type IAB	Scott and Taylor (1983) Jones (1992, 1994)				
A5	None		Low	No	No	Slow, phenocrysts and mesostasis at equilibrium
B1	Lithic chondrules	Dodd (1978a,b)	Low	No	No	Fast, considerable supercooling
	Clastic chondrules Metal-poor microporphyritic chondrules Type II	Dodd (1978a,b) Dodd (1978a,b) McSween (1977a,b)				

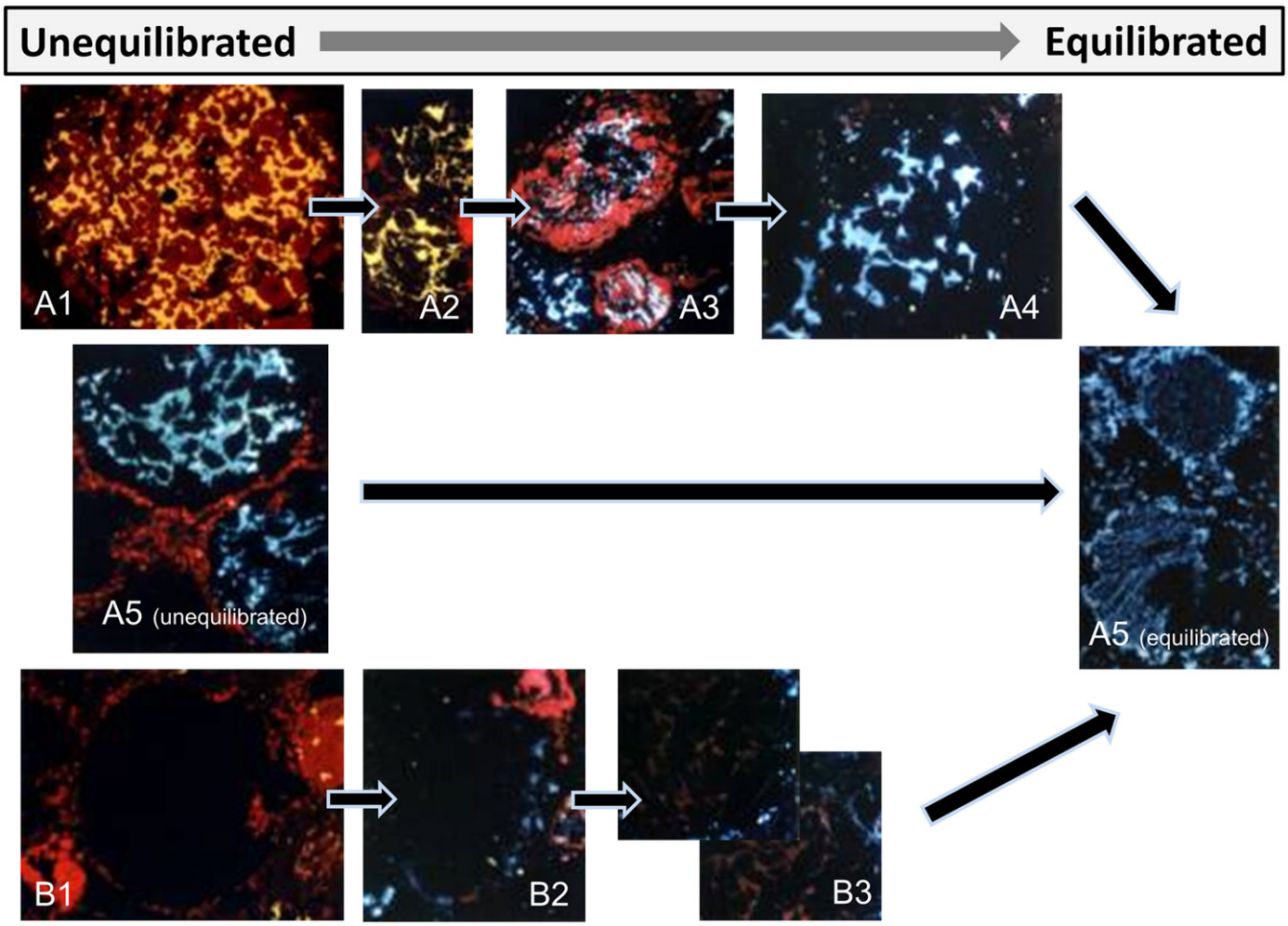

Fig. 30. Cathodoluminescence images of chondrules showing the variations that accompany metamorphism (DeHart et al., 1992). The three types present in unmetamorphosed chondrites are A1, B1 and A5 (unequilibrated) but with progressive metamorphism they all converge on A5 (equilibrated) passing through the intermediate classes of A2, A3, and A4 along one line and B2, B3 along the other. A5 chondrules are present at all levels of metamorphism, but homogenize as metamorphism progresses. (High-resolution versions of these images are available on-line as supplemental material to Akridge et al., 2004.).

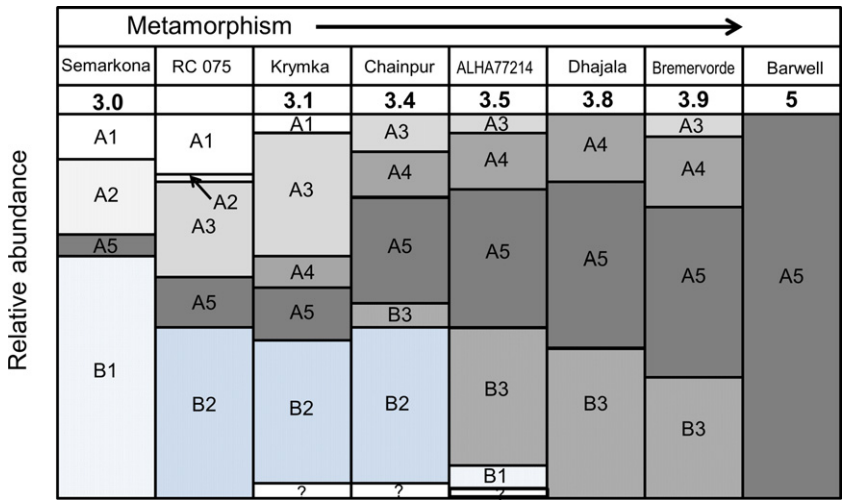

Fig. 31. The distribution (relative abundance by numbers) of chondrules over the compositional classes for seven type 3 ordinary chondrites and Barwell (L5). The classifications were made from low-powered photomicrographs of sections, using the CL to determine compositions of the major phases. It is possible to assign virtually all chondrules in the sections to compositional groups and, since composition and therefore the chondrule group varies with metamorphism (as well as formation conditions), it is possible to assign the especially significant Roosevelt County 075 meteorite to petrologic type 3.1 (Sears et al., 1995).

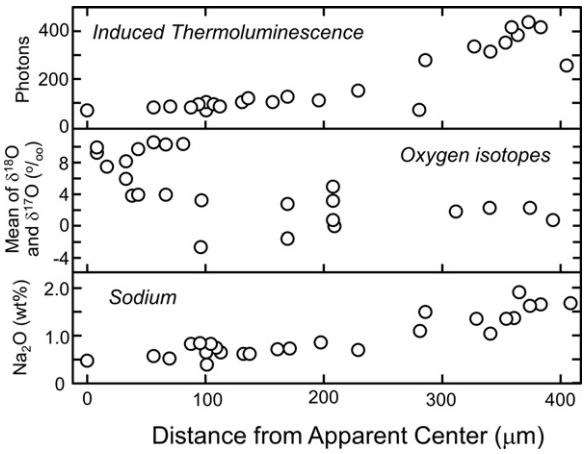

Fig. 32. Thermoluminescence, oxygen isotopes, and sodium as a function of apparent distance from the center of a large group A1 chondrule in Semarkona shown in Fig. 4. While induced thermoluminescence and sodium are highest towards the perimeter (as well as cathodoluminescence, see Fig. 4), and oxygen isotopes are heavier in the perimeter (Matsunami et al., 1993; Sears et al., 2009).

progression of chondrules through their respective metamorphic sequences (Fig. 30) is apparent in this diagram. This pattern of chondrule abundance was used by Sears et al. (1995) to assign a petrographic type to Roosevelt County 075.

It was the CL of a particularly large group of A1 chondrules that caught the attention of Matsunami et al. (1993) who obtained an induced TL image that illustrated the similarity of TL and CL. Regions of bright CL had higher induced TL (Fig. 1). These authors also found that the chondrule was chemically zoned, so the high CL–high TL region had high abundances of volatile elements compared to the interior. Subsequently Sears et al. (2009) obtained oxygen isotope data and found the mesostasis in the interior of the chondrule was isotopically heavy compared to the mesostasis in the outer regions and was fractionated in a mass-independent way (Fig. 32). These data suggest considerable mass transport during chondrule formation, in and out of the chondrule, and also the possibility that the non-mass-dependent fractionation of oxygen isotopes observed in meteorites might in some respects be related to chondrule formation.

5.3. Enstatite chondrites

Because of the high state of reduction and low bulk Mg/Si value, the silicate phase of enstatite chondrites is dominated by enstatite with very strong cathodoluminescence (Zhang et al., 1996a). This high state of reduction, which has attracted considerable attention, has resulted in a number of unusual minor phases (Keil, 1968). These help pin down formation conditions and, relevant to the present focus, suggest important differences in the thermal history of EH and EL chondrites. Sulfide chemistry suggests that EH chondrites cooled very rapidly after their last thermal event, whereas EL chondrites cooled slowly (Skinner and Luce, 1971; Zhang et al., 1996b).

The cathodoluminescence properties of enstatite and enstatite chondrites have been studied in considerable detail (Reid and Cohen, 1967; Grögler and Leiner, 1968; Keil, 1968; Leitch and Smith, 1982; McKinley et al., 1984; Marshall, 1988; Steele, 1989b; Dehart and Lofgren, 1994, 1995; Weisberg et al., 1994). The CL trends with petrographic type displayed by the enstatite chondrites were discussed by Zhang et al. (1996a) and high-resolution images of their CL were published by Akridge et al. (2004). The cathodoluminescence of EL chondrites is uniform throughout the petrographic type sequence, but the EH chondrites assume blue CL towards the higher types (Fig. 29). There is no simple compositional explanation for these differences but it seems to be associated with structure differences in the pyroxene of the two classes (Reid and Cohen, 1967). Pyroxene in the high petrologic type EH chondrites is in the disordered state while in the low EH types and throughout the EL chondrites the pyroxene is in the structurally ordered state. This would be consistent with the rapid cooling observed for the EH chondrites.

5.4. Carbonaceous chondrites

The CO chondrites show a pattern in CL properties with petrographic type very similar to that shown by ordinary chondrites, with the low types dominated by the red CL of forsterite, and the high types dominated by the blue CL of feldspar, with a gradational trend in between (Sears et al., 1991b). The color index varies with petrologic type in a way identical to the ordinary chondrites (Fig. 29). As discussed above, these trends are well understood in terms of changes in minerals and phases responsible for the observed TL and CL.

The CL properties of the Murchison meteorite have proved of special interest because of the variety of processes they reveal (Fig. 33). The information content of the CL mosaics published by Akridge et al. (2004) has not been fully exploited and this is especially true of Murchison. The Murchison CM chondrite plots at the low end of the blue-red index range (Fig. 29) because its CL is dominated by the intense red CL of forsterite. Murchison consists largely of large chondrules with various properties enclosed in a fine-grained matrix. There are clearly two major chondrule types, those containing forsterite with bright luminesce and those containing Fe that do not luminesce. All chondrules are rimmed with fine-grained material (Sears et al., 1993). These chondrules with their rims appear to have been corroded, to varying extents, by aqueous alteration. Significantly, the thickness of the rim varies with the nature of the chondrule, the luminescent chondrules having thick rims while the nonluminescent chondrules have very thin rims (Fig. S17). This has been explained in terms of the luminescent chondrules being group A1 which have suffered reduction and mass loss, the evaporated volatiles condensing on the chondrule, while the nonluminescent chondrules (group B1), suffered limited reduction and mass loss during chondrule formation. Thus the rims are recondensed material evaporated from the enclosed chondrule during chondrule formation. Before final lithification, the components of Murchison underwent aqueous alteration. A scenario describing this process, driven mostly by interpretations of the CL mosaic, is shown in Fig. S18.

5.5. Lunar samples

Akridge et al. (2004) show high-resolution photomosaics for four lunar highland regolith breccias, a pristine highland sample and lunar soil cores. The CL of the highland breccias was examined by Symes et al. (1998) and one of their sections is reproduced here with an explanatory sketch as Fig. 34. The highland breccias studied by these authors are from Fra Mauro and consist essentially of ejecta from the Imbrium impact. Between the clasts of these breccias is a matrix of lithified soil of which about 10% by volume consists of crystalline lunar spheres which appear yellow in the CL mosaic and stand out against the ubiquitous blue feldspar. The difference in the CL of the feldspar in the crystalline lunar spherules and the feldspar elsewhere signals major compositional differences and a different history. Symes et al. (1998) argued that they were formed from melt spheres ejected during impact. They argued that the same mechanics is possible for asteroids, where large impacts, those that produce transient craters comparable in diameter to the radius of

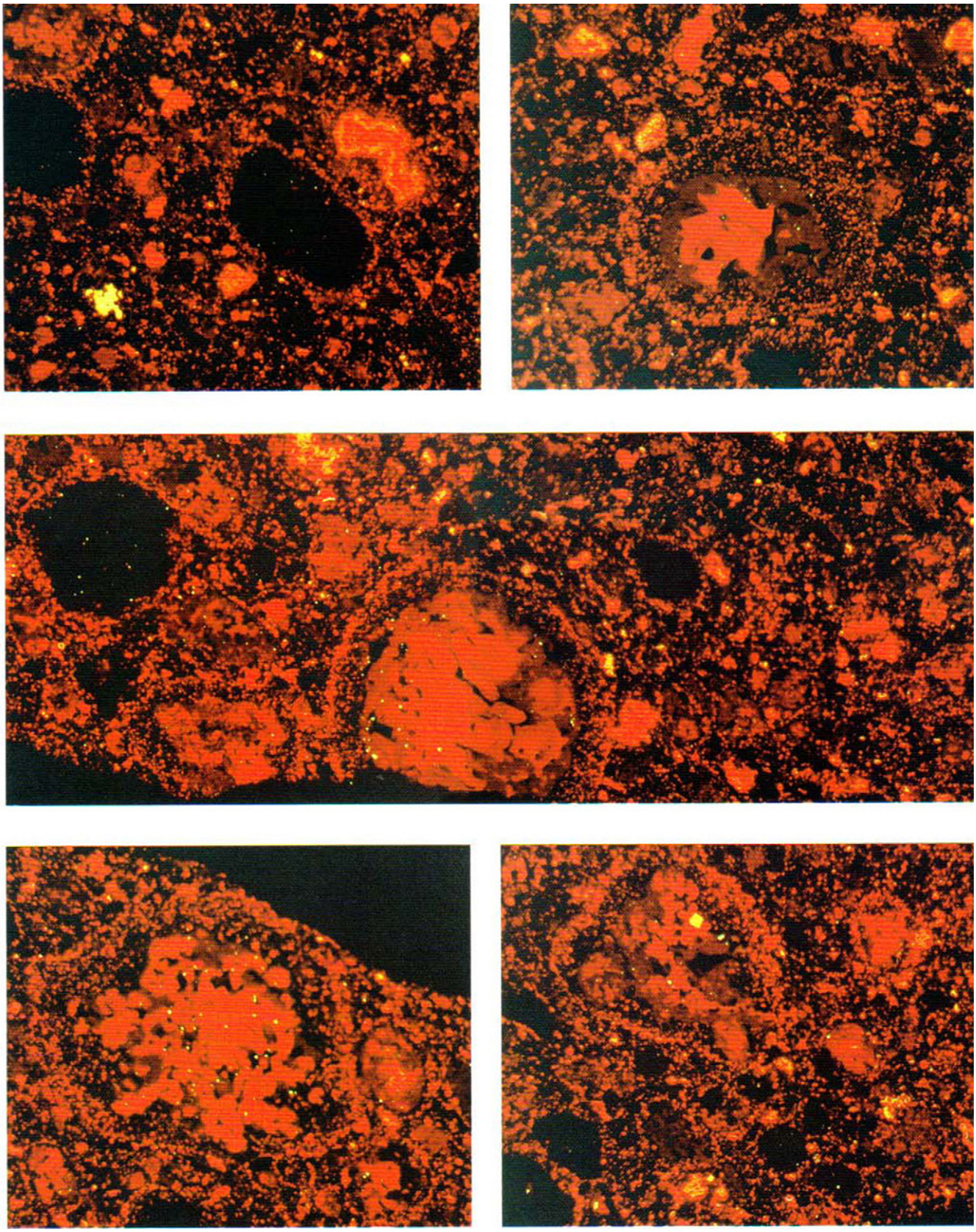

Fig. 33. Cathodoluminescence (CL) images of structures in the Murchison CM chondrite. (a, top left). Matrix region including two group B chondrules and an irregular refractory inclusion with red and yellow CL. (b, top right). Group A chondrule with a thick fine-grained rim and CL zoning in the large central olivine. (c, center). Large group A chondrule surrounded by a thick fine-grained rim. (d, bottom left). Another irregular group A chondrule with a thick fine-grained rim and numerous tiny fields of mesostasis with yellow CL. (e, bottom right). An irregular group A chondrule with a thick fine-grained rim and mesostasis which has one small region with yellow CL. Several small group B chondrules are in the lower half of the image, each with thin fine-grained rims. All images are to the same scale, the horizontal width of the four smaller figures is 150 mm (Sears et al., 1993).

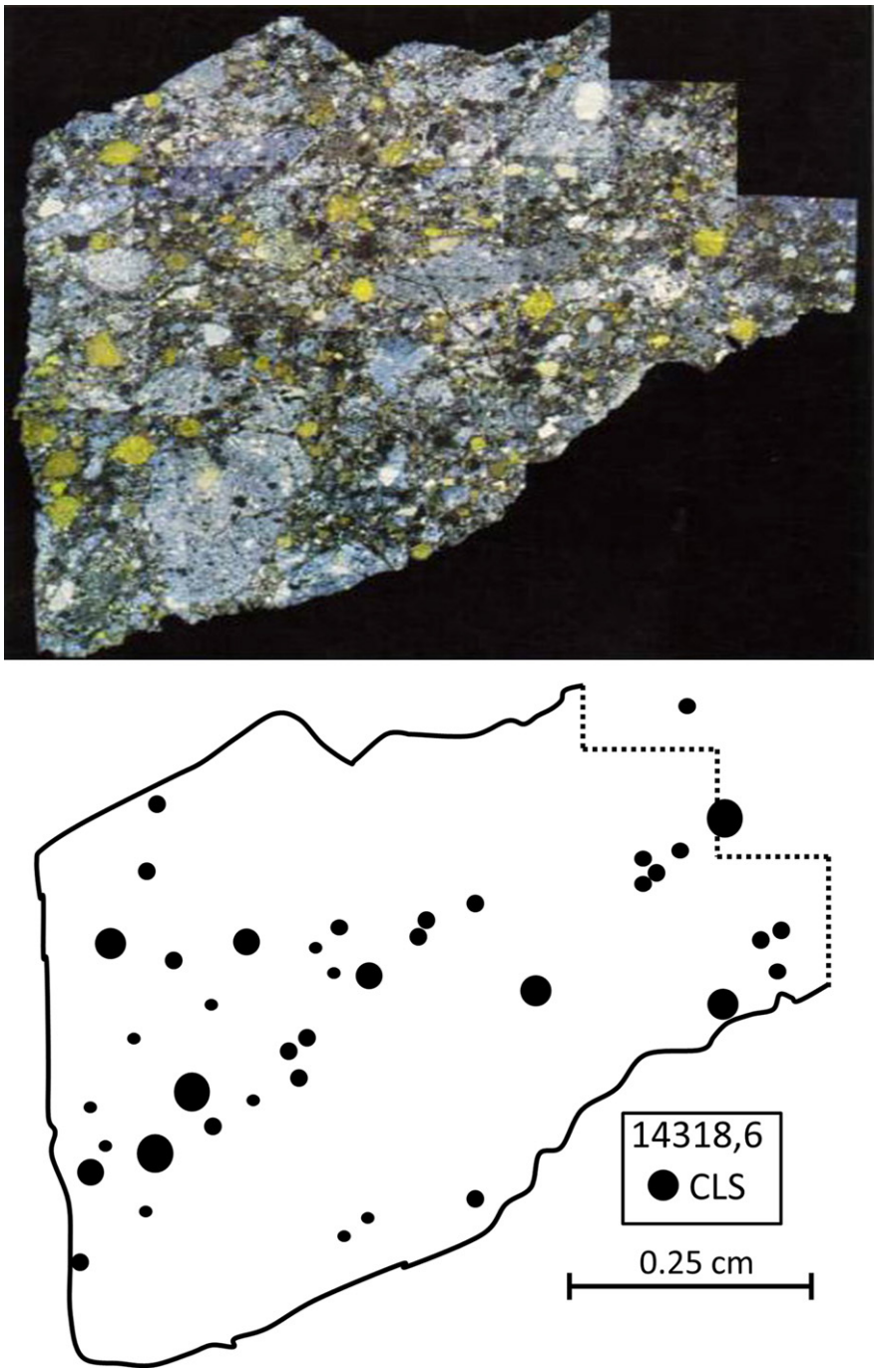

Fig. 34. Photomosaic of the cathodoluminescence of Apollo lunar regolith breccia 14318 and a map showing the location of crystalline lunar spherules and glass spherules. The spherules stand out as the yellow objects in a background of ubiquitous feldspar with blue CL. The areas free of crystalline lunar spherules are clasts (Symes et al., 1998).

the target object, could have produced meteoritic chondrules by impact.

Three samples from a lunar drill core were examined by Batchelor et al. (1997) who produced photomosaics of their cathodoluminescence. These were published at high resolution by Akridge et al. (2004). The samples show blue-green grains of feldspar luminescence which decreased in abundance with increasing maturity as measured by agglutinate content, inert gas content, solar flare track density, and the paramagnetic parameter (Fig. 35). Regolith working converts the feldspar grains to glasses and agglutinates which do not luminesce. This explains the decrease in TL sensitivity with increasing regolith maturity.

6. Thermoluminescence studies of small particles

6.1. Lunar grains

Probably the first study of the TL properties of small extraterrestrial particles was the Hoyt et al. (1972) study of grains from the Apollo 14 regolith. These authors found that the low-temperature TL (~200 °C) was being produced by one grain in 15, namely a small fraction of the feldspar, while the high-temperature TL was produced by grains rich in K or P. This might be consistent with the CL photomosaics discussed in Section 5.5 where the yellow CL due to calcic plagioclase while the blue CL was due to Na and K rich

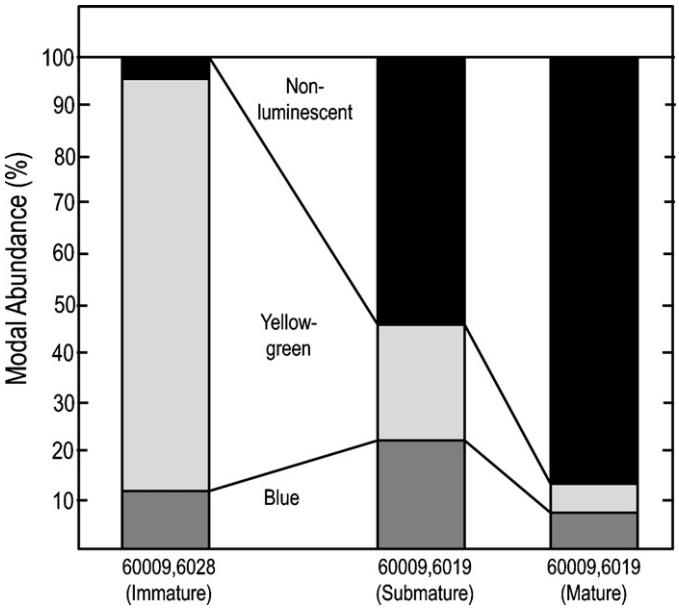

Fig. 35. Modal abundances of the major phases in terms of CL color in three Apollo 16 lunar soil samples from the 60009/10 core. Phases that exhibit luminescence (yellow-green or blue) are feldspar, while nonluminescent phases include heavily shocked feldspar, glass, pyroxene, olivine, and metal. The abundance of nonluminescent grains increases as a function of soil maturity in these samples at the expense of yellow-green luminescing grains (Batchelor et al., 1997).

feldspars. These authors found that while natural TL could provide an indication of regolith burial depth, they were not of sufficient accuracy to determine temperature gradients (Walker et al., 1972).

6.2. Micrometeorites

A final class of extraterrestrial materials to be considered are the small particles, which are becoming especially important with spacecraft missions returning tiny amounts of new extraterrestrial materials to Earth (Zolensky et al., 2000). For many decades, interplanetary dust particles have been collected by stratospheric aircraft flights and micrometeorites have been recovered from the ice of Antarctica (Grün, 2001). The challenge for thermoluminescence studies of such particles – as with most techniques – is their tiny size and weak TL signals. Sedaghatpour and Sears (2009) obtained signals from four 100–200 μm micrometeorite particles, and Craig and Sears (2009) obtained signals from six comparable size matrix particles from the type 3.0 Semarkona meteorite. The major conclusion is that while the bulk of these materials is amorphous and difficult to characterize, the TL peak temperature and TL peak width relationships suggest that TL signal was being produced by forsterite, not feldspar (Fig. S19). Forsterite is becoming an increasingly important component of primitive materials (Crovisier et al., 1997; Kloeck et al., 1989; Koike et al., 2002; Steele, 1986, 1989a; Zolensky et al., 2006).

6.3. Semarkona matrix

Most recently, Craig and Sears (2010) have found a way to reproducibly and reliably obtain data from 10 μm to 15 μm particles of the matrix of the Semarkona chondrite with the hope that it will eventually provide insights into the thermal history of interplanetary dust and cometary particles returned from the Stardust mission. The relationship between matrix, chondrules, and the bulk TL of Semarkona was discussed by Craig and Sears (2009). To extract independent information on radiation and thermal energy, Craig and Sears (2010) took the ratios of (1) natural TL to the induced TL (both at 400 °C in the glow curve) as a proxy for radiation dose absorbed, and (2) natural TL at 250 °C and the natural TL at 400 °C as a proxy for temperature experienced. Thus NTL400/ITL400 should increase with increased dose absorbed, NTL250/NTL400 should decrease with increased temperature. These authors identified four history regimes and noted the distribution of matrix fragments within these (Fig. S20). (1) Most fragments plot in the field corresponding to high temperatures and low radiation (region C), while regions corresponding to high radiation – high temperature (region A) and low temperature – low radiation (region D) are less well populated. The region of low temperature – high radiation (region B) is unpopulated. This was interpreted as reflecting the presence of radiation hot spots during cosmic radiation (e.g., feldspar grains since Ca has a high cross section for neutron capture), and different thermal gradients and rates of attenuation of radiation around those hot spots. These are probably the first data on microradiation environments in meteorites since the charged particle track work of the early 1970s, but demonstrates the feasibility of exploring the thermal and radiation history of 10 μm extraterrestrial particles using the thermoluminescence technique.

7. Concluding remarks

Over the last four or five decades, studies of the natural and induced TL properties and CL characteristics have been performed on most of the major forms of extraterrestrial material. Something of value has been obtained for most of these materials.

In the case of natural TL studies, the decision of the community was to include these measurements in the preliminary examination of Antarctic meteorites in order to identify meteorites with unusual thermal and radiation histories and provide information on orbits and terrestrial age. Such data have been obtained for large numbers of meteorites, from both the hot and cold deserts, especially if theoretical models and assumed environmental temperatures are applied. These data can sometimes be used to find trends in terrestrial age distribution on ice fields which leads to insights into concentration mechanisms. One large find of paired meteorites from the Allan Hills of Antarctica appears to have undergone a significant orbit change within the last 10^5 years.

In the case of type 3 chondrites, induced TL measurements provide a new and quantitative means of determining their petrographic (metamorphic) classification and the data are now in wide use. It also provides a means of some level of palaeothermometry, independent of mineral chemistry methods and is essentially insensitive to lack of chemical equilibration between minerals. Induced TL studies have been extended to other problems. Together with laboratory heating measurements, and measurements on analogous terrestrial minerals, they provide new insights into secular variation in the fall of chondrites to Earth, the shock history of chondrites, the post-shock cooling history of martian meteorites, the metamorphic history of eucrites, and the classification and regolith history of lunar samples.

Cathodoluminescence observations often supply petrographic and mineralogical information that enhances explanations for the TL data as well as providing an additional window through which to view the history of these objects. The metamorphic changes experienced by type 3 chondrites, enstatite chondrites, and eucrites, and the regolith history of lunar samples can be addressed in a way that is complementary but independent of other techniques such as petrography and I_s/FeO. In fact, it might be possible to infer metamorphic changes in the low type 3 ordinary chondrites with a precision greater than induced TL. The compositional variation in chondrule properties are well reflected in their CL properties that, unlike the petrographic chondrule classification schemes, reflect both primary differences and metamorphism and identify a previously undescribed chondrule class in low types. Chondrule like

objects in lunar breccias stand out especially well having bright yellow CL against a background of blue CL feldspars, thus enabling easy location and rapid statistical studies.

In the last few years techniques have been developed to measure increasingly smaller particles, micrometeorites and ~10 μm fragments of Semarkona matrix.

Thermoluminescence and cathodoluminescence studies provide a unique way of looking at fundamental processes experienced by extraterrestrial materials. Often they provide quantitative data and enable a precision not possible by other techniques, and they can also be applied to largely amorphous materials impossible or difficult to study by other techniques. Depending on how these techniques are used, they can be applied to a great diversity of problems, from planetary to geological.

Acknowledgments

We thank Associate Editor Klaus Keil for soliciting this Invited Review, for advice, encouragement, and for guiding us through the process, and Mike Weisberg and Steve Sutton for extremely helpful reviews. DS is grateful to all the students and colleagues who have worked with him on this topic over the last 40 years and who are responsible for the understandings that we have developed. He is also grateful to the many colleagues who took an interest in our work and offered the best kind of encouragement; they found our work useful. He is also grateful to the Research Corporation, NASA, NSF, and the State of Arkansas who supported the research. Finally, he is grateful to Hazel Sears who has shared this interest with him for 40 years and reviewed the present article. AS is grateful to Professor N. Bhandarin, Dr D. Sengupta, and Dr. Rabiul Biswas for their contributions and ideas. KN appreciates the support of the Visiting Researcher's Program of the Reactor Institute, Kyoto University, for ^{60}Co γ-ray irradiations of his samples and Professor Kojima and Dr. Imae, of the National Institute of Polar Research, for helpful suggestions concerning the classification of Japanese samples.

Appendix A. Supplementary data

Supplementary data associated with this article can be found, in the on-line version, at http://dx.doi.org/10.1016/j.chemer.2012.12.001.

References

Afiattalab, F., Wasson, J.T., 1980. Composition of the metal phases in ordinary chondrites: implications regarding classification and metamorphism. Geochim. Cosmochim. Acta 44, 431–446.

Aitken, M.J., 1985. Thermoluminescence Dating. Academic Press, Orlando, USA, 359 pp.

Aitken, M.J., 1999. Introduction to Optical Dating. Oxford University Press, Oxford, UK, 280 pp.

Akridge, J.M.C., Benoit, P.H., Sears, D.W.G., 2000. Terrestrial age measurements using natural thermoluminescence of a drained zone under the fusion crust of Antarctic ordinary chondrites. Meteorit. Planet. Sci. 35, 869–874, http://dx.doi.org/10.1111/j.1945-5100.2000.tb01470.x.

Akridge, J.M.C., Benoit, P.H., Sears, D.W.G., 2001. Determination of trapping parameters of the high temperature thermoluminescence peak in equilibrated ordinary chondrites. Radiat. Measure. 33, 109–117, http://dx.doi.org/10.1029/2003JE002198.

Akridge, D.G., Akridge, J.M.C., Batchelor, J.D., Benoit, P.H., Brewer, J., DeHart, J.M., Keck, B.D., Lu, J., Meier, A., Penrose, M., Schneider, D.M., Sears, D.W.G., Symes, S.J.K., Zhang, Y., 2004. Photomosaics of the cathodoluminescence of 60 sections of meteorites and lunar samples. J. Geophys. Res. 109 (E7), http://dx.doi.org/10.1029/2003JE002198, CiteID E07S03.

Alexander, C.M.O'D., Hutchison, R., Barber, D.J., 1989. Origin of chondrule rims and interchondrule matrices in unequilibrated ordinary chondrites. Earth Planet. Sci. Lett. 95, 187–207.

Ashworth, J.R., Barber, D.J., 1976. Lithification of gas-rich meteorites. Earth Planet. Sci. Lett. 30, 222–233.

Bart, G., Lipschutz, M.E., 1979. On volatile element trends in gas-rich meteorites. Geochim. Cosmochim. Acta 43, 1499–1504.

Barton, J.C., Wright, A.G., Watson, A.H., 1982. A direct measurement of the distribution in depth of Al-26 in the Estacado meteorite. Geochim. Cosmochim. Acta 46, 1963–1967.

Batchelor, J.D., Sears, D.W.G., 1991a. Metamorphism of eucrite meteorites studied quantitatively using thermoluminescence. Nature 349, 516–519.

Batchelor, J.D., Sears, D.W.G., 1991b. Thermoluminescence constraints on the metamorphic, shock and brecciation history of basaltic meteorites. Geochim. Cosmochim. Acta 55, 3831–3844.

Batchelor, J.D., Symes, S.J.K., Benoit, P.H., Sears, D.W.G., 1997. Thermoluminescence constraints on the thermal and mixing history of lunar surface materials and comparisons with basaltic meteorites. J. Geophys. Res. 102, 19,321–19,334.

Benoit, P.H., Sears, D.W.G., 1992. The breakup of a meteorite parent body and the delivery of meteorites to Earth. Science 255, 1685–1687.

Benoit, P.H., Sears, D.W.G., 1993a. Breakup and structure of an H-chondrite parent body: the H-chondrite flux over the last million years. Icarus 101, 188–200.

Benoit, P.H., Sears, D.W.G., 1993b. A recent meteorite fall in Antarctic with an unusual orbital history. Earth Planet. Sci. Lett. 120, 463–471.

Benoit, P.H., Sears, D.W.G., 1996. Rapid changes in the composition of the meteorite flux: the irradiation, orbital, and terrestrial history of Antarctic H chondrites and modern falls. Meteorit. Planet. Sci. 31, 81–86.

Benoit, P.H., Sears, D.W.G., 1997. Orbits of meteorites from natural TL. Icarus 125, 281–287.

Benoit, P.H., Sears, D.W.G., 1999. Accumulation mechanisms and the weathering of Antarctic equilibrated ordinary chondrites. J. Geophys. Res. – Planets 104, 14159–14168.

Benoit, P.H., Sears, D.W.G., McKeever, S.W.S., 1991. The natural thermoluminescence of meteorites – II. Meteorite orbits and orbital evolution. Icarus 94, 311–325.

Benoit, P.H., Sears, H., Sears, D.W.G., 1992. The natural thermoluminescence of meteorites – IV: ordinary chondrites at the Lewis Cliff ice field. J. Geophys. Res. 97, 4629–4647.

Benoit, P.H., Jull, A.J.T., Mckeever, S.W.S., Sears, D.W.G., 1993a. The natural thermoluminescence of meteorites VI: Carbon-14, thermoluminescence and the terrestrial ages of meteorites. Meteoritics 28, 196–203.

Benoit, P.H., Sears, D.W.G., McKeever, S.W.S., 1993b. Natural thermoluminescence and terrestrial ages of meteorites from a variety of temperature regimes. Radiat. Detect. Dosim. 47, 669–674.

Benoit, P.H., Sears, H., Sears, D.W.G., 1993c. The natural thermoluminescence of meteorites – V: ordinary chondrites at the Allan Hills vicinity. J. Geophys. Res. 98, 1875–1888.

Benoit, P.H., Roth, J., Sears, H., Sears, D.W.G., 1994. The natural thermoluminescence of meteorites 7: ordinary chondrites from the Elephant Moraine region, Antarctica. J. Geophys. Res. – Planets 99, 2073–2085.

Benoit, P.H., Sears, D.W.G., Symes, S.J.K., 1996. The thermal and radiation exposure history of lunar meteorites. Meteorit. Planet. Sci. 31, 869–875.

Benoit, P.H., Hartmetz, C.P., Batchelor, D.J., Symes, S.J.K., Sears, D.W.G., 2001. The induced thermoluminescence and thermal history of plagioclase feldspars. Am. Mineral. 76, 780–789.

Bevan, A.W.R., Binns, R.A., 1989. Meteorites from the Nullarbar region, Western Australia: I. Review of past recoveries and a procedure for naming new finds. Meteoritics 24, 127–133.

Bhandari, N., 1985. Thermal and radiation history of meteorites as revealed by their thermoluminescence records. Nucl. Tracks Radiat. Measure. 10, 269–273.

Bhandari, N., Lal, D., Rajan, R.S., Arnold, J.R., Marti, K., Moore, C.B., 1980. Atmospheric ablation in meteorites: a study based on cosmic ray tracks and neon isotopes. Nucl. Tracks 4, 213–262.

Bhandari, N., Sengupta, D., Jha, R., Goswami, J.N., 1985. TL and nuclear track studies in Shergotty and other SNC meteorites. Lunar Planet. Sci. XVI (Suppl. A), 3–4.

Binns, R.A., 1967. Structure and evolution of non-carbonaceous chondritic meteorites. Earth Planet. Sci. Lett. 2, 23–28.

Biswas, R.H., Morthekai, P., Gartia, R.K., Chawla, S., Singhvi, A.K., 2011. Thermoluminescence of the meteorite interior: a possible tool for the estimation of cosmic ray exposure ages. Earth Planet. Sci. Lett. 304, 36–44.

Boeckl, R., 1972. Terrestrial age of nineteen stony meteorites derived from their radiocarbon. Nature 236, 25–26.

Boetter-Jensen, L., 1997. Luminescence techniques: instruments and methods. Radiat. Measure. 27, 749–768.

Bonal, L., Quirico, E., Bourot-Denise, M., Montagnac, G., 2006. Determination of the petrologic type of CV3 chondrites by Raman spectroscopy of included organic matter. Geochim. Cosmochim. Acta 70, 1849–1863.

Bonal, L., Bourot-Denise, M., Quirico, E., Montagnac, G., Lewin, E., 2008. Organic matter and metamorphic history of CO chondrites. Geochim. Cosmochim. Acta 71, 1605–1623.

Bottke, W.F., Vokrouhlický, D., Rubicam, D.P., Nesvorný, D., 2006. The Yarkovsky and YORP effects: implications for asteroid dynamics. Ann. Rev. Earth Planet. Sci. 34, 157–191.

Boyle, R., 1664. Experiments and Considerations Touching Colours, See Guttenberg ebook http://www.gutenberg.org/files/14504/14504-h/14504-h.htm

Brearley, A.J., 1990. Carbon-rich aggregates in type 3 ordinary chondrites – characterization, origins, and thermal history. Geochim. Cosmochim. Acta 54, 831–850.

Browning, L., McSween, H., Zolensky, M., 1996. Correlated alteration effects in CM carbonaceous chondrites. Geochim. Cosmochim. Acta 60, 2621–2633.

Burke, J.G., 1986. Cosmic Debris: Meteorites in History. University of California Press, 445 pp.

Burns, R., 2005. Mineralogical Applications of Crystal Field Theory. Cambridge University Press, 576 pp.

Cassidy, W.A., 1990. A general description of the Lewis Cliff Ice tongue. In: Cassidy, W.A., Whillans, I.M. (Eds.), Workshop on Antarctic Meteorite Stranding Surfaces, LPI Tech. Rep. 90-93. Lunar and Planetary Institute, Houston, Texas, pp. 26–27.

Cassidy, W.A., 2003. Meteorites, Ice, and Antarctica: A Personal Account. Cambridge University Press, 364 pp.

Cassidy, W.A., Olsen, E., Yanai, K., 1977. Antarctica – a deep-freeze storehouse for meteorites. Science 198, 727–731.

Cassidy, W., Harvey, R., Schutt, J., Delisle, G., Yanai, K., 1992. The meteorite collection sites of Antarctica. Meteoritics 27, 490–525.

Chizmadia, L.J., Rubin, A.E., Wasson, J.T., 2002. Mineralogy and petrology of amoeboid olivine inclusions in CO3 chondrites: relationship to parent-body aqueous alteration. Meteorit. Planet. Sci. 37, 1781–1796.

Clayton, R.N., Mayeda, T.K., Goswami, J.N., Olsen, E.J., 1991. Oxygen isotopes studies of ordinary chondrites. Geochim. Cosmochim. Acta 55, 2317–2337.

Correcher, V., Sanchez-Munõz, L., Garcia-Guine, J., Delgado, A., 2007. Natural blue thermoluminescence emission of the recently fallen meteorite in Villalbeto de la Penã (Spain). Nucl. Instrum. Meth. Phy. Res. A 580, 637–640.

Cotton, F.A., Wilkinson, G.W., 1968. Advanced Inorganic Chemistry, 2nd ed. Interscience Publishers, 1136 pp.

Craig, J.P., Sears, D.W.G., 2009. The fine-grained matrix of the Semarkona LL3.0 ordinary chondrite: an induced thermoluminescence study. Meteorit. Planet. Sci. 44, 643–652, http://dx.doi.org/10.1111/j.1945-5100.2009.tb00760.x.

Craig, J.P., Sears, D.W.G., 2010. Natural and induced thermoluminescence data for twenty-five 10-15 μm particles form the LL3.0 ordinary chondrite Semarkona: implications for the narture and history of primitive solar system material. In: Lunar and Planetary Science Conference: Abstract no. 1401.

Crovisier, J., Leech, K., Bockelée-Morvan, D., Brooke, T.Y., Hanner, M.S., Altieri, B., Keller, H.U., Lellouch, E., 1997. The spectrum of Comet Hale-Bopp (C/1995 01) observed with the Infrared Space Observatory at 2.9 astronomical units from the sun. Science 275, 1904–1907.

Dalrymple, G.B., Doell, R.R., 1970. Thermoluminescence of lunar samples. Science 167, 713–715.

Dehart, J.M., Lofgren, G.E., 1994. The occurrence of blue luminescing enstatite in E3 and E4 chondrites. In: The Twenty-Fifth Lunar and Planetary Science Conference, Part 1, pp. 319–320.

Dehart, J.M., Lofgren, G.E., 1995. Formation and metamorphism in Enstatite chondrites. In: The Twenty-Sixth Lunar Planet. Sci. Conf., Part 1, pp. 325–326.

DeHart, J.M., Lofgren, G.E., Lu, J., Benoit, P.H., Sears, D.W.G., 1992. Chemical and physical studies of chondrites X: cathodoluminescence studies of metamorphism and nebular processes in type 3 ordinary chondrites. Geochim. Cosmochim. Acta 56, 3791–3807.

Dennison, J.F., Lipschutz, M.E., 1987. Chemical studies of H chondrites. II. Weathering effects in the Victoria Land, Antarctica, populations and comparison of two Antarctic populations with non-Antarctic falls. Geochim. Cosmochim. Acta 51, 741–754.

Derham, C.J., Geake, J.E., 1964. Luminescence of meteorites. Nature 201, 62–63.

Derham, C.J., Geake, J.E., Walker, G., 1964. Luminescence of enstatite achondrite meteorites. Nature 203, 134–136.

Dodd, R.T., 1969. Metamorphism of ordinary chondrites, a review. Geochim. Cosmochim. Acta 33, 161–203.

Dodd, R.T., 1978a. The composition and origin of large microporphyritic chondrules in the Manych L-3 chondrite. Earth Planet. Sci. Lett. 39, 52–66.

Dodd, R.T., 1978b. Compositions of droplet Chondrules in the Manych L-3 chondrite and the origin of Chondrules. Earth Planet. Sci. Lett. 40, 71–82.

Dodd, R.T., 1981. Meteorites, A Petrologic-Chemical Synthesis. Cambridge University Press, 368 pp.

Dodd, R.T., Van Schmus, W.R., Koffman, D.M., 1967. A survey of the unequilibrated ordinary chondrites. Geochim. Cosmochim. Acta 31, 921–951.

Eugster, O., Herzog, G.F., Marti, K., Caffee, M.W., 2006. Irradiation records, cosmic-ray exposure ages, and transfer times of meteorites. In: Laurette, D., McSween, H.Y. (Eds.), Meteorites and the Early Solar System II. , pp. 829–851.

Fredriksson, K., Keil, K., 1963. The light-dark structure in the Pantar and Kapoeta stone meteorites. Geochim. Cosmchim. Acta 27, 717–739.

Garlick, G.F.J., 1949. Luminescent Materials. Clarendon Press, 254 pp.

Garlick, G.F.J., Gibson, A.F., 1948. The electron trap mechanism of luminescence in sulphide and silicate phosphors. Proc. Phys. Soc. A 60, 574–590.

Garlick, G.F.J., Robinson, I., 1971. The thermoluminescence of lunar samples. In: Runcorn, S.K., Urey, H.C. (Eds.), The Moon, Proceedings from IAU Symposium no. 47 held at the University of Newcastle-Upon-Tyne England, 22-26 March, 1971. Symposium no. 47. International Astronomical Union, Dordrecht, Reidel, p. 324.

Garlick, G.F.J., Steigmann, G.A., Lamb, W.E., 1972. Explanation of transient lunar phenomena based on lunar samples studies. Nature 235, 39–40.

Geake, J.E., Walker, G., 1966a. Luminescence caused by proton impact with special reference to the lunar surface. Nature 211, 471–472.

Geake, J.E., Walker, G., 1966b. The luminescence spectra of meteorites. Geochim. Cosmochim. Acta 30, 929–937.

Geake, J.E., Walker, G., 1967. Laboratory investigations of meteorite luminescence. Proc. R. Soc. Lond. Ser. A Math. Phys. Sci. 296, 337–346.

Geake, J.E., Walker, G., Mills, A.A., Garlick, G.F.J., 1972. Luminescence of lunar material excited by electrons. Proc. Lunar Sci. Conf. 2, 2971–2979.

Gooding, J.L., Keil, K., 1981. Relative abundances of chondrule primary textural types in ordinary chondrites and their bearing on conditions of chondrule formation. Meteoritics 16, 17–43.

Grady, M.M., Swart, P.K., Pillinger, C.T., 1982. The variable carbon isotopic composition of type 3 ordinary chondrites. J. Geophys. Res. 87 (suppl.), A289–A296.

GRL, 1983. Geophys. Res. Lett. 10, 773–840.

Grossman, L., 1980. Refractory inclusions in the Allende. Ann. Rev. Earth Planet. Sci. 8, 559–608.

Gietzen, K.M., Lacy, C.H.S., Ostrowski, D.R., Sears, D.W.G., 2012. IRTF observations of S complex and other asteroids. Implications for surface compositions, the presence of clinopyroxenes, and their relationship to meteorites. Meteorit. Planet. Sci. 47, 1789–1808.

Grögler, N., Leiner, A., 1968. Cathodoluminescence and thermoluminescence observations of aubrites. In: McDacdougall, D.J. (Ed.), Thermoluminescence of Geological Materials. Academic Press, pp. 569–578.

Grossman, J.N., Brearley, A.J., 2005. The onset of metamorphism in ordinary and carbonaceous chondrites. Meteorit. Planet. Sci. 40, 87–122, http://dx.doi.org/10.1111/j.1945-5100.2005.tb00366.x.

Grün, E., 2001. Interplanetary Dust. Springer, Berlin, 804 pp.

Guimon, R.K., Weeks, K.S., Keck, B.D., Sears, D.W.G., 1984. Thermoluminescence as a palaeothermometer. Nature 311, 363–365.

Guimon, R.K., Keck, B.D., Sears, D.W.G., 1985. Chemical and physical studies of type 3 chondrites – IV: annealing studies of a type 3.4 ordinary chondrite and the metamorphic history of meteorites. Geochim. Cosmochim. Acta 19, 1515–1524.

Guimon, R.K., Symes, S.P., Sears, D.W.G., Benoit, P.H., 1995. Chemical and physical studies of type 3 chondrites XII: the metamorphic history of CV chondrites and their components. Meteoritics 30, 707–714.

Haq, M., Hasan, F.A., Sears, D.W.G., 1988. Thermoluminescence and the shock and reheating history of meteorites – IV: the induced TL properties of type 4-6 ordinary chondrites. Geochim. Cosmochim. Acta 52, 1679–1689.

Haq, M., Hasan, F.A., Sears, D.W.G., Moore, C.B., Lewis, C.F., 1989. Thermoluminescence and the origin of the dark matrix of Fayetteville and similar meteorites. Geochim. Cosmochim. Acta 53, 1435–1440.

Hartmetz, C.P., Ostertag, R., Sears, D.W.G., 1986. A thermoluminescence study of experimentally shock-loaded oligoclase and bytownite. Proc. 17th Lunar and Planet. Sci. Conf., Part 1 J. Geophys. Res. 91, E263–E274.

Harvey, E.N., 2005. A History of Luminescence: From the Earliest Times Until 1900. Dover Books, 692 pp.

Hasan, F.A., Haq, M., Sears, D.W.G., 1986. Thermoluminescence and the shock and reheating history of meteorites – III: the Shergottites. Geochim. Cosmochim. Acta 50, 1031–1038.

Hasan, F.A., Haq, M., Sears, D.W.G., 1987. Natural thermoluminescence levels in meteorites, I: 23 meteorites of known Al-26 content. J. Geophys. Res. 92, E703–E709.

Hasan, F.A., Score, R., Sears, D.W.G., 1989. The natural thermoluminescence survey of Antarctic meteorites – a discussion of methods of reporting natural TL data. Lunar Planet. Sci. XX, 383–384.

Heiken, G.H., Vaniman, D.T., French, B.M., 1991. Lunar Sourcebook – A User's Guide to the Moon. Cambridge University Press, 753 pp.

Herschel, A.S., 1881. Fall of a meteorite on March 14, 1881. Mon. Not. R. Astron. Soc. 41, 444.

Herschel, A.S., 1899. Triboluminescence. Nature 60, 29.

Heymann, D., 1967. Origin of hypersthene chondrites: ages and shock effects of black chondrites. Icarus 6, 189–221.

Houtermans, F.G., Leiner, A., 1969. Thermoluminescence of meteorites. J. Geophys. Res. 71, 3387–3396.

Howard, E.C., 1802. Experiments and observations on certain stony substances, which at different times are said to have fallen on the Earth; also on various kinds of native iron. Philos. Trans. R. Soc. 92, 168–212.

Hoyt Jr., H.P., Walker, R.M., Zimmerman, D.W., Zimmerman, J., 1972. Thermoluminescence of individual grains and bulk samples of lunar fines. Proc. Lunar Sci. Conf. 2, 2997–3007.

Huang, S., Akridge, G., Sears, D.W.G., 1996. Metal-silicate fractionation in the surface dust layers of accreting planetesimals, implications for the formation of ordinary chondrites and the nature of asteroid surfaces. J. Geophys. Res. Planets 101, 29,373–29,385.

Huss, G.R., 1991. Ubiquitous interstellar diamond and SiC in primitive chondrites – abundances reflect metamorphism. Nature 347, 159–162.

Huss, G.R., Lewis, R.S., 1994. Noble gases in presolar diamonds I, three distinct components and their implications for diamond origins. Meteoritics 29, 791–810.

Huss, G.R., Keil, K., Taylor, G.J., 1981. The matrices of unequilibrated ordinary chondrites, implications for the origin and history of chondrites. Geochim. Cosmochim. Acta 45, 33–51.

Huss, G.R., Rubin, A.E., Grossman, J.N., 2006. In: Lauretta, D.S., McSween Jr., H.Y. (Eds.), Thermal Metamorphism in Chondrites Meteorites and the Early Solar System II. University of Arizona Press, Tucson, p. 943, pp. 567–586.

Jones, R.H., 1992. On the relationship between isolated and chondrule olivine grains in the carbonaceous chondrite ALHA77307. Geochim. Cosmochim. Acta 56, 467–482.

Jones, R.H., 1994. Petrology of FeO-poor, porphyritic pyroxene chondrules in the Semarkona chondrite. Geochim. Cosmochim. Acta 58, 5325–5340.

Jull, A.J.T., Donahue, D.J., Linick, T.W., 1980. Carbon-14 activities in recently fallen meteorites and Antarctic meteorites. Geochim. Cosmochim. Acta 53, 2095–2100.

Jull, A.J.T., Cielaszyk, E., Cloudt, S., 1998. ^{14}C terrestrial ages of meteorites from Victoria Land, Antarctica and the infall rates of meteorites. In: Grady, M.M., Hutchison, R., McGall, G.J.H., Rothery, D.A. (Eds.), Meteorites, Flux with Time and Impact Effects, London. Special Publication 140. Geological Society of London, pp. 75–91.

Kieffer, S.W., 1975. Droplet chondrules. Science 189, 333–340.

Keil, K., 1968. Mineralogical and chemical relationships among enstatite chondrites. J. Geophys. Res. 73, 6945–6976.

Keil, K., 1982. Composition and origin of chondritic breccias. In: Workshop on Lunar Breccias and Soils and their Meteoritic Analogs. LPI Technical Report 82-02, pp. 65–83.
Keil, K., 2002. Geological history of asteroid 4 Vesta: the "smallest terrestrial planet". In: Bottke, W., Cellino, A., Paolicchi, P., Binzel, R.P. (Eds.), Asteroids III. Arizona LPI Publishing, pp. 573–585.
Kimura, M., Grossman, J.N., Weisberg, M.K., 2008. Fe-Ni metal in primitive chondrites: indicators of classification and metamorphic conditions for ordinary and CO chondrites. Meteorit. Planet. Sci. 43, 1161–1177.
Kloeck, W., Thomas, K.L., McKay, D.S., Palme, H., 1989. Unusual olivine and pyroxene composition in interplanetary dust and unequilibrated ordinary chondrites. Nature 339, 126–128.
Koeberl, C., Cassidy, W.A., 1991. Differences between Antarctic and non-Antarctic meteorites: an assessment. Geochim. Cosmochim. Acta 55, 3–18.
Koike, C., Chihara, H., Koike, K., Nakagawa, M., Okada, M., Tsuchiyama, A., Aoki, M., Awata, T., Atobe, K., 2002. Thermoluminescence of forsterite and fused quartz as a candidate for the extended red emission. Meteorit. Planet. Sci. 37, 1591–1598, http://dx.doi.org/10.1111/j.1945-5100.2002.tb00813.x.
Komovsky, G.F., 1961. Thermoluminescence of stony meteorites. Meteoritika 21, 64–69 (In Russian).
Korotev, R., 2005. Lunar geochemistry as told by lunar meteorites. Chem. Erde 65, 297–346, http://dx.doi.org/10.1016/j.chemer.2005.07.001.
Lalou, C., Nordemann, D., Labyrrie, J., 1970. Etude préliminaire de la thermoluminescence de la meteorite. Saint-Severin. Compt. Rendus de l'Acad. Sci., Paris Ser. D 270, 2401 (In French).
Lee, T., Papanastassiou, D.A., Wasserburg, G.J., 1976. Demonstration of ^{26}Mg excess in Allende and evidence for ^{26}Al. Geophys. Res. Lett. 3, 41–44.
Leitch, C.A., Smith, J.V., 1982. Petrography, mineral chemistry and origin of type I enstatite chondrites. Geochim. Cosmochim. Acta 46, 2083–2096.
Levy, P.W., 1978. Thermoluminescence studies having application to geology and archaeology. Phys. Chem. Tech. J. 3, 466–480.
Leiner, A., Geiss, J., 1968. Thermoluminescence measurements on chondritic meteorites. In: McDougall, D.J. (Ed.), Thermoluminescence of Geological Materials. Academic Press, NY, pp. 559–582.
Lipschutz, M.E., Biswas, S., McSween, H.Y., 1983. Chemical characteristics and origin of H chondrite regolith breccias. Geochim. Cosmochim. Acta 47, 169–179.
Marshall, D.J., 1988. Cathodoluminescence of Geological Materials. Unwin Hyman, Boston, 146 pp.
Matsui, H., Ninagawa, K., Imae, N., Kojima, H., 2010. Thermoluminescense study in the Japanese antarctic meteorites collection, Yamato 98 unequilibrated ordinary chondrites II. Meteorit. Planet. Sci. Suppl. 45, A129, id.5189.
Mason, B., 1971. In: Mason, B. (Ed.), Handbook of Elemental Abundances in Meteorites. Series in Extraterrestial Chemistry. Gordon and Breach, New York.
Matsunami, S., Ninagawa, K., Nishimura, S., Kubono, N., Yamamoto, I., Kohata, M., Wada, T., Yamashita, Y., Lu, J., Sears, D.W.G., Nishimura, H., 1993. Thermoluminescence and compositional zoning in the mesostasis of a Semarkona group A1 chondrule and new insights into the chondrule-forming process. Geochim. Cosmochim. Acta 57, 2102–2110.
Mazor, E., Anders, E., 1967. Primordial gases in the Jodzie howardite and the origin of gas-rich meteorites. Geochim. Cosmochim. Acta 31, 1441–1456.
McCoy, T.J., Scott, E.R.D., Jones, R.H., Keil, K., Taylor, G.J., 1991. Composition of chondrule silicates in LL3-5 chondrites and implications for their nebular history and parent body metamorphism. Geochim. Cosmochim. Acta 55, 601–619.
McKeever, S.W.S., 1980. The analysis of glow curves from meteorites. Mod. Geol. 7, 105–114.
McKeever, S.W.S., 1985. Thermoluminescence of Solids. Cambridge UP, 376 pages.
McKeever, S.W.S., Sears, D.W., 1980. Natural thermoluminescence of meteorites – a pointer to orbits? Mod. Geol. 7, 137–145.
McKeever, S.W.S., Yukihara, E.G., 2011. Optically Stimulated Luminescence. John Wiley and Sons, 378 pp.
McKie, D., McConnell, J.D.C., 1963. The kinetics of the low-high transformation in albite. I. Amelia albite under dry conditions. Min. Mag. 33, 581–588.
McKinley, S.G., Scott, E.R.D., Keil, K., 1984. Composition and origin of enstatite in E chondrites. J. Geophys. Res. 89 (Suppl.), B567–B572.
McNaughton, N.J., Fallick, A.E., Pillinger, C.T., 1982. Deuterium enrichments in type 3 ordinary chondrites. J. Geophys. Res. 87 (Suppl.), A297–A302.
McSween Jr., H.Y., 1977a. Carbonaceous chondrites of the Ornans type, a metamorphic sequence. Geochim. Cosmochim. Acta 41, 477–491.
McSween Jr., H.Y., 1977b. Petrographic variations among carbonaceous chondrites of the Vigarano type. Geochim. Cosmochim. Acta 41, 1777–1790.
Meeker, G.P., Wasserburg, G.J., Armstrong, J.T., 1983. Replacement textures in CAI and implications regarding planetary metamorphism. Geochim. Cosmochim. Acta 47, 707–721.
Melcher, C.M., 1981a. Thermoluminescence of meteorites and their terrestrial ages. Geochim. Cosmochim. Acta 45, 615–626.
Melcher, C.M., 1981b. Thermoluminescence of meteorites and their orbits. Earth Planet. Sci. Lett. 52, 39–54.
Michel, R., Leya, I., Borges, L., 1996. Production of cosmogenic nuclides in meteoroids: accelerator experiments and model calculations to decipher the cosmic ray record in extraterrestrial matter. Nucl. Instrum. Meth. Phys. Res. Sect. B 113, 434–444.
Michlovich, E.S., Wolf, S.F., Wang, M.-S., Vogt, S., Elmore, D., Lipschutz, M.E., 1995. Chemical studies of H chondrites. 5: Temporal variations of sources. J. Geophys. Res. 100, 3317–3333.
Mills, A.A., Sears, D.W., Hearsey, R., 1977. Apparatus for the measurement of thermoluminescence. J. Phys. E. Sci. Instrum. 10, 51–56.
Milton, D.J., de Carli, P.S., 1963. Maskelynite: formation by explosive shock. Science 140, 670–671.
Miono, S., Nakanishi, A., 1994. Terrestrial ages of the Antarctic meteorites measured by thermoluminescence of the fusion crust, II. Proc. NIPR Sym. Antarct. Meteorit. 7, 225–229.
Miono, S., Ono, H., Kujirai, H., Yoshida, M., Nakanishi, A., 1990. Terrestrial ages of Antarctic meteorites measured by thermoluminescence of the fusion crust. Proc. NIPR Sym. Antarct. Meteorit. 3, 240–243.
Müller, O., Zähringer, J., 1966. K-Ar-Altersbestimmungen an Eisenmeteoriten – III Kalium- und Argon-Bestimmungen. Geochim. Cosmochim. Acta 30, 1075–1092.
Nash, D.B., Greer, R.T., 1970. Luminescence properties of Apollo 11 lunar samples and implications for solar-excited lunar luminescence. Proc. Apollo 11 Lunar Sci. Conf. 2, 2341–2350.
Nesvorný, D., Ferraz-Mello, S., Holman, M., Morbidelli, A., 2002. Regular and chaotic dynamics in the mean-motion resonances: implications for the structure and evolution of the asteroid belt. In: Bottke, W.F., Cellino, A., Paolicchi, P., Binzel, R.P. (Eds.), Asteroids III. Tucson, University of Arizona Press, pp. 379–394.
Ninagawa, K., Hoshikawa, Y., Kojima, H., Matsunami, S., Benoit, P.H., Sears, D.W.G., 1998. Thermoluminescence of Japanese Antarctic ordinary chondrite collection. Antarct. Meteorit. Res. 11, 1–17.
Ninagawa, K., Soyama, K., Ota, M., Toyoda, S., Imae, N., Kojima, H., Benoit, P.H., Sears, D.W.G., 2000. Thermoluminescence studies of ordinary chondrites in the Japanese Antarctic meteorite collection, II: new measurements for thirty type 3 ordinary chondrites. Antarct. Meteorit. Res. 13, 112–120.
Ninagawa, K., Ota, M., Imae, N., Kojima, H., 2002. Thermoluminescence studies of ordinary chondrites in the Japanese Antarctic meteorite collection, III, Asuka and Yamato type 3 ordinary chondrites. Antarct. Meteorit. Res. 15, 114–121.
Ninagawa, K., Mieda, Y., Ueda, H., Imae, N., Kojima, H., Yanai, K., 2005. Thermoluminescence studies of ordinary chondrites in the Japanese Antarctic meteorite collection, IV. Asuka ordinary chondrites. Antarct. Meteorit. Res. 18, 1–16.
Nishiizumi, K., Arnold, J.R., Elmore, D., Ferraro, R.D., Gove, H.E., Finkel, R.C., Beukens, R.P., Chang, K.H., Kilius, L.R., 1979. Measurements of Cl-36 in Antarctic meteorites and Antarctic ice using a Van de Graaff accelerator. Earth Planet. Sci. Lett. 45, 285–292.
Nishiizumi, K., Elmore, D., Kubik, P.W., 1989. Update on terrestrial ages of Antarctic meteorites. Earth Planet. Sci. Lett. 93, 299–313.
Nishiizumi, K., Nagai, H., Imamura, M., Honda, M., Kobayashi, K., Kubik, P.W., Sharma, P., Wieler, R., Signer, P., Goswami, J.N., Sinha, N., Reedy, R.C., Arnold, J.R., 1990. Solar cosmic ray produced nuclides in the Salem meteorite. Meteoritics 25, 392.
Ostertag, R., 1983. Shock experiments on feldspar crystals. J. Geophys. Res. Suppl. 88, B364–B376.
Otto, J., 1992. New meteorite finds from the Algerian Sahara Desert. Chem. Erde 52, 33–40.
Papike, J.J., Karner, J.M., Shearer, C.K., Burger, P.V., 2009. Silicate mineralogy of martian meteorites. Geochim. Cosmochim. Acta 73, 7443–7748, http://dx.doi.org/10.1016/j.gca.2009.09.008.
Pasternak, E.S., 1978. Thermoluminescence of ordered and thermally disordered albite. Ph.D. Thesis. University of Pennsylvania, PA.
Rambaldi, E.R., Wasson, J.T., 1981. Metal and associated phases in Bishunpur, a highly unequilibrated ordinary chondrite. Geochim. Cosmochim. Acta 45, 1001–1015.
Rambaldi, E.R., Sears, D.W., Wasson, J.T., 1980. Si-rich grains in highly unequilibrated chondrites. Nature 287, 817–820.
Randall, J.T., Wilkins, M.H.F., 1945a. Phosphorescence and electron traps I. The study of trap distributions. Proc. R. Soc. Lond. A184, 366–389.
Randall, J.T., Wilkins, M.H.F., 1945b. Phosphoresence and electron traps 2. The interpretation of long-period phosphorescence. Proc. R. Soc. Lond. A184, 390–407.
Reed, S.J.B., 2005. Electron Microprobe Analysis and Scanning Eleectron Microscopy in Geology. Cambrideg University Press, Cambridge, UK, 192 pp.
Reid, A.M., Cohen, A.J., 1967. Some characteristics of enstatite from enstatite achondrites. Geochim. Cosmochim. Acta 31, 661–670.
Righter, K., Satterwhite, C., McBride, K., Harrington, R., 2011. The NASA antarctic meteorite curation laboratories. Meteorit. Mag. 17, 7–11.
Rubin, A.E., James, J.A., Keck, B.D., Weeks, K.S., Sears, D.W.G., Jarosewich, E., 1985. The colony meteorite and variations in CO3 chondrite properties. Meteoritics 20, 175–196.
Rubin, A.E., Trigo-Rodriguez, J.M., Huber, H., Wasson, J.T., 2007. Progressive aqueous alteration of CM carbonaceous chondrites. Geochim. Cosmochim. Acta 71, 2361–2382.
Schultz, L., Franke, L., 2004. Helium, neon, and argon in meteorites: a data collection. Meteorit. Planet. Sci. 39, 1889–1890.
Scott, E.R.D., Taylor, G.J., 1983. Chondrules and other components in C, 0, and E chondrites; similarities in their properties and origins. Proc. Lunar Planet. Sci. Conf. 14th J. Geophys. Res. 88, B275–B286.
Scott, E.R.D., Taylor, G.J., Maggiore, P., 1982. A new LL3 chondrite, Allan Hills A79003, and observations on matrices in ordinary chondrites. Meteoritics 17, 65–75.
Scott, E.R.D., Keil, K., Stoeffler, D., 1992. Shock metamorphism of carbonaceous chondrites. Geochim. Cosmochim. Acta 56, 4281–4293.
Scott, E.R.D., Jones, R.H., 1990. Disentangling nebula and asteroidal features of CO3 carbonaceous chondrites. Geochim. Cosmochim. Acta 54, 2485–2502.
Sears, D.W., 1974. Thermoluminescence and fusion crust studies of meteorites. PhD Thesis, University of Leicester.
Sears, D.W., 1975a. Thermoluminescence studies and the preatmospheric shape and mass of the Estacado meteorite. Earth Planet. Sci. Lett. 26, 97–104.
Sears, D.W., 1975b. Temperature gradients in meteorites produced by heating during atmospheric passage. Mod. Geol. 5, 155–164.

Sears, D.W., 1976. Edward Charles Howard and an early British contribution to meteoritics. J. Br. Aston. Assoc. 86, 133–139.
Sears, D.W., 1980. Thermoluminescence of meteorites; relationships with their K-Ar age and their shock and reheating history. Icarus 44, 190–206.
Sears, D.W.G., 2004. The Origin of Chondrules and Chondrites. Cambridge University Press, Cambridge.
Sears, D.W., Durrani, S.A., 1980. Thermoluminescence and the terrestrial age of meteorites: some recent results. Earth Planet. Sci. Lett. 46, 159–166.
Sears, D.W.G., Hasan, F.A., 1986. Thermoluminescence and Antarctic meteorites. In: Annexstad, J.O., Schultz, L., Wanke, H. (Eds.), Proceedings of the 2nd Workshop on Antarctic Meteorites. 83-100. LPI Technical Rept. 86-01. Lunar and Planetary Institute, Houston.
Sears, D.W., McKeever, S.W.S., 1980. Measurement of thermoluminescence sensitivity of meteorites. Mod. Geol. 7, 201–207.
Sears, D.W., Mills, A.A., 1973. Temperature gradients and atmospheric ablation rates for the Barwell meteorite. Nat. Phys. Sci. 242, 25–26.
Sears, D.W., Mills, A.A., 1974. Thermoluminescence and the terrestrial age of meteorites. Meteoritics 9, 47–67.
Sears, D.W.G., Weeks, K.S., 1983. Chemical and physical studies of type 3 chondrites – II, thermoluminescence of sixteen type 3 ordinary chondrites and relationships with oxygen isotopes. Proc. 14th Lunar Planet. Sci. Conf., Part 1 J. Geophys. Res. 88, B301–B311.
Sears, D.W.G., Grossman, J.N., Melcher, C.L., Ross, L.M., Mills, A.A., 1980. Measuring metamorphic history of unequilibrated ordinary chondrites. Nature 287, 791–795.
Sears, D.W.G., Lu Jie, Keck, B.D., Batchelor, J.D., 1991a. Metamorphism of CO and CO-like chondrites and comparisons with type 3 ordinary chondrites. Proc. Nat. Inst. Polar Res. Sym. Antarct. Meteorit. 4, 319–345.
Sears, D.W.G., Benoit, P.H., Batchelor, J.D., 1991b. Evidence for differences in the thermal histories of Antarctic and non-Antarctic H chondrites with cosmic ray exposure ages <20 Ma. Geochim. Cosmochim. Acta 55, 1192–1197.
Sears, D.W.G., Benoit, P.H., Sears, H., Batchelor, J.D., Symes, S., 1991c. The natural thermoluminescence of meteorites: III. Lunar and basaltic meteorites. Geochim. Cosmochim. Acta 55, 3167–3180.
Sears, D.W.G., Benoit, P.H., Lu, J., 1993. Two groups each with distinctive rims in Murchison recognized by cathodoluminescence. Meteoritics 28, 669–675.
Sears, D.W.G., Symes, S.P., Guimon, R.K., Benoit, P.H., 1995. Chemical and physical studies of type 3 chondrites XII: the metamorphic history of CV chondrites and their components. Meteoritics 30, 707–714.
Sears, D.W.G., Symes, S.J.K., Akridge, D.G., Batchelor, J.D., Benoit, P.H., 1997. Some induced thermoluminescence and thermal modeling constraints on the metamorphic history of eucrites and eucrite-related meteorites. Meteorit. Planet. Sci. 32, 917–927.
Sears, D.W.G., Saxton, J.M., Lyon, I.C., 2009. Mass-independent fractionation of oxygen isotopes in the mesostasis of a chondrule from the Semarkona LL3.0 ordinary chondrite. Geochim. Cosmochim. Acta 73, 3948–3962.
Sears, D.W.G., Yozzo, J., Ragland, C., 2011. The natural thermoluminescence of Antarctic meteorites and their terrestrial ages and orbits: A 2010 update. Meteorit. Planet. Sci. 46 (1), 79–91, http://dx.doi.org/10.1111/j.1945-5100.2010.01139.x.
Sedaghatpour, F., Sears, D.W.G., 2009. Characterization of Antarctic micrometeorites by thermoluminescence. Meteorit. Planet. Sci. 44, 653–664, http://dx.doi.org/10.1111/j.1945-5100.2009.tb00761.x.
Sen Gupta, D., Bhandari, N., Watanabe, S., 1997a. Terrestrial ages of Antarctic meteorites based on the thermoluminescence levels induced in the fusion crust. Braz. J. Phys. 27, http://dx.doi.org/10.1590/S0103-97331997000300001.
Sen Gupta, D., Bhandari, N., Watanabe, S., 1997b. Formation age of Lonar Meteor Crater, India. Revista de Física Aplicada e Instrumentação 12, 1–7.
Singhvi, A.K., Pal, S., Bhandari, N., 1982. Ablation characteristics of meteorites based on thermoluminescence and track studies. Phys. Chem. Tech. 6, 404–408.
Sipiera, P.P., Becker, M.J., Kawachi, Y., 1987. Classificiation of 26 chondrites from Roosevelt County, New Mexico. Meteoritics 22, 151–155.
Sippel, R.F., Spencer, A.B., 1970. Luminescence petrography and properties of lunar crystalline rocks and breccias. Proc. Apollo 11 Lunar Sci. Conf. 3, 2413.
Skinner, B.J., Luce, F.D., 1971. Solid solutions of the type Ca, Mg, Mn, Fe. S and their use as geothermometers for the Enstatite Chondrites. Am. Mineral. 56, 1269–1296.
Smith, J.V., 1974. Feldspar Minerals. Springer-Verlag, Dordrecht.
Steele, I.M., 1986. Compositions and textures of relic forsterite in carbonaceous and unequilibrated ordinary chondrites. Geochim. Cosmochim. Acta 50, 1379–1395.
Steele, I.M., 1989a. Compositions of isolated forsterites in Ornans C3O. Geochim. Cosmochim. Acta 53, 2069–2079.
Steele, I.M., 1989b. Cathodoluminescence mineralogy of meteorites. In: 20th Lunar Planet. Sci. Conf., # 1052.
Steele, I.M., 1998. Forsterite in ALHA77307, evidence for multiple origins. In: 29th Lunar Planet. Sci. Conf., # 1731.
Stöffler, D., Bischoff, A., Buchwald, V., Rubin, A.E., 1988. Shock effects in meteorites. In: Kerridge, J.F., Matthews, M.S. (Eds.), Meteorites and the Early Solar System. Univ. of Arizona, Tucson, pp. 165–202.
Stöffler, D., Keil, K., Scott, E.R.D., 1991. Shock metamorphism of ordinary chondrites. Geochim. Cosmochim. Acta 55, 3845–3867.
Symes, S.J.K., Sears, D.W.G., Akridge, D., Huang, S., Benoit, P.H., 1998. The crystalline lunar spherules, their formation and implications for the origin of meteoritic chondrules. Meteorit. Planet. Sci. 33, 13–29.
Suess, H.E., Wänke, H., Wlotzka, F., 1964. On the origin of gas-rich meteorites. Geochim. Cosmochim. Acta 28, 595–600.
Sutton, S.R., 1985. Thermoluminescence measurements on shock-metamorphosed sandstone and dolomite from meteor crater, Arizona. I – Shock dependence of thermoluminescence properties. II Thermoluminescence age of meteor crater. J. Geophys. Res. 90, 3683–3700.
Sutton, S.R., Crozaz, G., 1983. Thermoluminescence and nuclear particle tracks in ALHA-81005. Evidence for a brief transit time. Geophys. Res. Lett. 10, 809–812.
Sutton, S.R., Walker, R.M., 1986. Thermoluminescence of Antarctic meteorites: a rapid screening technique for terrestrial age estimation, pairing studies and identification of specimens with unusual prefall histories. In: Lunar and Planetary Inst. International Workshop on Antarctic Meteorites, pp. 104–106.
Takeda, K., Ninagawa, K., 2005. Cathodoluminescence and thermoluminescence studies of CR Chondrites. Meteorit. Planet. Sci. 40, A150, Supplement, 68th Annual Meeting of the Meteoritical Society. #5030.
Takeda, H., Mori, H., Delaney, J.S., Prinz, M., Harlow, G.E., 1983. Mineralogical comparison of antarctic and non-antarctic HED howardites-eucrites-diogenites. In: Achondrites 8th Symp. Antarct. Meteorit., Memoirs NIPR #30, pp. 181–205.
Van Schmus, W.R., Wood, J.A., 1967. A chemical-petrologic classification for the chondritic meteorites. Geochim. Cosmochim. Acta 31, 747–765.
Vaz, J.E., 1971. Asymmetric distribution of thermoluminescence in the Ucera meteorite. Nat. Phys. Sci. 230, 23, http://dx.doi.org/10.1038/physci230023a0.
Vaz, J.E., Sears, D.W., 1977. Artificially-induced thermoluminescence gradients in stony meteorites. Meteoritics 12, 47–60.
Wacker, J.F., 1990. ^{26}A1 survey of antarctic meteorites. In: Cassidy, W.A., Whillans, I.M. (Eds.), Workshop on Antarctic Meteorite Stranding Surfaces. LPI Technical Report 90-03. , p. 54.
Walker, R.M., Zimmerman, D.W., Zimmerman, J., 1972. Thermoluminescence of Lunar Samples: measurement of temperature gradients in core material. The Moon 4, 308–314.
Wagner, G.A., 1985. Thermoluminescence studies on Jilin meteorite. Earth Planet. Sci. Lett. 72, 304–306.
Weisberg, M.K., Prinz, M., Clayton, R.N., Mayeda, T.K., 1993. The CR (Renazzo-type) carbonaceous chondrite group and its implications. Geochim. Cosmochim. Acta 57, 1567–1586.
Weisberg, M.K., Prinz, M., Fogel, R.A., 1994. The evolution of enstatite and chondrules in unequilibrated enstatite chondrites: evidence from iron-rich pyroxene. Meteoritics 29, 362–373.
Weisberg, M.K., McCoy, T.J., Krot, A.N., 2006. Systematics and evaluation of meteorite classification. In: Laurette, D., McSween, H.Y. (Eds.), Meteorites and the Early Solar System II. , pp. 19–52.
Wilkening, L., 1976. Carbonaceous chondritic xenoliths and planetary-type noble gases in gas-rich meteorites. In: Proc. Lunar Sci. Conf. 7th, pp. 3549–3559.
Willis, J., Goldstein, J.I., 1981. Solidification zoning and metallographic cooling rates of chondrites. Nature 293, 126–127.
Wintle, A.G., 1973. Anomalous fading of thermoluminescence in mineral samples. Nature 245, 143–144.
Wintle, A.G., 1977. Detailed study of a thermoluminescent mineral exhibiting anomalous fading. J. Lumin. 15, 385–393.
Wlotzka, F., 1985. Olivine-spinel and olivine-ilmenite thermometry in chondrites of different petrologic. Lunar Planet. Sci. XVI, 918–919.
Wlotzka, F., 1987. Equilibration temperatures and cooling rates of chondrites, a new approach. Meteoritics 22, 529.
Wlotzka, F., 1990. The meteoritical bulletin No. 69. Meteoritics 25, 237–239.
Wlotzka, F., 1991. The meteoritical bulletin No 70. Meteoritics 26, 68–69.
Wolf, S.F., Lipschutz, M.E., 1992. Comparison differences among Antarctic populations: discriminant analysis of H chondrites from Victoria Land and Queen Maud Land. Lunar Planet. Sci. XXIII, 1545–1546.
Yanai, K., Kojima, H., 1991. Varieties of lunar meteorites recovered from Antarctica. Proc. NIPR Symp. Antarct. Meteorit. 4, 70–90.
Zhang, Y., Benoit, P.H., Sears, D.W.G., 1996a. Pyroxene structures, cathodoluminescence and the thermal history of the enstatite chondrites. Meteorit. Planet. Sci. 31, 87–96.
Zhang, Y., Benoit, P.H., Sears, D.W.G., 1996b. The thermometry of enstatite chondrites, A brief review and update. Meteorit. Planet. Sci. 31, 647–655.
Zolensky, M.E., Pieters, C., Clark, B., Papike, J.J., 2000. Small is beautiful: the analysis of nanogram-sized astromaterials. Meteorit. Planet. Sci. 35, 9–29, http://dx.doi.org/10.1111/j.1945-5100.2000.tb01970.x.
Zolensky, M.E., et al., 2006. Mineralogy and petrology of Comet 81P/Wild 2 nucleus samples. Science 314, 1735–1739, http://dx.doi.org/10.1126/science.1135842.